

Fluctuations of conserved charges in relativistic heavy ion collisions: An introduction

Masayuki Asakawa¹ and Masakiyo Kitazawa¹

¹Department of Physics, Osaka University, Toyonaka, Osaka 560-0043, Japan

December 22, 2021

Abstract

Bulk fluctuations of conserved charges measured by event-by-event analysis in relativistic heavy ion collisions are observables which are believed to carry significant amount of information on the hot medium created by the collisions. Active studies have been done recently experimentally, theoretically, and on the lattice. In particular, non-Gaussianity of the fluctuations has acquired much attention recently. In this review, we give a pedagogical introduction to these issues, and survey recent developments in this field of research. Starting from the definition of cumulants, basic concepts in fluctuation physics, such as thermal fluctuations in statistical mechanics and time evolution of fluctuations in diffusive systems, are described. Phenomena which are expected to occur in finite temperature and/or density QCD matter and their measurement by event-by-event analyses are also elucidated.

1 Introduction

1.1 Background

The medium described by quantum chromodynamics (QCD) is expected to have various phase transitions with variations of external thermodynamic parameters such as temperature T . Although the basic degrees of freedom of QCD, quarks and gluons, are confined into hadrons in the vacuum, they are expected to be liberated at extremely high temperature and form a new state of the matter called the quark-gluon plasma (QGP). It is also known that the chiral symmetry, which is spontaneously broken in vacuum, is restored at extremely hot and/or dense environment. These phase transitions at vanishing baryon chemical potential (μ_B) are investigated with lattice QCD Monte Carlo simulations. The numerical analyses show that the phase transition is a smooth crossover [1, 2]. On the other hand, various models predict that there exists a discontinuous first order phase transition at nonzero μ_B . The existence of the endpoint of the first order transition, the QCD critical point [3], and possibly multiple critical points [4], are anticipated in the phase diagram of QCD on T - μ_B plane [5, 6, 7].

After the advent of the relativistic heavy ion collisions, the quark-gluon plasma has come to be created and investigated on the Earth. At the Relativistic Heavy Ion Collider (RHIC) [8] and the Large Hadron Collider (LHC) [9], active experimental studies on the QGP have been being performed. The discovery of the strongly-coupled property of the QGP near the crossover region [8, 9] is one of the highlights of these experiments. With the top RHIC energy $\sqrt{s_{NN}} = 200$ GeV and LHC energy $\sqrt{s_{NN}} = 2.76$ TeV, hot medium with almost vanishing μ_B is created [10, 11]. On the other hand, the chemical freezeout picture for particle abundances [12] suggests that the net-baryon number density and μ_B of the hot medium increase as $\sqrt{s_{NN}}$ is lowered down to $\sqrt{s_{NN}} \simeq 5 - 10$ GeV [11, 13]. The relativistic heavy ion collisions, therefore, can investigate various regions of the QCD phase diagram on T - μ_B plane by changing the collision energy $\sqrt{s_{NN}}$. Such an experimental program is now ongoing at RHIC, which is called the beam-energy scan (BES) program [14]. The upgraded stage of the BES called the BES-II is planned to start in 2019 [15]. The future experiments prepared at FAIR [16], NICA [17] and J-PARC will also contribute to the study of the medium with large μ_B . The searches of the QCD critical point [18] and the first-order phase transition are among the most interesting subjects in this program.

In relativistic heavy ion collisions, after the formation of the QGP the medium undergoes confinement transition before they arrive at the detector. During rescatterings in the hadronic stage, the signals formed in the QGP tend to be blurred. In order to study the properties of QGP in these experiments, therefore, it is important to choose observables which are sensitive to the medium property in the early stage.

Recently, as unique hadronic observables which reflect thermal property of the primordial medium created by relativistic heavy ion collisions, the bulk fluctuations have acquired much attentions [19]. Although these observables are hadronic ones, it is believed that they reflect the thermal property in the early stage [20]. They are believed to be good observables in investigating the deconfinement transition [21, 22, 23] and finding the location of the QCD critical point [18, 24, 25]. Active experimental studies have been carried out [26, 27, 28, 29, 30, 31, 32, 33] as well as analyses on the numerical simulations on the lattice [34, 35]. In particular, fluctuations of conserved charges and their higher order cumulants representing non-Gaussianity [23, 36, 37] are actively studied recently. The purpose of this review is to give a basic introduction to the physics of fluctuations in relativistic heavy ion collisions, and give an overview of the recent experimental and theoretical progress in this field of research.

1.2 Fluctuations

Before starting the discussion of relativistic heavy ion collisions, we first give a general review on fluctuations briefly. When one measures an observable in some system, the result of the measurements would take different values for different measurements, even if the measurement is performed with an ideal detector with an infinitesimal resolution. This distribution of the result of measurements is referred to as fluctuations. In typical thermal systems, the fluctuations are predominantly attributed to thermal effects, which can be calculated in statistical mechanics. Quantum effects also give rise to fluctuations.

In contrast to standard observables, fluctuations are sometimes regarded as the noise associated with the measurement and thus are obstacles. As expressed by Landauer as “The noise is the signal” [38], however, the fluctuations sometimes can become invaluable physical observables in spite of their obstacle characters. Here, in order to spur the motivations of the readers we list three examples of the physics in which fluctuations play a crucial role.

1. **Brownian motion:** The first example is a historical one on Brownian motion. As first discovered by Brown in 1827, small objects, such as pollens, floating on water show a quick and random motion. Due to this motion, the position of the pollen after several time duration fluctuates even if the initial position is fixed. The origin of this motion was first revealed by Einstein. In his historical paper in 1905 [39], Einstein pointed out that the Brownian motion is attributed to the thermal motion of water molecules. This prediction was confirmed by Perrin, who calculated the Avogadro constant based on this picture [40]. In this era, the existence of atoms had not been confirmed, yet. These studies served as a piece of the earliest evidence for the existence of molecules and atoms. In other words, human beings saw atoms for the first time behind fluctuations.

This example tells us that fluctuations are powerful tools to diagnose microscopic physics. One century after Einstein’s era, now that we know substructures of atoms, hadrons, and quarks and gluons, it seems a natural idea to utilize fluctuations in relativistic heavy ion collisions in exploring subnuclear physics. In this review, a Brownian particle model for diffusion of fluctuations will be discussed in Sec. 5.4.

2. **Cosmic microwave background:** The second example is found in cosmology. As a remnant of Big Bang and as a result of transparent to radiation, our Universe has 2.7 K thermal radiation called cosmic microwave background (CMB) [41]. The temperature of this radiation is almost uniform in all directions in the Universe, but has a tiny fluctuation at different angles. This fluctuation is now considered as the remnant of quantum fluctuations in the primordial Universe. With this picture the power spectrum of this fluctuation tells us various properties of our Universe [42]; for example, our Universe has started with an inflational expansion 13.8 billion years ago. In other words, we can see the hot primordial Universe behind the fluctuation of CMB.

This example tells us that fluctuations can be powerful tools to trace back the history of a system. It thus seems a natural idea to utilize fluctuations to investigate the early stage of the “little bang” created by relativistic heavy ion collisions. A common feature in the study of fluctuations in CMB and heavy ion collisions is that the non-Gaussian fluctuations acquire attentions. In fact, the non-Gaussianity of the CMB has been one of the hot topics in this community [43, 44], although the Planck spacecraft has not succeeded in the measurement of statistically significant non-Gaussianity thus far [45].

3. **Shot noise:** The final example is the fluctuations of the electric current in an electric circuit called the shot noise. The electric current at a resistor R is generally fluctuating. Even without an applied voltage, the current has thermal noise proportional to T/R , which is called the Johnson-Nyquist noise [46, 47]. On the other hand, there is a contribution of the noise which takes place

when a voltage is applied and is proportional to the average current $\langle I \rangle$. When a circuit has a potential barrier, variance of such a noise tends to be proportional to $e^* \langle I \rangle$, where e^* is the electric charge of the elementary degrees of freedom carrying electric current. (This proportionality comes from the Poisson nature of the noise as will be clarified in Sec. 3.2.3.) This noise is called the shot noise [48]. Because of this proportionality, this fluctuation can be used to investigate the quasi-particle property. When the material undergoes the phase transition to superconductivity, for example, electrons are “confined” into Cooper pairs and the electric charge carried by the elementary degrees of freedom is doubled. This behavior is in fact observed in the measurement of the shot noise [49]. More surprisingly, in the materials in which the fractional quantum Hall effect is realized, the shot noise behaves as if there were excitations having fractional charges [50].

This example tells us that the fluctuations are powerful tools to investigate elementary degrees of freedom in the system although they are macroscopic observables. It thus seems a natural idea to utilize this property of fluctuations to explore the confinement/deconfinement property of quarks in relativistic heavy ion collisions. In fact, this is a relatively old idea in heavy ion community [21, 22, 23]. It is also notable that the non-Gaussianity of the shot noise has been observed in mesoscopic systems [51].

1.3 Bulk fluctuations in relativistic heavy ion collisions

In this review, among various fluctuations we focus on the bulk fluctuations of conserved charges. When one measures a charge in a phase space in some system, the amount of the charge, Q , fluctuates measurement by measurement. We refer to the distribution of Q as the bulk fluctuation (or, simply fluctuation). When we perform this measurement in a spatial volume in a thermal system, this fluctuation is called the thermal fluctuation.

The bulk fluctuations are closely related to correlation functions. The total charge Q in a phase space V is given by the integral of the density of the charge $n(x)$ as

$$Q = \int_V dx n(x), \quad (1)$$

where x is the coordinate in the phase space. The variance of Q thus is given by

$$\langle \delta Q^2 \rangle_V = \langle (Q - \langle Q \rangle_V)^2 \rangle_V = \int_V dx_1 dx_2 \langle \delta n(x_1) \delta n(x_2) \rangle, \quad (2)$$

where $\delta n(x) = n(x) - \langle n \rangle$. In this equation, the left-hand side is the quantity that we call (second-order) bulk fluctuation, while the integrand on the right-hand side is called correlation function. Equation (2) shows that $\langle \delta Q^2 \rangle_V$ can be obtained from the correlation function by taking the integral. If one knows the value of $\langle \delta Q^2 \rangle_V$ for all V the correlation function can also be constructed from $\langle \delta Q^2 \rangle_V$. In this sense, the correlation function carries the same physical information as the bulk fluctuation, and the choice of observables, bulk fluctuation or correlation function, is a matter of taste for the second-order fluctuation $\langle \delta Q^2 \rangle_V$. (For higher orders, correlation functions contain more information than bulk fluctuations.) Phenomenological studies on the correlation functions of conserved charges in relativistic heavy ion collisions are widely performed, especially in terms of the so-called balance function [52]. The relation between the correlation functions and bulk fluctuations are also discussed in the literature [53, 54, 55]. In this review, however, we basically stick to bulk fluctuations in our discussion.

In relativistic heavy ion collisions, the bulk fluctuations are observed by the event-by-event analyses. In these analyses, the number of some charge or a species of particle observed by the detector is counted event by event. The distribution of the numbers counted in this way is called event-by-event fluctuation. As we will discuss in detail in Sec. 4, the fluctuations observed in this way are believed to

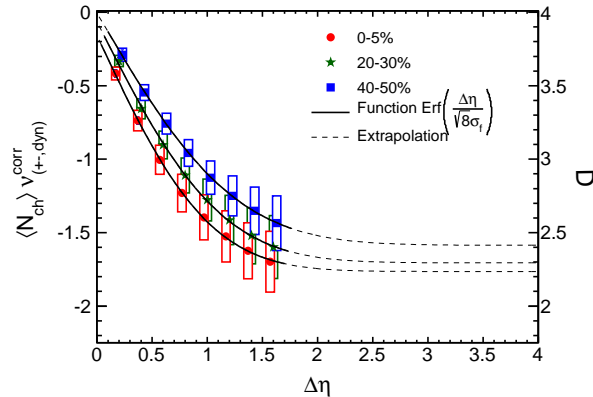


Figure 1: Rapidity window ($\Delta\eta$) dependence of net-electric charge fluctuation measured by ALICE collaboration at LHC [27]. The right vertical axis is the D-measure D , the magnitude of net-electric charge fluctuation in a normalization that the value should become $3 \sim 4$ in an equilibrated hadronic medium [22].

carry information on the thermal fluctuation in the primordial stage. The event-by-event fluctuations, however, are not the thermal fluctuations themselves. The hot media created by collisions are dynamical systems, and the detector can only measure their final states. Moreover, fluctuations other than thermal fluctuations contribute to event-by-event fluctuations. Careful treatment and interpretation, therefore, are required in comparing the event-by-event fluctuations with theoretical analysis on thermal fluctuations. As will be discussed in Sec. 4, however, there are sufficient reasons to expect that event-by-event fluctuations can be compared with thermal fluctuations with an appropriate treatment.

In Figs. 1 and 2, we show two examples of recent experimental results on event-by-event analyses of bulk fluctuations. Figure 1 shows the experimental result obtained by ALICE Collaboration at LHC [27]. This figure shows the variance of the net-electric charge; the right vertical axis shows the quantity called D-measure, i.e. the variance normalized in such a way that the value in the equilibrated hadronic medium becomes $3 \sim 4$ [22]. The horizontal axis is the rapidity window $\Delta\eta$ to count the particle number. The figure shows that the experimental result has a nontrivial suppression, which cannot be described by the equilibrated hadronic degrees of freedom. The result thus suggests that the net-electric charge fluctuation at the LHC energy contains non-hadronic or non-thermal physics in the primordial medium. The origin of the suppression in Fig. 1 will be discussed in Sec. 3.3. The experimental result also shows that the fluctuation is more suppressed for larger $\Delta\eta$. This behavior will be discussed in detail in Sec. 5.2.

In Fig. 2, we show the experimental results on the non-Gaussian fluctuations measured by STAR Collaboration at RHIC [28, 32]. The two panels show the same quantity, the ratios of the net-proton number cumulants, as a function of the collision energy $\sqrt{s_{NN}}$; since the baryon chemical potential μ_B of the hot medium becomes smaller as $\sqrt{s_{NN}}$ increases [11, 13], these plots can be interpreted as the μ_B dependence of the cumulants. The right panel [32] is the updated version of the left panel [28]; the quality of the experimental analysis is ever-improving in this field [32]. In the right panel, the vertical axes are quantities which is expected to take unity in the equilibrated hadronic medium. The panel shows that these quantities take values which are close to the hadronic one but have statistically-significant deviation from those values. These deviations are believed to be important observables to explore the QCD phase structure. In this review, we will elucidate the meanings of the vertical axes in Fig. 2 and the reason why these quantities are widely discussed.

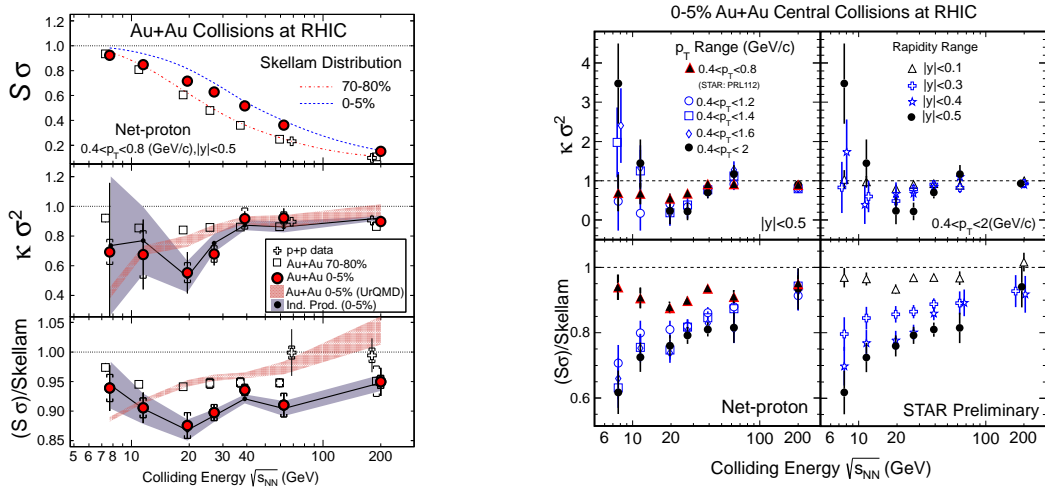


Figure 2: Ratios of net-proton number cumulants measured by STAR Collaboration at RHIC [28, 32]. The right panel [32] is the updated version of the left panel [28].

1.4 Contents of this review

In this review, we give a pedagogical introduction to the physics of fluctuations in relativistic heavy ion collisions. In particular, one of the objectives of the introductory part is to understand the meanings of Figs. 1 and 2. We aimed at answering, for example, the following questions in this review:

- What are the *cumulants*? Why should we focus on these quantities in the discussion of non-Gaussian fluctuations? Why are the cumulants sometimes called susceptibility, and what are the relation of cumulants with moments, skewness and kurtosis?
- Meanings of the vertical axes of Figs. 1 and 2. How to understand these experimental data?
- What happens in the fluctuation observables in heavy ion collisions if the hot medium undergoes a phase transition to deconfinement transition, or passes near the QCD critical point?
- Why can the event-by-event fluctuation be compared with thermal fluctuations? Why should one *not* directly compare the event-by-event fluctuations with thermal fluctuations?
- The concept of “equilibration of the fluctuation of conserved charges.” What is the difference of this concept from the “local equilibration,” and why should we distinguish them?

In addition to the answers to these questions, we have tried to describe recent progress in this field of research.

The outline of this review is as follows. In the next section, we give a pedagogical review on the probability distribution function, which is a basic quantity describing fluctuations. The cumulants are introduced here, and their properties, especially the extensive nature, are discussed. In Sec. 3, we discuss the thermal fluctuations, i.e. the fluctuations in an equilibrated medium. The behaviors of cumulants in the QCD phase diagram is also considered. Sections 4 – 6 are devoted to a review on the event-by-event fluctuations in experimental analyses. In Sec. 4, we summarize general properties of the event-by-event fluctuations. Various cautions in the interpretation of these quantities are given in this section. In Sec. 5, we focus on the non-equilibrium property of the event-by-event fluctuations, by describing the time evolution of fluctuations using stochastic formalisms. In Sec. 6, we consider a model for probability distribution functions which treats the efficiency problem in the observation of

fluctuations. The difference between net-baryon and net-proton number cumulants are also discussed here. We then give a short summary in Sec. 7.

2 General introduction to probability distribution function

Because fluctuation is a distribution of some observable, it is mathematically represented by probability distribution functions. For example, if one repeats a measurement of an observable in an equilibrated medium many times, the result of the measurement would fluctuate measurement by measurement. The distribution of the result of the measurement is represented by a histogram. After accumulating the results of many measurements, the histogram with an appropriate normalization can be regarded as the probability distribution function. This distribution is nothing other than the fluctuation. In many contexts, the width of the distribution is particularly called fluctuations.

In this section, as preliminaries of later sections we give a pedagogical introduction to basic concepts in probability. We introduce moments and cumulants as quantities characterizing probability distribution functions. Advantages of cumulants, especially for the description of non-Gaussianity of distribution functions, are elucidated. We also discuss properties of specific distribution functions, Poisson, Skellam, binomial and Gauss distributions. The properties of these distribution functions play important roles in later sections for interpreting fluctuation observables in relativistic heavy ion collisions.

2.1 Moments and cumulants

We start from a probability distribution function $P(m)$ satisfying $\sum_m P(m) = 1$ for an integer stochastic variable m . One of the set of quantities which characterizes $P(m)$ is the moments. The n -th order moment is defined by

$$\langle m^n \rangle = \sum_m m^n P(m), \quad (3)$$

where the bracket on the left-hand side represents the statistical average with $P(m)$. If the moments for all $n > 0$ exists, they carry all information encoded in $P(m)$. For a probability distribution function $P(x)$ for a continuous stochastic variable x , the moments are defined by

$$\langle x^n \rangle = \int dx x^n P(x), \quad (4)$$

where the integral is taken over the range of x .

To calculate the moments for a given probability distribution $P(m)$, it is convenient to introduce the moment generating function,

$$G(\theta) = \sum_m e^{m\theta} P(m) = \langle e^{m\theta} \rangle. \quad (5)$$

Moments are then given by the derivatives of $G(\theta)$ as

$$\langle m^n \rangle = \left. \frac{d^n}{d\theta^n} G(\theta) \right|_{\theta=0}. \quad (6)$$

For the continuous case the generating function is defined by

$$G(\theta) = \int dx e^{x\theta} P(x). \quad (7)$$

For many practical purposes, it is more convenient to use *cumulants* rather than moments for characterizing a probability distribution. To define the cumulants, we start from the cumulant generating function,

$$K(\theta) = \ln G(\theta). \quad (8)$$

The cumulants of $P(m)$ are then defined by

$$\langle m^n \rangle_c = \left. \frac{d^n}{d\theta^n} K(\theta) \right|_{\theta=0}. \quad (9)$$

As we will see below, cumulants have several useful features for describing fluctuations, especially their non-Gaussianity.

Before discussing the advantages of cumulants, let us clarify the relation between moments and cumulants. These relations are obtained straightforwardly from their definitions Eqs. (6) and (9). For example, to write cumulants in terms of moments, we calculate as follows:

$$\langle m \rangle_c = \left. \frac{d}{d\theta} \ln G(\theta) \right|_{\theta=0} = \frac{G^{(1)}(0)}{G(0)} = \langle m \rangle, \quad (10)$$

$$\langle m^2 \rangle_c = \left. \frac{d^2}{d\theta^2} \ln G(\theta) \right|_{\theta=0} = \frac{G^{(2)}(0)}{G(0)} - \frac{(G^{(1)}(0))^2}{(G(0))^2} = \langle m^2 \rangle - \langle m \rangle^2 = \langle \delta m^2 \rangle, \quad (11)$$

where $G^{(n)}(\theta)$ represents the n -th derivative of $G(\theta)$ and we have used $G(0) = \sum_m P(m) = 1$. In the last equality we defined $\delta m = m - \langle m \rangle$. By repeating a similar manipulation, one can extend the relation to an arbitrary order. The results for third- and fourth-orders are given by

$$\langle m^3 \rangle_c = \langle \delta m^3 \rangle, \quad (12)$$

$$\langle m^4 \rangle_c = \langle \delta m^4 \rangle - 3\langle \delta m^2 \rangle^2. \quad (13)$$

Note that the first-order cumulant is equal to the first-order moment, or the expectation value. The second- and third-order cumulants are given by the central moments,

$$\langle \delta m^n \rangle = \langle (m - \langle m \rangle)^n \rangle. \quad (14)$$

In particular, the second-order cumulant $\langle \delta m^2 \rangle$ corresponds to the *variance*. This quantity is sometimes called simply fluctuation, because for many purposes the cumulants higher than the second-order are not physically significant. The cumulants for $n \geq 4$ are given by nontrivial combinations of central moments with n -th and lower orders.

All cumulants except for the first-order one are represented by central moments and do not depend on the average $\langle m \rangle$. To prove this statement, we consider a probability distribution function $P'(m) = P(m - m_0)$ in which the distribution is shifted by m_0 compared with $P(m)$. The cumulant generating function of $P'(m)$ is calculated to be

$$\begin{aligned} K'(\theta) &= \ln \sum_m e^{m\theta} P'(m) = \ln \sum_m e^{m\theta} P(m - m_0) = \ln \sum_m e^{(m+m_0)\theta} P(m) \\ &= \ln \sum_m e^{m\theta} P(m) + m_0\theta = K(\theta) + m_0\theta, \end{aligned} \quad (15)$$

where $K(\theta)$ is the cumulant generating function of $P(m)$. Equation (15) shows that the difference between $K'(\theta)$ and $K(\theta)$ is a term $m_0\theta$. The derivatives of $K'(\theta)$ and $K(\theta)$ higher than the first-order thus are equivalent. Therefore, the cumulants higher than the first-order do not depend on $\langle m \rangle$, and they are represented only by central moments.

The expressions of moments in terms of cumulants are similarly obtained as follows:

$$\langle m \rangle = \left. \frac{d}{d\theta} e^{K(\theta)} \right|_{\theta=0} = K^{(1)}(0) e^{K(0)} = \langle m \rangle_c, \quad (16)$$

$$\langle m^2 \rangle = \left. \frac{d^2}{d\theta^2} e^{K(\theta)} \right|_{\theta=0} = (K^{(2)}(0) + (K^{(1)}(0))^2) e^{K(0)} = \langle m^2 \rangle_c + \langle m \rangle_c^2, \quad (17)$$

and so forth. Up to the fourth-order, one obtains

$$\begin{aligned} \langle m^3 \rangle &= \langle m^3 \rangle_c + 3\langle m^2 \rangle_c \langle m \rangle_c + \langle m \rangle_c^3, \\ \langle m^4 \rangle &= \langle m^4 \rangle_c + 4\langle m^3 \rangle_c \langle m \rangle_c + 3\langle m^2 \rangle_c^2 + 6\langle m^2 \rangle_c \langle m \rangle_c^2 + \langle m \rangle_c^4. \end{aligned} \quad (18)$$

2.2 Sum of two stochastic variables

An important property of cumulants becomes apparent when one considers the sum of two stochastic variables. Let us consider two integer stochastic variables m_1 and m_2 which respectively obey probability distribution functions $P_1(m_1)$ and $P_2(m_2)$ which are not correlated. Then, the probability distribution of the sum of two stochastic variables, $m = m_1 + m_2$, is given by

$$P(m) = \sum_{m_1, m_2} \delta_{m, m_1 + m_2} P(m_1) P(m_2). \quad (19)$$

(To understand Eq. (19), one may, for example, imagine the probability distribution of the sum of the numbers of two dices.) The moment and cumulant generating functions for $P(m)$ are calculated to be

$$\begin{aligned} G(\theta) &= \sum_m e^{m\theta} P(m) = \sum_m e^{m\theta} \sum_{m_1, m_2} \delta_{m, m_1 + m_2} P_1(m_1) P_2(m_2) \\ &= \sum_{m_1} e^{m_1\theta} P_1(m_1) \sum_{m_2} e^{m_2\theta} P_2(m_2) = G_1(\theta) G_2(\theta), \end{aligned} \quad (20)$$

$$K(\theta) = \ln G(\theta) = K_1(\theta) + K_2(\theta), \quad (21)$$

where $G_i(\theta) = \sum_m e^{m\theta} P_i(m)$ and $K_i(\theta) = \ln G_i(\theta)$ are the moment and cumulant generating functions of P_i , respectively, for $i = 1$ and 2 . By taking n derivatives of the both sides of Eq. (21), one finds

$$\langle m^n \rangle_c = \langle m_1^n \rangle_c + \langle m_2^n \rangle_c. \quad (22)$$

This result shows that the cumulants of the probability distribution for the sum of two independent stochastic variables are simply given by the sum of the cumulants. (This is the reason why the cumulants are called in this way.) Note that this result is obtained for two *independent* stochastic variables; when the distributions of m_1 and m_2 are correlated, Eq. (22) no longer holds.

2.3 Cumulants in statistical mechanics

In statistical mechanics, results of measurement of observables in a volume V are fluctuating, and one can define their cumulants from the distribution of the results. From Eq. (22) one can argue an important property of the cumulants in statistical mechanics that the cumulants of extensive variables in grand canonical ensemble are *extensive variables*.

To see this, let us consider the number N of a conserved charge in a volume V in grand canonical ensemble. From the distribution of the result of measurements, one can define the cumulants $\langle N^n \rangle_{c, V}$ of the charge. Next, let us consider the cumulants of the particle number in a twice larger volume,

$\langle N^n \rangle_{c,2V}$. This system can be separated into two subsystems with an equal volume V . In statistical mechanics, it is usually assumed that the subsystems are uncorrelated when the volume is sufficiently large, and the property of the system does not depend on the shape of V . Therefore, the particle number in the total system is regarded as the sum of the two independent particle numbers in the two subsystems. From Eq. (22), $\langle N^n \rangle_{c,2V}$ thus are represented as

$$\langle N^n \rangle_{c,2V} = 2\langle N^n \rangle_{c,V}. \quad (23)$$

By similar arguments one obtains,

$$\langle N^n \rangle_{c,\lambda V} = \lambda \langle N^n \rangle_{c,V} \quad (24)$$

for an arbitrary number λ . Equation (24) shows that the cumulants of N in statistical mechanics are extensive variables. As special cases of this property, the average particle number $\langle N \rangle$ and the variance $\langle \delta N^2 \rangle$ in statistical mechanics are extensive variables.

From Eq. (24), the cumulants in volume V can be written as

$$\langle N^n \rangle_{c,V} = \chi_n V. \quad (25)$$

Here, χ_1 is the density of the particle, and χ_2 is the quantity which is referred to as susceptibility because of the linear response relation discussed in Sec. 3.1.3. We call χ_n for $n \geq 3$ as generalized susceptibilities.

Remarks on the extensive nature of the cumulants are in order. First, the above argument is valid only when the volume of the system is sufficiently large. When the spatial extent of the volume is not large enough, the correlation between two adjacent volumes becomes non-negligible. This would happen when the spatial extent of the volume is comparable with the microscopic correlation lengths. Next, in the above argument we have implicitly assumed grand canonical ensemble in addition to the equilibration. The argument, for example, is not applicable to subvolumes in canonical ensemble in which the number of N in the total system is fixed. In this case, the fixed total number gives rise to correlation between subvolumes; because the total number is fixed, if the particle number in a subvolume is large the particle number in the other subvolume tends to be suppressed. This correlation violates the assumption of independence between the particle numbers in subvolumes unless the subvolume is small enough compared with the total volume.

2.4 Examples of distribution functions

Now, we see some specific distribution functions, which play important roles in relativistic heavy ion collisions.

2.4.1 Binomial distribution

The binomial distribution function is defined by the number of ‘‘successes’’ of N independent trials, each of which yields a success with probability p . The binomial distribution function is given by

$$B_{p,N}(m) = {}_N C_m p^m (1-p)^{N-m}, \quad (26)$$

where

$${}_N C_m = \frac{N!}{m!(N-m)!} \quad (27)$$

is the binomial coefficient. It is easy to show that $\sum_m B_{p,N}(m) = 1$ using the binomial theorem. The moment and cumulant generating functions of the binomial distribution are calculated to be

$$\begin{aligned} G_B(\theta) &= \sum_m e^{m\theta} B_{p,N}(m) = \sum_m {}_N C_m (e^\theta p)^m (1-p)^{N-m} \\ &= (1-p + e^\theta p)^N, \end{aligned} \quad (28)$$

$$K_B(\theta) = N \ln(1-p + e^\theta p). \quad (29)$$

From Eq. (29), the cumulants of the binomial distribution function are given by

$$\langle m^n \rangle_c = \xi_n N \quad (30)$$

with explicit forms of ξ_n up to the fourth-order

$$\xi_1 = p, \quad \xi_2 = p(1-p), \quad \xi_3 = p(1-p)(1-2p), \quad \xi_4 = p(1-p)(1-6p+6p^2). \quad (31)$$

Equation (30) shows that the cumulants of the binomial distribution are proportional to N , which is a reasonable result from the extensive nature of cumulants.

The sum of two stochastic variables obeying independent binomial distribution functions with an equal probability p is again distributed with a binomial one. This can be shown by explicitly deriving the identity,

$$B_{p,N_1+N_2}(m) = \sum_{m_1, m_2} \delta_{m, m_1+m_2} B_{p,N_1}(m_1) B_{p,N_2}(m_2). \quad (32)$$

An alternative way to prove this statement is to use Eqs. (22) and (30). Suppose that m_1 and m_2 obey the binomial distribution $B_{p,N_1}(m_1)$ and $B_{p,N_2}(m_2)$, respectively. From Eq. (22), one finds that the cumulants of the sum $m = m_1 + m_2$ are given by $\langle m^n \rangle_c = \xi_n (N_1 + N_2)$, which are nothing but the cumulants of the binomial distribution $B_{p,N_1+N_2}(m)$. Because all cumulants are those of the binomial distribution, the distribution of $m_1 + m_2$ is given by the binomial one.

2.4.2 Poisson distribution

The Poisson distribution function is defined by the number of successes of independent trials, each of which yields a success with infinitesimal probability. The Poisson distribution is thus obtained by taking the $p \rightarrow 0$ limit of the binomial distribution function with fixed $\lambda = pN$. Replacing the binomial coefficients in Eq. (26) as ${}_N C_m \rightarrow N^m/m!$, which is valid in this limit, and using the definition of Napier's number $e = \lim_{p \rightarrow 0} (1+p)^{1/p}$ in Eq. (26), one obtains

$$P_\lambda(m) = \frac{\lambda^m}{m!} e^{-\lambda}. \quad (33)$$

The cumulant generating function of Eq. (33) is obtained as

$$K_\lambda(\theta) = \lambda(e^\theta - 1). \quad (34)$$

By taking derivatives of Eq. (34), one finds that all the cumulants of the Poisson distribution are the same,

$$\langle m^n \rangle_c = \lambda \quad (\text{for any } n \geq 1). \quad (35)$$

This property will be used frequently in later sections. This result also shows that the Poisson distribution is characterized by a single parameter λ , while the binomial distribution function is characterized by the two parameters, p and N .

The sum of two stochastic variables obeying two independent Poissonian obeys Poissonian,

$$P_{\lambda_1+\lambda_2}(m) = \sum_{m_1, m_2} \delta_{m, m_1+m_2} P_{\lambda_1}(m_1) P_{\lambda_2}(m_2), \quad (36)$$

as one can explicitly show easily. Similarly to the case of the binomial distribution, however, a much easier way to show this is to use Eqs. (22) and (35).

The Poisson distribution is one of the most fundamental distribution function, as it naturally appears in various contexts. One interesting example among them is the classical ideal gas. One can show that the distribution of the number of a classical free particles in a volume in grand canonical ensemble obeys the Poisson distribution. To show this, the following intuitive argument suffices. First, consider a canonical ensemble for a volume V_c with a fixed particle number N_c . The grand canonical ensemble is defined by a subvolume V in this system in the limit $r \equiv V/V_c \rightarrow 0$. Next, consider a particle in this system. The probability that this particle exists in the subvolume V is given by r . Moreover, because we consider classical free particles, the probability that each particle is in the subvolume is uncorrelated. The probability distribution function of the particle number N in V thus is given by the binomial distribution with probability r . Because the grand canonical ensemble is defined by $r \rightarrow 0$ limit with fixed $N = rN_c = VN_c/V_c$, the distribution in this limit obeys Poissonian. In Sec. 3.2 we will explicitly calculate the cumulants in the classical ideal gas and show that they satisfy Eq. (35). When the effect of quantum statistics, Bose-Einstein or Fermi-Dirac, shows up, this argument does not hold owing to the quantum correlation even for ideal gas.

2.4.3 Skellam distribution

Although the sum of stochastic variables obeying independent Poisson distributions again obeys Poissonian, the *difference* of two stochastic variables obeying independent Poisson distributions is not given by a Poisson distribution. This is obvious from the fact that the difference can take a negative value, while the Poisson distribution $P_\lambda(m)$ take nonzero values only for positive m . The difference,

$$S_{\lambda_1, \lambda_2}(m) = \sum_{m_1, m_2} \delta_{m, m_1-m_2} P_{\lambda_1}(m_1) P_{\lambda_2}(m_2), \quad (37)$$

is called the Skellam distribution. The generating functions of the Skellam distribution are calculated to be

$$G(\theta) = \sum_m e^{m\theta} \sum_{m_1, m_2} \delta_{m, m_1-m_2} P_{\lambda_1}(m_1) P_{\lambda_2}(m_2) \quad (38)$$

$$= \sum_{m_1} e^{m_1\theta} P_{\lambda_1}(m_1) \sum_{m_2} e^{-m_2\theta} P_{\lambda_2}(m_2) \quad (39)$$

$$= G_{\lambda_1}(\theta) G_{\lambda_2}(-\theta), \quad (40)$$

$$K(\theta) = K_{\lambda_1}(\theta) + K_{\lambda_2}(-\theta), \quad (41)$$

where generating functions $G_\lambda(\theta)$ and $K_\lambda(\theta)$ are those of Poisson distribution. By taking derivatives of this result with Eq. (34), one obtains

$$\langle m^n \rangle_c = \langle m_1^n \rangle_c + (-1)^n \langle m_2^n \rangle_c = \lambda_1 + (-1)^n \lambda_2 \quad (42)$$

for the Skellam distribution. This result shows that all even cumulants take a common value $\lambda_1 + \lambda_2$, while the odd cumulants take $\lambda_1 - \lambda_2$. This result also shows that the Skellam distribution is characterized by two parameters, λ_1 and λ_2 , or alternatively odd and even cumulants.

The explicit analytic form of $S(m)$ is given by

$$S_{\lambda_1, \lambda_2}(m) = e^{-(\lambda_1 + \lambda_2)} \left(\frac{\lambda_1}{\lambda_2} \right) I_m \left(2\sqrt{\lambda_1 \lambda_2} \right), \quad (43)$$

where $I_m(z)$ is the modified Bessel function of the first kind.

The Skellam distribution plays an important role in later sections, because they describe the distribution of net particle number, i.e. the difference of the numbers of particles and anti-particles, in the classical ideal gas. The fluctuation of net-baryon number in hadron resonance gas, for example, obeys the Skellam distribution.

2.4.4 Gauss distribution

So far we have considered stochastic variables taking integer values. An example of a distribution with a continuous stochastic variable is the Gauss distribution, which is defined by

$$P_G(x) = \frac{1}{\sigma\sqrt{2\pi}} \exp \left[-\frac{(x - x_0)^2}{2\sigma^2} \right]. \quad (44)$$

The normalization factor is required to satisfy $\int_{-\infty}^{\infty} dx P_G(x) = 1$. The generating functions are calculated to be

$$\begin{aligned} G(\theta) &= \int dx e^{\theta x} \frac{1}{\sigma\sqrt{2\pi}} \exp \left[-\frac{(x - x_0)^2}{2\sigma^2} \right] = \exp \left[x_0\theta + \frac{1}{2}\sigma^2\theta^2 \right], \\ K(\theta) &= x_0\theta + \frac{1}{2}\sigma^2\theta^2. \end{aligned} \quad (45)$$

We thus have

$$\langle x \rangle = x_0, \quad \langle x^2 \rangle_c = \sigma^2, \quad (46)$$

and

$$\langle x^n \rangle_c = 0 \quad \text{for } n \geq 3. \quad (47)$$

The results in Eqs. (46) and (47) can, of course, also be obtained by explicitly calculating $\langle x \rangle = \int dx x P_G(x)$ and $\langle x^2 \rangle_c = \langle \delta x^2 \rangle = \int dx (x - x_0)^2 P_G(x)$, and so forth.

Equations (46) and (47) show that the cumulants higher than the second-order vanish for the Gauss distribution. In other words, nonzero higher order cumulants characterize deviations from the Gauss distribution function. This is the reason why the cumulants are used as quantities representing non-Gaussianity.

2.5 Variance, skewness and kurtosis

Till now, we have discussed cumulants as quantities characterizing distribution functions. When one wants to describe the deviation from the Gauss distribution, it is sometimes convenient to use the quantities called skewness S and kurtosis κ [56]. These quantities are defined as

$$S = \frac{\langle x^3 \rangle_c}{\langle x^2 \rangle_c^{3/2}} = \frac{\langle x^3 \rangle_c}{\sigma^3}, \quad \kappa = \frac{\langle x^4 \rangle_c}{\langle x^2 \rangle_c^2} = \frac{\langle x^4 \rangle_c}{\sigma^4}, \quad (48)$$

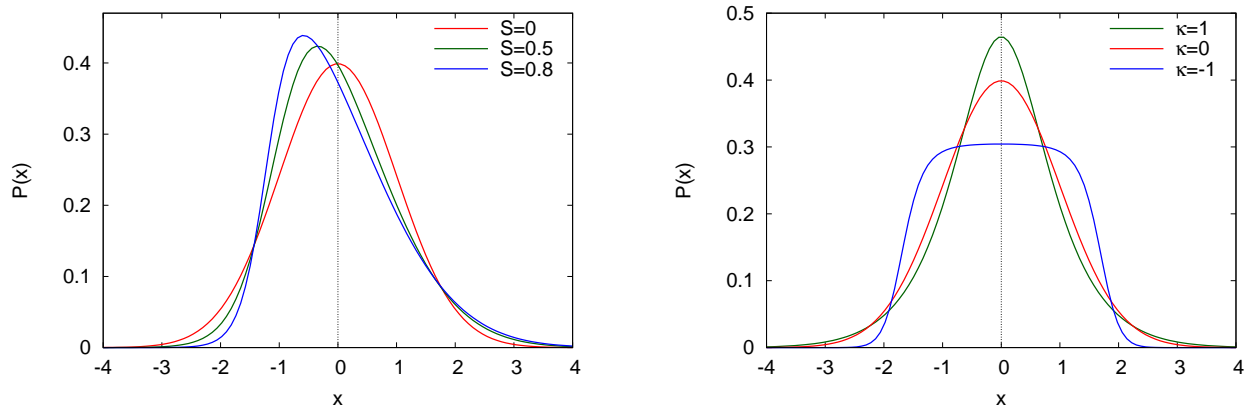


Figure 3: Typical distribution functions having nonzero skewness (left) and kurtosis (right). The average and variance are set to $\langle x \rangle = 0$ and $\sigma = 1$.

where σ^2 is the variance defined by $\sigma^2 = \langle x^2 \rangle_c$. The skewness and kurtosis are interpreted as the third- and fourth-order cumulants of the renormalized stochastic variable $\tilde{x} = x/\sigma$ satisfying $\langle \tilde{x}^2 \rangle_c = 1$,

$$S = \langle \tilde{x}^3 \rangle_c, \quad \kappa = \langle \tilde{x}^4 \rangle_c. \quad (49)$$

In Fig. 3, we show typical distribution functions having nonzero skewness and kurtosis. All distribution functions shown in the figure satisfy $\langle x \rangle = 0$ and $\langle x^2 \rangle_c = 1$. As shown in the left panel, the skewness represents the asymmetry of the distribution function. The kurtosis, on the other hand, typically describes the “sharpness” of the distribution compared with the Gaussian one as in the right panel.

When the non-Gaussianity of a distribution function is discussed, the set of variables to be used, S and κ , or the third and fourth-order cumulants, should be chosen depending on the problem. When the distribution is expected to obey some specific one of which the cumulants are known, the cumulants are much more convenient. For example, when the distribution is expected to obey the Poisson one and the difference from this distribution is concerned, one may focus on the cumulants normalized by the average, $\langle m^n \rangle_c / \langle m \rangle^n$, which become unity in the Poisson distribution. The deviation from the Poisson distribution is then characterized by the difference of the ratio from unity. As we will see in Sec. 3, for example, the fluctuation of net-baryon number in the equilibrated hadronic medium is well described by the Skellam distribution. If the fluctuation carries some physics which cannot be described by hadronic degrees of freedom in equilibrium, it may deviate from the Skellam one. In order to find this deviation, the best observable to be used is the ratios of cumulants between even or odd orders [23], which become unity for the Skellam distribution as discussed in Sec. 2.4.3. Another example is the distribution of the topological charge, Q , in QCD. A model called the dilute instanton gas model for the topological sector in QCD predicts that the distribution of the topological charge is given by the Skellam one with $\langle Q \rangle = 0$ [57]. The proximity of the ratios of the even order cumulants to unity thus is a useful measure to judge the validity of this model. Recently, the measurements of the topological cumulants are actively performed on the lattice [58, 59, 60].

Contrary to the ratios of cumulants, the magnitudes of skewness and kurtosis in the Poisson distribution depend on the average λ as

$$S = \lambda^{-1/2}, \quad \kappa = \lambda^{-1}. \quad (50)$$

These quantities become arbitrary small as λ becomes larger. This behavior is related to the central limit theorem in statistics, which states that the sum of independent events approaches a Gauss distribution

as the number of events to be summed is increased. Because the Poisson distribution can be interpreted as the result of the sum of independent events, it approaches the Gauss distribution for large λ . The S and κ , the quantities characterizing the deviation from the Gauss distribution, become arbitrarily small in this limit. Similar tendency is also expected in the large volume limit of fluctuation observables in statistical mechanics. Fluctuations in macroscopic systems are well described by Gauss distributions, and S and κ become irrelevant in the large volume limit. On the other hand, the higher order cumulants take nonzero values even in this limit. There, however, are practical difficulties in the measurement of higher order cumulants in large systems. In addition to the difficulty in the exact measurement of observables in large systems, there is a fundamental problem that the statistical error of higher order cumulants grows as the volume increases, as discussed in the next subsection.

2.6 Error of the cumulants

Related to the above discussion on non-Gaussianity in large systems, we give some remarks on the statistical error associated with the measurement of higher order cumulants.

The statistical error $\Delta\hat{O}$ of an observable \hat{O} is estimated as

$$(\Delta\hat{O})^2 = \frac{\langle(\hat{O} - \langle\hat{O}\rangle)^2\rangle}{N_{\text{stat}} - 1} = \frac{\langle\delta\hat{O}^2\rangle}{N_{\text{stat}} - 1}, \quad (51)$$

where N_{stat} is the number of statistics, i.e. the number of the measurements of \hat{O} , and the expectation value is taken over this statistical ensemble.

Let us consider an extensive observable N in statistical mechanics, such as particle number. As discussed already, cumulants of N are extensive observables proportional to the volume V . Now, we start from the first-order cumulant. Usually, the density $\rho = N/V$ of this quantity is concerned rather than N . By substituting ρ into \hat{O} in Eq. (51), one obtains

$$(\Delta\rho)^2 = \frac{\langle\delta N^2\rangle}{V^2 N_{\text{stat}}} = \frac{\chi_2}{V N_{\text{stat}}}, \quad (52)$$

where in the last equality we used the extensive nature of the second-order cumulant Eq. (25). We have also assumed that $N_{\text{stat}} \gg 1$ and used an approximation $N_{\text{stat}} - 1 \simeq N_{\text{stat}}$ in the denominator. The result Eq. (52) shows that the error of ρ is proportional to $V^{-1/2}$, which is a well-known result. With a fixed N_{stat} , the error of ρ becomes smaller as V becomes larger.

Next, we consider the statistical error of the second-order cumulant of N . By substituting δN^2 in \hat{O} , the error is calculated to be

$$\begin{aligned} (\Delta(\delta N^2))^2 &= \frac{\langle((\delta N^2) - \langle\delta N^2\rangle)^2\rangle}{N_{\text{stat}}} = \frac{\langle\delta N^4\rangle - \langle\delta N^2\rangle^2}{N_{\text{stat}}} = \frac{\langle N^4\rangle_{\text{c}} + 2\langle N^2\rangle_{\text{c}}^2}{N_{\text{stat}}} \\ &= \frac{\chi_4 V + 2(\chi_2 V)^2}{N_{\text{stat}}}. \end{aligned} \quad (53)$$

In this derivation, we have used the central moments as basic quantities rather than moments. This choice suppresses the correlation between first- and second-order moments. The central moments are converted to cumulants in the third equality. From Eq. (53), the error of the susceptibility χ_2 is obtained by dividing both sides by V^2 as

$$(\Delta\chi_2)^2 = \frac{\chi_4 V^{-1} + 2\chi_2^2}{N_{\text{stat}}} = \frac{2\chi_2^2}{N_{\text{stat}}} + \mathcal{O}(V^{-1}). \quad (54)$$

This result shows that the error of χ_2 does not have V dependence for sufficiently large V . Contrary to the first-order case, the increase of V does not reduce the statistical error of χ_2 .

Similarly, the error of the higher order cumulants can be estimated by substituting the definition of the cumulants in Eq. (51). The higher order cumulants are represented by central moments in general as shown in sec. 2.1. (To obtain the explicit forms, one may substitute $G^{(1)} = 0$ in Eqs. (10)–(13) and so forth.) It is therefore instructive to first see the error of the central moments. The n -th order central moment is represented by the sum of the product of cumulants

$$\langle m^{n_1} \rangle_c \langle m^{n_2} \rangle_c \cdots \langle m^{n_i} \rangle_c, \quad (55)$$

with $n = n_1 + n_2 + \cdots + n_i$ and $n_i \geq 2$. Moreover, one can easily show that the coefficients of all terms in this decomposition are positive and nonvanishing. Now, because the cumulants are proportional to V , the term which is leading in V in large volume is the one containing the product of the largest number of the cumulants. For even n , it is $(\langle N^2 \rangle_c)^{n/2}$ and one obtains the behavior of the central moments in large V as

$$\langle (\delta N)^n \rangle \sim (\langle N^2 \rangle_c)^{n/2} (1 + \mathcal{O}(V^{-1})) \sim (\chi_2 V)^{n/2} + \mathcal{O}(V^{n/2-1}). \quad (56)$$

For odd n , one obtains $\langle (\delta N)^n \rangle \sim V^{(n-1)/2}$.

Using these dependences on V , the statistical error of the central moments is given by

$$(\Delta(\delta N^n))^2 = \frac{\langle \delta N^{2n} \rangle - \langle \delta N^n \rangle^2}{N_{\text{stat}}} \sim \frac{(\chi_2 V)^n}{N_{\text{stat}}}, \quad (57)$$

where in the last step we have used Eq. (56) and the fact that the terms proportional to V^n never cancel out between $\langle \delta N^{2n} \rangle$ and $\langle \delta N^n \rangle^2$. Subleading terms in V^{-1} are neglected on the far right-hand side. The error of the n -th order central moment thus is proportional to $\sqrt{V^n/N_{\text{stat}}}$ for large V and N_{stat} .

Now, we come back to the statistical error of higher order cumulants. As discussed already, the cumulants can be represented by the central moments. Substituting the cumulants in \mathcal{O} into Eq. (51) and representing them in terms of central moments, the error of the cumulants is given by the sum of the product of the central moments. It is then concluded that the error of the cumulants in the leading order in V should be same as Eq. (57) unless the highest order terms in V cancel out. The error of the generalized susceptibility thus is expected to behave as

$$\Delta\chi_n \sim \sqrt{\frac{\chi_2^n V^{n-2}}{N_{\text{stat}}}}, \quad (58)$$

for large V and N_{stat} . Eq. (58) shows that the error of χ_n for $n \geq 3$ grows as V becomes larger and the measurement of non-Gaussian cumulants becomes more and more difficult as the spatial volume becomes larger. This V dependence is highly contrasted to the error of standard observables Eq. (52), which becomes smaller as V becomes larger. The proportionality coefficients in Eq. (58) up to the fourth-order are presented in Ref. [61].

In relativistic heavy ion collisions, non-Gaussian cumulants have been observed up to the fourth-order. These measurements are possible because the size of the system observed by detectors is not large; the particle number in each event is at most of order 10^3 . The growth of the statistical error of higher order cumulants is a well known feature, and discussed in various contexts; see for example Refs. [62, 63, 64].

2.7 Cumulants for multiple variables

Next, we discuss probability distribution functions for multiple stochastic variables and their moments and cumulants.

Let us consider a probability distribution function $P(m_1, m_2)$ for integer stochastic variables m_1 and m_2 . The moments of this distribution are defined by

$$\langle m_1^{n_1} m_2^{n_2} \rangle = \sum_{m_1, m_2} m_1^{n_1} m_2^{n_2} P(m_1, m_2). \quad (59)$$

By defining the moment generating function as

$$G(\theta_1, \theta_2) = \sum_{m_1, m_2} e^{\theta_1 m_1} e^{\theta_2 m_2} P(m_1, m_2) = \langle e^{\theta_1 m_1} e^{\theta_2 m_2} \rangle, \quad (60)$$

the moments are given by

$$\langle m_1^{n_1} m_2^{n_2} \rangle = \frac{\partial^{n_1}}{\partial \theta_1^{n_1}} \frac{\partial^{n_2}}{\partial \theta_2^{n_2}} G(\theta_1, \theta_2) \Big|_{\theta_1=\theta_2=0} \quad (61)$$

similarly to the case of a single variable. The cumulants for $P(m_1, m_2)$ are similarly defined with the cumulant generating function $K(\theta_1, \theta_2) = \ln G(\theta_1, \theta_2)$ as

$$\langle m_1^{n_1} m_2^{n_2} \rangle_c = \frac{\partial^{n_1}}{\partial \theta_1^{n_1}} \frac{\partial^{n_2}}{\partial \theta_2^{n_2}} K(\theta_1, \theta_2) \Big|_{\theta_1=\theta_2=0}. \quad (62)$$

It is easy to extend the argument in Sec. 2.1 to relate the moments and cumulants to this case. The relation of the cumulants with moments for $n_1 = 0$ or $n_2 = 0$ is equal to the previous case. For the mixed cumulants, it is, for example, calculated to be

$$\begin{aligned} \langle m_1 m_2 \rangle_c &= \frac{\partial}{\partial \theta_1} \frac{\partial}{\partial \theta_2} \ln G(\theta_1, \theta_2) \Big|_{\theta_1=\theta_2=0} = \frac{\partial}{\partial \theta_1} \left(\frac{\partial G(\theta_1, \theta_2)}{\partial \theta_2} G(\theta_1, \theta_2)^{-1} \right) \Big|_{\theta_1=\theta_2=0} \\ &= \left(G(\theta_1, \theta_2)^{-1} \frac{\partial^2 G(\theta_1, \theta_2)}{\partial \theta_1 \partial \theta_2} - G(\theta_1, \theta_2)^{-2} \frac{\partial G(\theta_1, \theta_2)}{\partial \theta_1} \frac{\partial G(\theta_1, \theta_2)}{\partial \theta_2} \right) \Big|_{\theta_1=\theta_2=0} \\ &= \langle \delta m_1 \delta m_2 \rangle \end{aligned} \quad (63)$$

and so forth. Equation (63) shows that the mixed second-order cumulant is given by the mixed central moment, or correlation.

For a probability distribution function for k stochastic variables m_1, \dots, m_k , the generating functions are defined by

$$G(\theta_1, \dots, \theta_k) = \sum_{m_1, m_2, \dots, m_k} \left(\prod_{i=1}^k e^{\theta_i m_i} \right) P(m_1, \dots, m_k), \quad (64)$$

$$K(\theta_1, \dots, \theta_k) = \ln G(\theta_1, \dots, \theta_k). \quad (65)$$

With these generating functions, the moments and cumulants are defined similarly. From these definitions, it is obvious that the cumulants for multi-variable distribution functions are extensive variables in grand canonical ensembles.

2.8 Some advanced comments

2.8.1 Cumulant expansion

From the definition of cumulants Eq. (9), the cumulant generating function is expanded as

$$K(\theta) = \sum_{n=1}^{\infty} \frac{\theta^n}{n!} \langle m^n \rangle_c. \quad (66)$$

By substituting $\theta = 1$ in Eq. (8), one obtains

$$K(1) = \ln \langle e^m \rangle = \ln \sum_m e^m P(m) = \sum_{n=1}^{\infty} \frac{\langle m^n \rangle_c}{n!}. \quad (67)$$

Equation (67) is called the cumulant expansion, and plays effective roles in obtaining various properties of higher order cumulants; examples are found in Appendix A and Ref. [65].

A remark here is that the cumulant expansion Eq. (67) has the same structure as the linked cluster theorem in field theory [66]. In fact, if one regards the “connected part” of correlation functions as the cumulant, the theorem is completely equivalent with the cumulant expansion.

2.8.2 Factorial moments and factorial cumulants

Up to now we have discussed moments and cumulants as quantities characterizing probability distribution functions. One of other sets of such quantities is factorial moments and factorial cumulants. The factorial moments are defined as

$$\langle m^n \rangle_f = \langle m(m-1) \cdots (m-n+1) \rangle = \left. \frac{d^n}{ds^n} G_f(s) \right|_{s=1} \quad (68)$$

with the factorial moment generating function

$$G_f(s) = \sum_m s^m P(m) = G(\ln s). \quad (69)$$

The factorial cumulants are then defined by the factorial cumulant generating function,

$$K_f(s) = \ln G_f(s) = K(\ln s), \quad (70)$$

as

$$\langle m^n \rangle_{fc} = \frac{d^n}{ds^n} K_f(s). \quad (71)$$

In the discussion of physical property of fluctuations, the standard moments and cumulants tend to be more useful than the factorial moments and cumulants. For example, as we will see in the next section the cumulants of conserved charges are directly related to the partition function and have more apparent physical meanings owing to the linear response relation. For some analytic procedure and theoretical purposes, however, the factorial moments and cumulants make analyses more concise; see, for example, Refs. [67, 68, 69, 70].

To relate the moments and cumulants with factorial ones, one may use relations between the two generating functions, such as $K(\theta) = K_f(e^\theta)$ or $K_f(s) = K(\ln s)$: By taking derivatives with respect to θ or s , their relations are obtained similarly to the procedure to obtain the relations between moments and cumulants presented in Sec. 2.1.

3 Bulk fluctuations in equilibrium

In this section we consider the properties of thermal fluctuations, i.e. the fluctuations in equilibrated medium. After describing a general property of fluctuations in quantum statistical mechanics, we calculate the fluctuations in ideal gas. This simple analysis allows us to understand many interesting properties of thermal fluctuations, such as the magnitude of cumulants in the hadronic medium [23]. We also review the linear response relations, which connect cumulants of conserved charges with the

corresponding *susceptibilities*, i.e. magnitude of the response of the system against external force. The linear response relations for higher order cumulants enable us to introduce physical interpretation to the behavior of cumulants in the QCD phase diagrams [37]. Thermal fluctuations in the hadron resonance gas model and anomalous behavior of fluctuations expected to take place near the QCD critical point are also reviewed. We also give a brief review on the recent progress in the study of fluctuations in lattice QCD numerical simulations.

The anomalous behaviors of fluctuation observables in an equilibrated medium discussed in this section serves as motivations of experimental analyses of fluctuations. It, however, should be remembered that the fluctuations discussed in this section are not directly observed in relativistic heavy ion collisions, as will be discussed in detail in Secs. 4, 5 and 6.

3.1 Cumulants in quantum statistical mechanics

In this subsection, we first take a look at general properties of fluctuations, in particular, the cumulants of conserved charges, in quantum statistical mechanics.

3.1.1 Cumulants of conserved charges

We consider a system described by a Hamiltonian H in a volume V and assume that this system has an observable \hat{N} which is a conserved charge. Because \hat{N} is conserved, \hat{N} commutes with H ,

$$[H, \hat{N}] = 0. \quad (72)$$

The grand canonical ensemble of this system with temperature T and chemical potential μ for \hat{N} is characterized by the density matrix

$$\rho = \frac{1}{Z} e^{-(H - \mu \hat{N})/T}, \quad (73)$$

with the grand partition function

$$Z = \text{tr}[e^{-(H - \mu \hat{N})/T}], \quad (74)$$

where the trace is taken over all quantum states. The expectation value of an observable \hat{O} is given by

$$\langle \hat{O} \rangle = \text{tr}[\hat{O} \rho]. \quad (75)$$

As in the previous section, one can define the moments and cumulants of \hat{O} in quantum statistical mechanics. The moments $\langle \hat{O}^n \rangle$ are simply given by the expectation values of powers of \hat{O} . The cumulants are then defined from the moments and the relations such as Eqs. (10) - (13), which relate moments and cumulants.

We note that the moments and cumulants defined in this way are interpreted as those for the distribution of the particle number in a volume V . To be more specific, imagine that you were able to count the particle number in V in the equilibrated medium exactly at some time. The obtained particle numbers then would fluctuate measurement by measurement around the average. The moments and cumulants are those of this fluctuation.

The cumulants of the conserved charge \hat{N} in quantum statistical mechanics are given by derivatives of the grand potential $\Omega = -T \ln Z$ with respect to μ/T . The first-order cumulant, i.e. the expectation value, $\langle N \rangle$ is given by

$$\frac{\partial(-\Omega/T)}{\partial(\mu/T)} = \frac{1}{Z} \text{tr}[\hat{N} e^{-(H - \mu \hat{N})/T}] = \langle N \rangle. \quad (76)$$

The second derivative gives the second-order cumulant as

$$\begin{aligned} \frac{\partial^2(-\Omega/T)}{\partial(\mu/T)^2} &= \frac{\partial}{\partial(\mu/T)} \left(\frac{1}{Z} \text{tr}[\hat{N} e^{-(H-\mu\hat{N})/T}] \right) = \frac{1}{Z} \text{tr}[\hat{N}^2 e^{-(H-\mu\hat{N})/T}] - \left(\frac{1}{Z} \text{tr}[\hat{N} e^{-(H-\mu\hat{N})/T}] \right)^2, \\ &= \langle \delta \hat{N}^2 \rangle = \langle \hat{N}^2 \rangle_c \end{aligned} \quad (77)$$

with $\delta \hat{N} = \hat{N} - \langle \hat{N} \rangle$. Similar manipulations lead to

$$\langle \hat{N}^n \rangle_c = \frac{\partial^n(-\Omega/T)}{\partial(\mu/T)^n}. \quad (78)$$

To show this relation, one may use the fact that Z is the moment generating function Eq. (5) up to normalization constant,

$$\langle N^n \rangle = \frac{1}{Z} \text{tr}[N^n e^{-(H-\mu\hat{N})/T}] = \frac{1}{Z} \frac{\partial^n Z}{\partial(\mu/T)^n}. \quad (79)$$

The normalization of Eq. (5) affects the definition of the cumulant generating function in Eq. (8) only by a constant. Since the constant does not alter derivatives, derivatives of the logarithm of Z give the cumulants.

As already discussed in Sec. 2.3, the cumulants of \hat{N} are extensive variables. This property can easily be shown using the fact that the grand potential is an extensive variable, and thus can be written using the grand potential per unit volume, ω , as

$$\Omega = \omega V. \quad (80)$$

The cumulants are thus given by

$$\langle \hat{N}^n \rangle_c = \frac{\partial^n(-\omega/T)V}{\partial(\mu/T)^n} \equiv \chi_n V, \quad (81)$$

where on the far right-hand side we introduced the cumulant per unit volume,

$$\chi_n = \frac{\partial^n(-\omega/T)}{\partial(\mu/T)^n}. \quad (82)$$

The quantities χ_n defined here is called susceptibilities, as the reason will be explained in Sec. 3.1.3.

The extensive property of cumulants Eq. (81) gives a constraint on the correlation function of particle number density. The particle number \hat{N} in a volume V is related to the particle density $n(\mathbf{x})$ as

$$\hat{N} = \int_V d\mathbf{x} n(\mathbf{x}). \quad (83)$$

The extensive property Eq. (81) then implies that

$$\langle n(\mathbf{x}_1)n(\mathbf{x}_2) \cdots n(\mathbf{x}_i) \rangle_c = \chi_i \delta(\mathbf{x}_1 - \mathbf{x}_2) \delta(\mathbf{x}_2 - \mathbf{x}_3) \cdots \delta(\mathbf{x}_{i-1} - \mathbf{x}_i), \quad (84)$$

because this is the only choice that is consistent with Eq. (81) for any choice of volume V . Equation (84) shows that the particle densities at different positions in coordinate space have no correlations. This result is consistent with Eq. (80) and the discussion in Sec. 2.3. For the validity of Eq. (80), the volume V has to be large enough. When the volume is not large enough so that the microscopic correlation length is not negligible, Eq. (80) is no longer valid. In such a case, Eqs. (81) or (84) is not satisfied, either.

3.1.2 Cumulants of non-conserved quantities

Here, it is worth emphasizing that the above discussion is applicable only for conserved charges, because it makes full use of the commutation relation Eq. (72). To see this, let us consider the cumulants of a non-conserved quantity \hat{N}' , which does not commute with H . Even for this case, one can define a *would-be* grand partition function,

$$Z' = \text{tr}[e^{-(H-\mu'\hat{N}')/T}], \quad (85)$$

where μ' would be interpreted as something like the chemical potential for \hat{N}' . With this definition, however, Eq. (85) is *not* the moment generating function of \hat{N}' . In fact, derivatives of Z' with respect to μ'/T are calculated to be

$$\frac{\partial}{\partial(\mu'/T)} Z' = \text{tr}[\hat{N}' e^{-(H-\mu'\hat{N}')/T}] = Z' \langle \hat{N}' \rangle, \quad (86)$$

$$\frac{\partial^2}{\partial(\mu'/T)^2} Z' = \int_0^{1/T} d\tau \text{tr}[\hat{N}' e^{-(H-\mu'\hat{N}')\tau} \hat{N}' e^{-(H-\mu'\hat{N}')(1/T-\tau)}] \neq Z' \langle \hat{N}'^2 \rangle, \quad (87)$$

where in Eqs. (86) and (87) we used the cyclic property of trace and a relation

$$\frac{d}{dt} e^{M(t)} = \int_0^1 ds e^{sM} \frac{dM}{dt} e^{(1-s)M} \quad (88)$$

for a linear operator M . Equation (87) shows that the second derivative of Z' does not give the second moment. Similarly, higher derivatives of Z' do not give the moments $\langle \hat{N}'^n \rangle_c$. As shown in Eq. (86) only the first derivative still gives the expectation value $\langle \hat{N}' \rangle$. Because Z' is no longer proportional to the moment generating function, $\Omega' = -T \ln Z'$ is not the cumulant generating function any more, either.

Because the cumulants of conserved charges are determined from the partition function or the grand potential by taking derivatives, the cumulants of the conserved charge are defined unambiguously once the grand potential is given in a theory. This, however, is not true for non-conserved quantities.

When the construction of grand potential is difficult, one may use an alternative way to define the cumulants. When the operator \hat{O} for an observable is explicitly known in a theory, in principle one can calculate the moments of \hat{O} by calculating the expectation value $\langle \hat{O}^n \rangle$. The cumulants are then also determined using the relations in Sec. 2.1. This method is applicable to both conserved and non-conserved quantities. To use this method, however, one has to have the explicit form of the operator, as well as their powers, in the theory. The conserved charges are related to the symmetry of the theory via Noether's theorem and their operators can be usually defined as the Noether currents. For non-conserved quantities, however, the corresponding operator is sometimes unclear. For example, the operator for the “total pion number” in QCD is not known. This problem makes the concept of cumulants of non-conserved quantities ambiguous. In lattice QCD Monte Carlo simulations, for example, one can calculate the cumulants of net-electric charge, which is a conserved charge in QCD, while the cumulants of total pion number, which is not conserved in QCD, cannot be determined. It is also worthwhile to note that the powers of an operator, \hat{O}^n , can be nontrivial in field theory because of ultraviolet divergence, even when the operator \hat{O} is known. In this case an appropriate regularization is required to define them. In this sense, the definition of the cumulant using the grand potential Eq. (78) is convenient because it only requires the grand potential. Analyses of the cumulants of conserved charges in Lattice QCD, for example, make use of this definition [34].

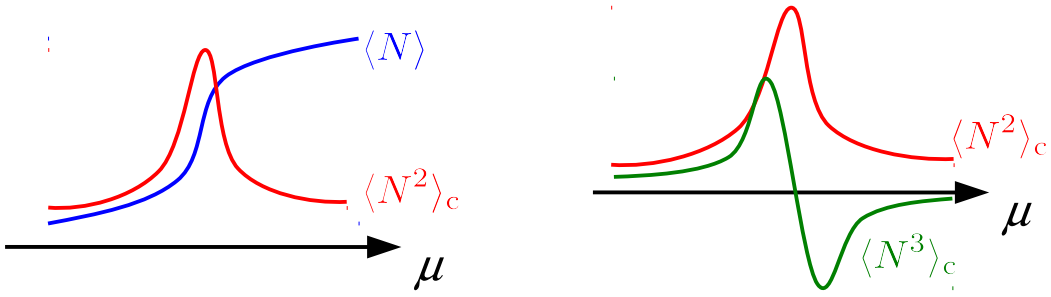


Figure 4: Dependences of various cumulants on μ .

3.1.3 Linear response relation

An important property of the cumulants of conserved charges in thermal medium is the linear response relation. From Eq. (78) one obtains

$$\chi_2 = \frac{\langle \hat{N}^2 \rangle_c}{V} = \frac{\partial}{\partial(\mu/T)} \frac{\langle \hat{N} \rangle}{V}. \quad (89)$$

The right-hand side of Eq. (89) represents the magnitude of the variation of density $\langle \hat{N} \rangle/V$ induced by the change of the corresponding external force, μ . In this sense, χ_2 is called susceptibility. The relation Eq. (89) shows that the susceptibility is *equivalent* to the fluctuation of \hat{N} per unit volume. One can generally derive similar relations between a susceptibility and fluctuation of conserved charges, which are referred to as the linear response relations.

The linear response relation allows us to obtain a geometrical interpretation for the behavior of the second order cumulant. Suppose that we know $\langle \hat{N} \rangle$ as a function of μ for a given T . Then, Eq. (89) tells us that $\langle \hat{N}^2 \rangle_c$ is enhanced for μ at which $\langle \hat{N} \rangle$ has a steep rise; see the left panel of Fig. 4. On the other hand, if $\langle \hat{N}^2 \rangle_c$ has a peak structure at some μ , it means that $\langle \hat{N} \rangle$ has a steep rise around this μ . As we will see in Sec. 3.3.3, this simple argument is quite useful in interpreting the behavior of fluctuations near the QCD critical point.

The linear response relation can be extended to higher order cumulants. From Eq. (78) one also obtains the relations for higher orders,

$$\chi_{n+1} = \frac{\langle \hat{N}^{n+1} \rangle_c}{V} = \frac{\partial}{\partial(\mu/T)} \frac{\langle \hat{N}^n \rangle_c}{V} = \frac{\partial \chi_n}{\partial(\mu/T)}. \quad (90)$$

This relation shows that the $(n+1)$ -th order cumulant plays a role of the susceptibility of n -th order one. In this sense it is reasonable to call Eq. (82) as (generalized) susceptibility. Moreover, because the behavior of the $(n+1)$ -th order cumulant is proportional to the μ derivative of the n -th order one, similarly to the second-order case this relation introduces an geometric interpretation for the behaviors of the higher order cumulants. For example, as shown in the right panel in Fig. 4, when the second-order cumulant $\langle \hat{N}^2 \rangle_c$ has a peak structure as a function of μ the third-order one $\langle \hat{N}^3 \rangle_c$ changes the sign there [37]. Note that $\langle \hat{N}^2 \rangle_c$ is positive definite but the cumulants higher than second-order can take positive and negative values. Because of the positivity of $\langle \hat{N}^2 \rangle_c$, $\langle \hat{N} \rangle$ as a function of μ is concluded to be a monotonically-increasing function, but the second and higher order cumulants are not.

We finally note that the relation like Eq. (89) is not valid for non-conserved quantities, because μ' derivatives in Eq. (87) do not give the moment.

3.1.4 Cumulants of energy

Similarly to conserved charges, it is possible to relate the cumulants of energy, which is also a conserved charge, with the partition function Z [37]. To obtain the relations, one takes $1/T$ derivative of Z with μ/T fixed. This can be done by introducing two independent variables

$$\beta = 1/T, \quad \alpha = \mu/T, \quad (91)$$

and take β derivative of Z . Because β derivative is given by

$$\frac{\partial}{\partial \beta} = \frac{\partial(1/T)}{\partial \beta} \frac{\partial}{\partial(1/T)} + \frac{\partial \mu}{\partial \beta} \frac{\partial}{\partial \mu} = \frac{\partial}{\partial(1/T)} - T\mu \frac{\partial}{\partial \mu}, \quad (92)$$

the derivative is calculated to be

$$\begin{aligned} \left. \frac{\partial Z}{\partial(-1/T)} \right|_{\mu/T} &= -\frac{\partial}{\partial \beta} Z = \left(-\frac{\partial}{\partial(1/T)} + T\mu \frac{\partial}{\partial \mu} \right) Z = \text{tr}[H e^{-(H-\mu\hat{N})/T}] \\ &= Z\langle H \rangle. \end{aligned} \quad (93)$$

Similarly, one can show $\frac{\partial^n Z}{\partial(-\beta)^n} = Z\langle H^n \rangle$. The cumulants of energy are then obtained as

$$\langle H^n \rangle_c = \left. \frac{\partial^n \ln Z}{\partial(-1/T)^n} \right|_{\mu/T} = \left(-\frac{\partial}{\partial(1/T)} + T\mu \frac{\partial}{\partial \mu} \right)^n \frac{-\Omega}{T}. \quad (94)$$

It is also possible to construct the mixed cumulants between energy and the conserved charge as

$$\langle \hat{N}^{n_1} H^{n_2} \rangle_c = \frac{\partial^{n_1}}{\partial(\mu/T)^{n_1}} \langle H^{n_2} \rangle_c. \quad (95)$$

The linear response relation for this case is given by

$$\left. \frac{\partial \langle H \rangle}{\partial T} \right|_{\mu/T} = \frac{\langle H^2 \rangle_c}{T^2}. \quad (96)$$

The left-hand side of this equation is the increase of the energy per unit T , i.e. the specific heat with fixed μ/T . Equation (96) thus shows that the fluctuation of energy divided by the square of the temperature is equal to specific heat.

3.2 Ideal gas

Next, let us consider the cumulants of a conserved charge in ideal gas. We start from ideal gas composed of a single species of particles. Because the particles do not interact with each other, the particle number N is automatically a conserved charge. The grand potential of the ideal gas per unit volume ω is given by [71].

$$-\frac{\omega}{T} = g \int \frac{d^3 p}{(2\pi)^3} \ln(1 \mp e^{-(E(p)-\mu)/T})^{\mp 1}, \quad (97)$$

where g represents the degeneracy such as spin degrees of freedom. The minus and plus signs on the right-hand side corresponds to bosons and fermions, respectively. $E(p)$ is the energy dispersion of the particle; for non-relativistic and relativistic cases with mass m , $E(p) = p^2/2m$ and $E(p) = \sqrt{m^2 + p^2}$, respectively.

Cumulants of N per unit volume is given by taking μ derivatives of Eq. (97). For example, the first-order cumulant gives the density ρ as

$$\rho = \frac{\langle N \rangle}{V} = \frac{\partial(-\omega/T)}{\partial(\mu/T)} = g \int \frac{d^3p}{(2\pi)^3} \frac{1}{e^{(E(p)-\mu)/T} \mp 1}, \quad (98)$$

which is the well-known Bose-Einstein and Fermi-Dirac distribution functions. The second-order cumulant is similarly calculated as

$$\chi_2 = \frac{\langle N^2 \rangle_c}{V} = \frac{\partial^2(-\omega/T)}{\partial(\mu/T)^2} = g \int \frac{d^3p}{(2\pi)^3} \frac{e^{(E(p)-\mu)/T}}{(e^{(E(p)-\mu)/T} \mp 1)^2}. \quad (99)$$

Next, let us consider the dilute limit $\rho/T^3 \ll 1$. From Eq. (98), this limit is realized when $e^{(E(p)-\mu)/T} \gg 1$, or equivalently

$$E(p) - \mu \gg T, \quad (100)$$

for all p . In this case, the integrand in Eq. (97) is approximated as $\ln(1 \mp e^{-(E(p)-\mu)/T}) \mp 1 \simeq e^{-(E(p)-\mu)/T}$ and Eq. (97) reduces to the grand potential of the free classical (Boltzmann) gas,

$$-\frac{\omega}{T} = g \int \frac{d^3p}{(2\pi)^3} e^{-(E(p)-\mu)/T} = g e^{\mu/T} \int \frac{d^3p}{(2\pi)^3} e^{-E(p)/T}. \quad (101)$$

For the relativistic case with $E(p) = \sqrt{m^2 + p^2}$, Eq. (100) is satisfied for $m - \mu \gg T$. In this case, the integral in Eq. (101) is rewritten using the modified Bessel function of the second kind $K_n(x)$ [72] as

$$\omega = -g \frac{m^2 T^2}{2\pi^2} e^{\mu/T} K_2\left(\frac{m}{T}\right). \quad (102)$$

With Eq. (101), higher order susceptibilities are easily calculated to be

$$\frac{\langle N^n \rangle_c}{V} = \frac{\partial^n(-\omega/T)}{\partial(\mu/T)^n} = -\frac{\omega}{T}, \quad (103)$$

for all $n \geq 1$. This result shows that all cumulants are identical. From this result and the discussion in Sec. 2.4.2, the distribution of the particle number for the free Boltzmann gas is given by the Poisson distribution. An intuitive explanation of this result is given in Sec. 2.4.2.

In relativistic quantum field theory, all charged particles are always accompanied by their antiparticles carrying the opposite charge. For a particle with chemical potential μ , the chemical potential of its antiparticle is $-\mu$. The grand potential is thus given by

$$-\frac{\omega}{T} = g \int \frac{d^3p}{(2\pi)^3} \left[\ln(1 \mp e^{-(E(p)-\mu)/T}) \mp 1 + \ln(1 \mp e^{-(E(p)+\mu)/T}) \mp 1 \right]. \quad (104)$$

For massless particles with $E(p) = p$, the integral in Eq. (104) can be carried out analytically. For fermions, the result is

$$\omega = -g \left(\frac{7\pi^2}{360} T^4 + \frac{1}{12} T^2 \mu^2 + \frac{1}{24\pi^2} \mu^4 \right). \quad (105)$$

3.2.1 Particles with non-unit charge

Next, we consider an ideal gas in which the charge carried by the particles is not unity in some unit. Such a case is realized, for example, when two particles each of which carry a unit charge form a molecule. If all particles are confined into molecules and the residual interaction between the molecules is weak enough, the system can be regarded as free gas of doubly charged particles.

Let us consider free gas of particles with charge r that is a rational number. Because of the definition of chemical potential, the chemical potential of the particle is $r\mu$. If the system is dilute enough so that it can be regarded as free Boltzmann gas, the grand potential is given by

$$-\frac{\omega}{T} = g \int \frac{d^3p}{(2\pi)^3} e^{-(E(p)-r\mu)/T} = g e^{r\mu/T} \int \frac{d^3p}{(2\pi)^3} e^{-E(p)/T}. \quad (106)$$

The expectation value of the total charge Q is obtained by μ/T derivative of Eq. (106) as

$$\frac{\langle Q \rangle}{V} = \frac{\partial(-\omega/T)}{\partial(\mu/T)} = r g e^{r\mu/T} \int \frac{d^3p}{(2\pi)^3} e^{-E(p)/T} = r\rho \quad (107)$$

with $\rho = \langle N \rangle / V$ being the particle density. Similarly, the cumulants of the total charge Q are obtained by taking μ/T derivatives of Eq. (106) as

$$\frac{\langle Q^n \rangle_c}{V} = \frac{\partial^n(-\omega/T)}{\partial(\mu/T)^n} = r^n \rho. \quad (108)$$

We thus obtain the relation between cumulants

$$\frac{\langle Q^{n_1} \rangle_c}{\langle Q^{n_2} \rangle_c} = r^{n_1 - n_2}. \quad (109)$$

This result shows that the magnitude of cumulants is drastically changed when the charge carried by the effective degrees of freedom in the system changes. This property of cumulants leads to possibility to diagnose the quasi-particle property of the system with cumulants.

In relativistic heavy ion collisions, the use of this property of cumulants as diagnostic tools for the deconfinement transition, at which quarks carrying fractional charges are liberated, was first suggested in Refs. [21, 22] for the second order cumulant. The idea is then extended to higher order ones in Ref. [23]. We will discuss these studies in more detail later.

3.2.2 Mixture of differently charged particles and net particle number

Next, let us consider the ideal classical gas composed of several particle species with different charges. To be specific, we consider a system composed of particles with charges r_1, r_2, \dots, r_n . Using the chemical potential μ of the charge, the grand potential per unit volume is given by

$$-\frac{\omega}{T} = \sum_i g_i \int \frac{d^3p}{(2\pi)^3} e^{-(E(p)-r_i\mu)/T}. \quad (110)$$

By taking μ/T derivatives of Eq. (110), cumulants of the charge, Q , are obtained as

$$\langle Q^n \rangle_c = \sum_i r_i^n \rho_i, \quad (111)$$

with $\rho_i = \langle N_i \rangle / V$ being the density of particles labeled by i . Note that uncharged particles do not contribute to $\langle Q^n \rangle_c$.

In QCD, conserved charges are given by the net-particle number, i.e. the difference between particle and antiparticle numbers. From Eq. (111), the cumulants of the net-particle number Q are given by

$$\langle Q^n \rangle_c = \langle N \rangle + (-1)^n \langle \bar{N} \rangle, \quad (112)$$

where $\langle N \rangle$ and $\langle \bar{N} \rangle$ are the numbers of particles and antiparticles, respectively. This result shows that the distribution of the net-particle number is given by the Skellam one.

3.2.3 Shot noise

At this point, it is worthwhile to comment on an example of fluctuations in completely different physical systems. We consider the shot noise, i.e. the fluctuation of electric currents in electric circuits with a potential barrier. It is known that the magnitude of the shot noise is proportional to the charge of the elementary excitation of the system. As we show in this subsection, this property comes from the Poissonian nature of the electric current, and shares the same mathematics as we have discussed above.

The shot noise is the fluctuation of the electric current at a potential barrier that an electron can pass through with a small probability per unit time. (In the original study of Schottky, fluctuation in a vacuum tube was investigated [48].) In typical experiments, correlation between electrons is well suppressed so that the probability of electrons to pass through the potential barrier can be regarded as independent with one another. Then, the number of electrons which pass through the barrier in some time interval is given by the Poisson distribution to a good approximation. The time evolution of the number of electrons which go through the barrier is well described by the Poisson *process* [73]. In typical experiments, the magnitude of the fluctuation of electric current is measured from the power spectrum in frequency space assuming white noise. Here, however, for simplicity we focus on the amount of the charge in a time interval and do not consider time evolution.

Because the number of electrons N which pass through the potential barrier in a time interval Δt is given by the Poisson distribution, the cumulants of N satisfy $\langle N^n \rangle_c = \langle N \rangle$ for $n \geq 1$. The amount of charge Q which passes through the barrier in Δt is related to N as $Q = eN$ with the charge of the electron, e . The second-order cumulant of Q is then given by

$$\frac{\langle Q^2 \rangle_c}{\langle Q \rangle} = \frac{e^2 \langle N^2 \rangle_c}{e \langle N \rangle} = e, \quad (113)$$

where in the second equality we have used the Poissonian nature of N . Equation (113) suggests that the ratio $\langle Q^2 \rangle_c / \langle Q \rangle$ can be used to measure the charge of the electron [48].

In superconducting materials, electrons are “confined” into Cooper pairs, which are doubly charged, when the material undergoes the phase transition to superconductor. The charge e in Eq. (113) then should be replaced with the one of the Cooper pairs, $2e$, and the ratio $\langle Q^2 \rangle_c / \langle Q \rangle$ should become twice larger than that in the normal material. In fact, such a behavior is observed experimentally [49]. The shot noise is also successfully applied to investigate the fractional quantum Hall effect, in which the shot noise behaves as if the elementary charge became fractional [50]. While the shot noise is usually measured up to the second-order, in some systems higher order cumulants are observed [51].

Finally, we remark that the physics considered here is completely different from thermal fluctuations; the former is the fluctuations associated with nonequilibrium diffusion processes, while the latter is the fluctuations in equilibrated media. Nevertheless, there is a common feature, proportionality between the fluctuation and the elementary charge, owing to the common underlying mathematics.

3.3 Fluctuations in QCD

Now we turn to the thermal fluctuations in QCD. After a review on fluctuations in the hadron resonance gas model, which well describes thermodynamics of QCD at low temperature and density, we consider

the behaviors of fluctuations in the deconfined medium and near the QCD critical point. Recently, the cumulants of conserved charges have been actively studied in lattice QCD numerical simulations [23, 74, 75, 76, 77, 78, 79, 80, 81, 82, 83, 84, 85, 86, 87, 88, 89, 90, 91]; see for reviews Refs. [34, 35]. The established knowledge in this field is also summarized in the following.

3.3.1 Hadron resonance gas (HRG) model

We first consider the medium at low temperature and density. It is well known that the medium at low T and chemical potentials is well described by hadronic degrees of freedom. When the condition Eq. (100) is well satisfied for all hadrons and the interactions between hadrons can be neglected, the contributions of individual hadrons on thermodynamics can be regarded as those in free Boltzmann gas. In this case, the grand potential is given by

$$-\frac{\omega_{\text{HRG}}}{T} = \sum_i g_i \int \frac{d^3p}{(2\pi)^3} e^{-(E(p)-q_B^{(i)}\mu_B - q_Q^{(i)}\mu_Q - q_S^{(i)}\mu_S)/T}, \quad (114)$$

where i runs over all species of hadrons. Here, we have introduced three chemical potentials, μ_B , μ_Q and μ_S , which are baryon, electric charge and strange chemical potentials, respectively. g_i is the degeneracy of the hadron labeled by i , and $q_c^{(i)}$ with $c = B, Q$ and S represents the baryon, electric charge and strange numbers carried by the hadron i , respectively. The grand potential Eq. (114) containing all known hadrons [92] as free particles is called the hadron resonance gas (HRG) model [12]. From the chemical freezeout temperature and chemical potential determined in relativistic heavy ion collisions [93], it is known that the condition Eq. (100) is well satisfied for the hot medium after chemical freezeout for all hadrons except for pions with the mass $m_\pi \simeq 140$ MeV. It is known that the HRG model well reproduces the thermodynamic quantities calculated on the lattice QCD below the pseudo-critical temperature $T \lesssim T_c \simeq 150$ MeV for vanishing chemical potentials [34]. Although the HRG model contains only free particles, there is an argument that by incorporating resonance states the effects of interaction between hadrons is effectively taken into account [94, 95].

Now let us calculate the cumulants of conserved charges, net-baryon, net-electric charge and net-strange numbers in the HRG model based on Eq. (114). We first consider the net-baryon number cumulants, which are obtained by taking μ_B derivatives of Eq. (114). The baryon number carried by baryons and anti-baryons are $q_B^{(i)} = +1$ and $q_B^{(i)} = -1$, respectively, while the mesonic degrees of freedom do not carry the baryon number and do not contribute to the fluctuation of net-baryon number in the HRG model. The net-baryon number cumulants thus are calculated to be

$$\begin{aligned} \langle N_{\text{B,net}}^n \rangle_c &= \frac{\partial^n (-\omega_{\text{HRG}}/T)}{\partial (\mu_B/T)^n} = -\frac{\omega_B}{T} - (-1)^n \frac{\omega_{\bar{B}}}{T} \\ &= \langle N_B \rangle + (-1)^n \langle N_{\bar{B}} \rangle, \end{aligned} \quad (115)$$

where ω_B and $\omega_{\bar{B}}$ denote the contributions of all baryons and anti-baryons to the grand potential ω_{HRG} , respectively, and N_B and $N_{\bar{B}}$ are the baryon and anti-baryon numbers, respectively. The result Eq. (115) shows that the fluctuation of the net-baryon number in the HRG model is given by the Skellam distribution and the ratios of cumulants between even or odd orders are unity [23],

$$\frac{\langle N_{\text{B,net}}^{n+2m} \rangle_c}{\langle N_{\text{B,net}}^n \rangle_c} = 1, \quad (116)$$

for integer n and m .

Next, we consider the net-electric charge. Contrary to the net-baryon number, there are hadronic resonances having $q_Q^{(i)} = \pm 2$, such as $\Delta^{++}(1232)$, in addition to $q_Q^{(i)} = 0$ and ± 1 states. Due to these

resonances, the fluctuation of net-electric charge is not given by the Skellam distribution. The cumulants of net-electric charge is given by

$$\langle N_{Q,\text{net}}^n \rangle_c = \langle N_{q_Q=1} \rangle + (-1)^n \langle N_{q_Q=-1} \rangle + 2^{n-1} \{ \langle N_{q_Q=2} \rangle + (-1)^n \langle N_{q_Q=-2} \rangle \}, \quad (117)$$

with $\langle N_{q_Q=m} \rangle$ being the density of hadrons having the electric charge $q_Q = m$. Owing to the $q_Q = \pm 2$ states, higher order cumulants tend to become larger than the Skellam one. The same argument applies to the net-strange number, while the contribution of $q_S = \pm 2$ states is a little more suppressed because of their heavy masses; the lightest of such baryons is Ξ^0 and $\bar{\Xi}^0$ with the mass 1315 MeV. For net-electric charge fluctuations, Bose-Einstein statistics of pions also gives rise to deviations from the Skellam distribution, while the effect of Fermi-Dirac statistics of baryons on Eq. (116) is well suppressed in the hadronic medium relevant to relativistic heavy ion collisions.

Next we consider the mixed cumulants in the HRG model. As an example, the correlation of net-baryon and net-strange numbers is given by

$$\langle N_{B,\text{net}} N_{S,\text{net}} \rangle_c = \frac{\partial^2 (\omega_{\text{HRG}}/T)}{\partial (\mu_B/T) \partial (\mu_S/T)} = \sum_i q_B^{(i)} q_S^{(i)} \langle N_i \rangle. \quad (118)$$

Equation (118) shows that the contributions to $\langle N_{B,\text{net}} N_{S,\text{net}} \rangle_c$ come from hadrons with $q_B^{(i)} \neq 0$ and $q_S^{(i)} \neq 0$. The lightest hadron having nonzero q_B and q_S is $\Lambda(1115)$ and $\bar{\Lambda}(1115)$ with the mass $m_\Lambda = 1115$ MeV. Because the mass of the nucleon and the mass of the lightest strange meson, K^\pm , are smaller than m_Λ , the density of Λ is suppressed compared with hadrons having only either $q_B^{(i)} \neq 0$ or $q_S^{(i)} \neq 0$. Therefore, the magnitude of $\langle N_{B,\text{net}} N_{S,\text{net}} \rangle_c$ should be suppressed

$$\langle N_{B,\text{net}} N_{S,\text{net}} \rangle_c \ll \langle N_{B,\text{net}} \rangle \langle N_{S,\text{net}} \rangle_c, \quad (119)$$

in the HRG model with small μ_B and μ_S [96]. Various mixed cumulants in the HRG model can be understood in a similar manner.

If the fluctuation observables in relativistic heavy ion collisions are well described by the hadronic degrees of freedom in equilibrium, the cumulants of conserved charges should be consistent with those in the HRG model. Conversely, if the fluctuations show deviation from those in the HRG model, they serve as experimental signals of non-hadronic and/or non-thermal physics. In this sense, the cumulants in the HRG model are usually compared with the experimental results as the ‘‘baseline’’ [97]. In particular, because the ratios between cumulants take a simple form in the HRG model, they are useful observables to investigate these nontrivial physics. In Fig. 2, the ratio of net-proton number cumulants, $\kappa\sigma^2 = \langle N_{p,\text{net}}^4 \rangle_c / \langle N_{p,\text{net}}^2 \rangle_c$ and $S\sigma / (\text{Skellam}) = \langle N_{p,\text{net}}^3 \rangle_c / \langle N_{p,\text{net}} \rangle$ are plotted¹. The figure shows that the ratios of the cumulants show statistically-significant deviations from the HRG baseline. This experimental result clearly shows that the ratio carries information on physics which cannot be described by the HRG model, such as the onset of the deconfined phase, existence of QCD critical point, or some non-equilibrium phenomena.

3.3.2 Onset of deconfinement transition

Next, we focus on the deconfined medium. At extremely high temperature, the quarks can be regarded as approximately free particles owing to asymptotic freedom. The cumulants of conserved charges thus

¹In QCD, net-proton number is not a conserved charge, and the definition of its cumulants is ambiguous. In the HRG model, on the other hand, the net-proton number is a conserved charge because protons and anti-protons in the HRG model are free particles, and its cumulants are well defined. For the same reason as for net-baryon number, this model gives $\langle N_{p,\text{net}}^4 \rangle_c / \langle N_{p,\text{net}}^2 \rangle_c = \langle N_{p,\text{net}}^3 \rangle_c / \langle N_{p,\text{net}} \rangle = 1$. However, they, of course, are not the net-baryon number in QCD [98, 99]. Problems with the use of net-proton number as a proxy of net-baryon number will be discussed in Secs. 4 and 6.

are given by those of ideal quark gas in this case. If Fermi-Dirac statistics were negligible there, the cumulants of net-quark number would become the Skellam ones,

$$\langle N_{q,\text{net}}^n \rangle_c = \langle N_q \rangle + (-1)^n \langle N_{\bar{q}} \rangle, \quad (120)$$

with N_q ($N_{\bar{q}}$) being the quark (anti-quark) number. By recalling that all quarks and anti-quarks carry $\pm 1/3$ baryon number, Eq. (120) is converted to net-baryon number cumulant as

$$\langle N_{B,\text{net}}^n \rangle_c = \frac{1}{3^n} [\langle N_q \rangle + (-1)^n \langle N_{\bar{q}} \rangle], \quad (121)$$

where we have used $N_{q,\text{net}} = 3N_{B,\text{net}}$. From this result, the ratio of the net-baryon number is given by

$$\frac{\langle N_{B,\text{net}}^{n+2} \rangle_c}{\langle N_{B,\text{net}}^n \rangle_c} = \frac{1}{9}, \quad (122)$$

i.e. compared with Eq. (116) the ratio is about one order suppressed when the deconfined medium is realized [23]. This change of the ratio is reminiscent of the shot noise in the fractional quantum Hall effect discussed in Sec. 3.2.3.

The above argument, however, is modified by the Fermi-Dirac statistics of quarks, because the masses of quark quasi-particles m_q would not satisfy $m_q/T \gg 1$ in the deconfined phase. For massless quarks, the net-quark number cumulants can be calculated with Eq. (105). By taking μ/T derivatives of Eq. (105), we have

$$\frac{\langle N_{q,\text{net}}^3 \rangle_c}{\langle N_{q,\text{net}} \rangle_c} = \frac{6}{\pi^2} \left(1 + \frac{1}{\pi^2} \frac{\mu^2}{T^2} \right)^{-1}, \quad \frac{\langle N_{q,\text{net}}^4 \rangle_c}{\langle N_{q,\text{net}}^2 \rangle_c} = \frac{6}{\pi^2} \left(1 + \frac{3}{\pi^2} \frac{\mu^2}{T^2} \right)^{-1}, \quad (123)$$

while all cumulants $\langle N_{q,\text{net}}^n \rangle_c$ for $n \geq 5$ vanish. This result shows that for massless quarks the ratios of cumulants are suppressed compared with the Skellam value, Eq. (122). The inclusion of Fermi-Dirac statistics thus does not alter the suppression of higher order cumulants in the deconfined medium.

The electric charge q_f carried by quarks are $\pm 1/3$ and $\pm 2/3$ depending on the flavor f . Assuming the Boltzmann statistics we have

$$\langle N_{Q,\text{net}}^n \rangle_c = \sum_f q_f^2 (\langle N_f \rangle + (-1)^n \langle N_{\bar{f}} \rangle). \quad (124)$$

Because of quarks with $q_f = \pm 2/3$, especially up quarks, the suppression of higher order cumulants compared with the HRG values is much milder compared with the net-baryon number in Eq. (121). The baryon number cumulants thus are better observable to see the deconfinement phase transition.

The ratios of cumulants have been actively analyzed in lattice QCD numerical simulations. In Fig. 5 we show an example of the recent analysis on the ratio of net-baryon number cumulants $\langle N_{B,\text{net}}^4 \rangle_c / \langle N_{B,\text{net}}^2 \rangle_c$ [83]. The figure shows that the ratio is consistent with the HRG value Eq. (116) below the pseudo-critical temperature $T_c \simeq 150 - 160$ MeV, while the ratio suddenly drops above T_c and approaches the free Fermi gas value at high T .

Recently, more sophisticated ways to investigate the medium properties near T_c using the higher order and mixed cumulants have been studied in the lattice community. In Ref. [81], various (mixed) cumulants are investigated in combinations which vanish in the HRG model. For example, from Eq. (116) one finds that $\langle N_{B,\text{net}}^4 \rangle_c - \langle N_{B,\text{net}}^2 \rangle_c = 0$ in the HRG model. Similar combinations are found also by considering mixed cumulants such as Eq. (118). In Fig. 6, three combinations of net-baryon and net-strange number cumulants which vanish in the HRG model obtained on the lattice are plotted [81]. The figure shows that these combinations are indeed consistent with zero for $T \lesssim T_c$, but suddenly becomes

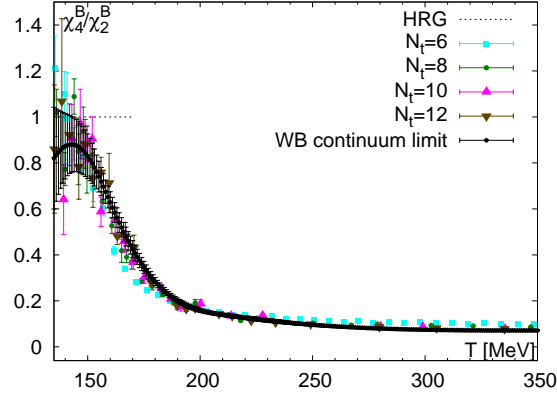


Figure 5: Ratio of the fourth- and second-order baryon number susceptibilities $\chi_4^B/\chi_2^B = \langle N_{B,\text{net}}^4 \rangle_c / \langle N_{B,\text{net}}^2 \rangle_c$ calculated on the lattice [83]. Points labeled by “WB continuum limit” are the value of χ_4^B/χ_2^B after taking the continuum (small lattice spacing) limit.

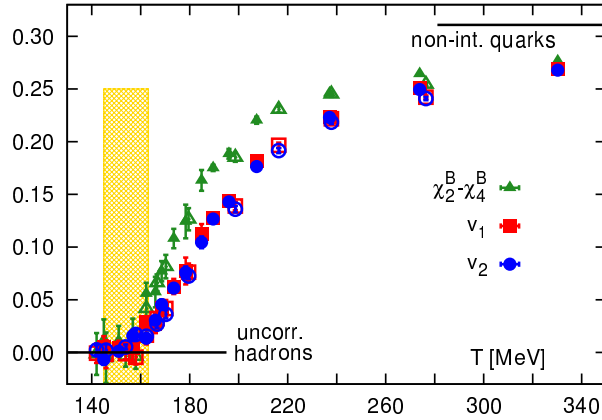


Figure 6: Combination of the net-baryon and net-strange number cumulants, $\langle N_{B,\text{net}}^4 \rangle_c - \langle N_{B,\text{net}}^2 \rangle_c$, v_1 and v_2 which are chosen so that they vanish in the HRG model [81]. The horizontal line labeled “uncorr. hadrons” indicates the values in the HRG model.

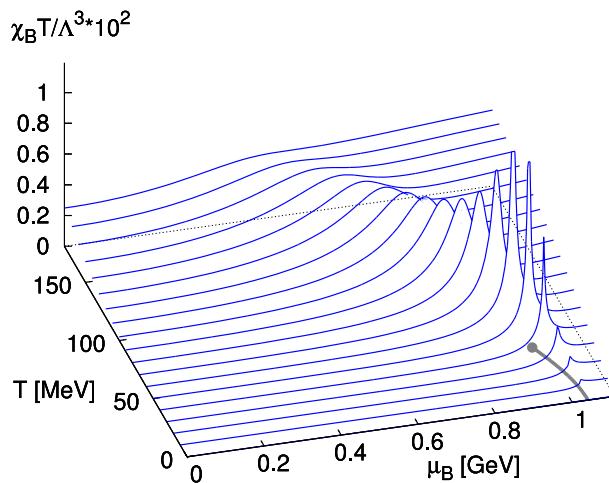


Figure 7: Plot of the baryon number susceptibility $\chi_B = \langle N_{B,\text{net}}^2 \rangle / V$ as a function of T and μ_B obtained in a chiral effective model [37].

nonzero above T_c . This result suggests that the medium is well described by the hadronic degrees of freedom up to near T_c , but the non-hadronic physics shows up around T_c . Similar ideas are applied to investigate the flavor hierarchy in the breakdown of the HRG model [81, 84, 87]. These studies suggest that fluctuations are useful observables to understand quasi-particle properties in the medium although they are static quantities.

Finally, we note that the cumulants at extremely high T and μ_B can be analyzed perturbatively [100, 101, 102]. The comparisons between these perturbative analyses with lattice results have been done [81].

3.3.3 QCD critical point

Around the boundary between the confined and deconfined phases, anomalous behaviors of fluctuation observables associated with the phase transition are expected to occur. In particular, the QCD phase diagram in the T - μ_B plane is expected to have the QCD critical point(s), which is the endpoint of the first-order phase transition line [3, 4, 5]. (An example of the phase diagram is shown in the bottom surface of Fig. 7.) Because the phase transition at this point is of second-order, various fluctuation observables diverge there. It is known that this point belongs the same universality class as in the 3d Z_2 Ising model, which is the same universality class as the critical point in the phase diagram of water belongs to, and the critical exponents are determined by the universality arguments². The anomalous behaviors associated with the critical point should become experimental observables to find this point [18, 24, 25].

An order parameter to characterize the QCD critical point is the chiral condensate $\sigma = \langle \bar{\psi}\psi \rangle$. Associated with the softening of the effective potential, the correlation length and fluctuation of the σ field diverge at the critical point. Owing to this divergence, fluctuations of fields which couple to σ also diverges. Because the net-baryon number has a coupling with the σ field [106, 107, 103, 108] with nonzero current quark mass and μ_B , the net-baryon number fluctuation diverges at the critical point. From studies on the baryon number susceptibility [109] based on chiral effective models [106, 110, 111, 112, 113, 114, 37, 115, 116], it is known that the baryon number susceptibility has a ridge structure along the crossover line [106] as illustrated in Fig. 7.

² It is known [103, 104] that the dynamical universality class of this point belongs to that of the model H in the classification of Hohenberg and Halperin [105].

Near the QCD critical point, higher order cumulants of conserved charges also behave anomalously. In Ref. [36], the higher order cumulants are calculated as a function of the correlation length of σ field up to the fourth-order. It is pointed out that the higher order cumulants are more sensitive to the correlation length. Another interesting property of higher order cumulants is that they change the sign near the critical point [37, 117, 118]. As discussed in Sec. 3.1.3, the net-baryon number cumulants are given by the μ_B derivative of the cumulant lower by one order as

$$\langle N_{B,\text{net}}^{n+1} \rangle_c = \frac{\partial \langle N_{B,\text{net}}^n \rangle_c}{\partial (\mu_B/T)}. \quad (125)$$

From this relation and the ridge structure of the baryon number susceptibility $\chi_2^B = \langle N_{B,\text{net}}^2 \rangle_c / V$ along the phase boundary as shown in Fig. 7, it is immediately concluded that $\chi_3^B = \langle N_{B,\text{net}}^3 \rangle_c / V$ changes the sign at the phase boundary near the QCD critical point [37]. The same conclusion is also obtained for mixed cumulants between net-baryon and energy E such as $\langle N_{B,\text{net}}^2 E \rangle_c / V$ [37]. By taking one more μ_B derivative, one can also conclude similarly that $\chi_4^B = \langle N_{B,\text{net}}^4 \rangle_c / V$ becomes negative along the phase boundary near the QCD critical point. This behavior can also be confirmed by the universality argument of the 3d Z_2 universality class [118].

For $\mu_B = 0$, from the mapping of the scaling parameters in the QCD phase diagram, similar argument is applicable to T derivatives of even order cumulants, which leads to $\chi_{2(n+1)}^B \sim \partial \chi_{2n}^B / \partial T$ [115]. From this relation it is pointed out that χ_6^B becomes negative near the phase boundary for small μ_B [117].

Besides the baryon number cumulants, those of electric charge and strangeness also behave anomalously near the critical point. The anomalous behaviors in these quantities, however, are weaker than those of the baryon number cumulants. The electric charge susceptibility $\chi_2^Q = \langle N_{Q,\text{net}}^2 \rangle_c / V$, for example, is obtained by μ_Q derivatives of ω . This derivative is rewritten in terms of the baryon and isospin chemical potentials, μ_B and μ_I , as $\partial / \partial \mu_Q = (\partial / \partial \mu_B + \partial / \partial \mu_I) / 2$ [37]. The electric susceptibility thus is given by

$$\chi_2^Q = \frac{\partial^2(-\omega/T)}{\partial (\mu_Q/T)^2} = \frac{1}{4} \left(\frac{\partial}{\partial (\mu_B/T)} + \frac{\partial}{\partial (\mu_I/T)} \right)^2 \frac{-\omega}{T} = \frac{1}{4} (\chi_2^B + \chi_2^I), \quad (126)$$

where $\chi_2^I = (\partial^2(-\omega/T)) / (\partial (\mu_I/T)^2)$ is the isospin susceptibility. In the last equality in Eq. (126) we have neglected the cross term $(\partial^2 \omega) / (\partial \mu_B \partial \mu_I)$ which vanishes in the isospin symmetric medium. The isospin susceptibility does not have a divergence at the critical point in an isospin symmetric medium [25]. Equation (126) shows that the effect of the divergence in χ_2^B is relatively suppressed in χ_2^Q .

In order to compare the cumulants of conserved charges obtained in effective models or lattice QCD numerical simulations with experimental data, the ratios of cumulants are calculated on the chemical freezeout line [93] in the literature [119, 120, 121, 122, 63, 64, 123, 124, 125]. Recently, the use of fluctuation observables for the determination of the freezeout temperature (of fluctuations) is also proposed [126, 34, 91]. These analyses would be used as a qualitative guide to understand the experimental results on the ratios of cumulants. As will be discussed in the next sections, however, the event-by-event analyses in relativistic heavy ion collisions measure the fluctuations in the final state, which are not the thermal fluctuation at some early stage in the time evolution of the hot medium. Because of this difference, their direct comparison with theories may lead to wrong conclusions; while the event-by-event fluctuations would carry information on early thermodynamics, this information must be extracted by correcting various contributions associated with the experiment. This is the subject which will be addressed in the following sections. We also note that the theoretical studies on the net-baryon number cumulants are sometimes compared with the experimental results on net-proton number cumulants, which are not the same quantities as the former; this problem will be discussed in Sec. 6.

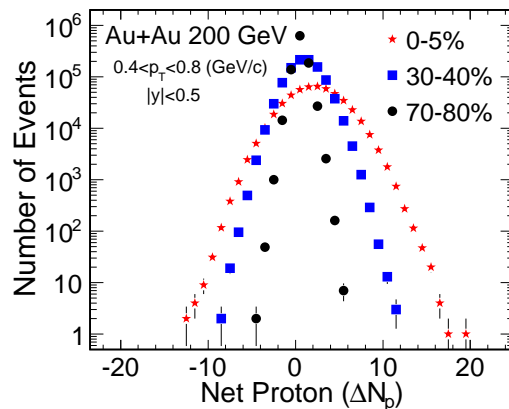


Figure 8: Event-by-event histogram of net-proton number cumulants measured by STAR collaboration at RHIC [26].

4 Event-by-event fluctuations

In Sec. 3, we have seen that the cumulants of conserved charges in an equilibrated medium behave characteristically reflecting the onset of deconfinement or the existence of the critical point. The goal of the measurement of fluctuations in relativistic heavy ion collisions is to find these behaviors in fluctuation observables. In these experiments, fluctuations are observed by event-by-event analyses. In this method, the numbers of particles of identified species are observed in some coverage of a detector in each event. The distribution of the numbers for individual events is called event-by-event fluctuation. It is believed that fluctuations observed in this way carry information on the thermal fluctuation in early stage in the time evolution of the hot medium.

In this and succeeding two sections, we discuss event-by-event analysis. In particular, we take a closer look at the relation between event-by-event and thermal fluctuations. In this section, we first give an overview of event-by-event analysis, and discuss why, when and how event-by-event fluctuations can be compared with thermal ones³. Two specific problems are discussed in later sections separately. In Sec. 5, we address the effect of the diffusion of fluctuations in later stages. It will be discussed that the rapidity window dependences of fluctuation observables can be used to understand this effect. We then consider the problem of efficiency correction in event-by-event analysis in Sec. 6. The difference between net-baryon and net-proton number cumulants will also be discussed there.

4.1 Event-by-event analysis

In event-by-event analysis of fluctuation observables in relativistic heavy ion collisions, some observables, such as the numbers of specific particles, are observed in some coverage of a detector in each event. The numbers then take different values for each event. As an example, in Fig. 8 we show the event-by-event histogram of net-proton number observed by STAR collaboration [26]. Regarding the histogram as the probability distribution function, one can construct the cumulants of the particle number from this event-by-event distribution⁴.

³ The experimental setting of event-by-event analysis and associated problems is summarized nicely in a review Ref. [20].

⁴ In actual experimental analyses, the procedure to obtain the cumulants is more complicated. For details, see Refs. [61, 69].

4.1.1 Conserved charges in heavy ion collisions

Among various fluctuation observables, those of conserved charges are believed to have suitable properties to investigate early thermodynamics. First, as we have discussed in Sec. 3.1, the cumulants of conserved charges in thermal medium are well defined and can be obtained unambiguously in a given theory. Moreover, through the linear response relations the cumulants of conserved charges are directly related to the property of the medium. Second, as we will discuss in Sec. 5 in detail, the time evolution of fluctuations is typically slow for conserved charges. The slow variation enables us to investigate the medium property in the early stage from event-by-event analysis, although the measurement is performed for the final state [21, 22].

In QCD, the net-flavor numbers are conserved charges besides energy, momentum and angular momentum. In heavy ion collisions, the numbers of net-baryon, net-electric charge and net-strangeness, which are given by the linear combinations of net-flavor numbers, are frequently used instead of the net-flavor numbers. Among these three charges, the net-electric charge is most directly observable in heavy ion collisions, because the detectors for heavy ion collisions can observe almost all charged particles entering the detector with particle identification. Figure 1 is an example of the experimental result of net-electric charge fluctuation [28]. Higher order cumulants of net-electric charge have been also measured by STAR collaboration recently [30].

The measurement of net-baryon number is more difficult, because the typical detectors cannot identify neutral baryons, in particular neutrons which account for about half of the total baryons. Because of this problem, net-proton number cumulants are measured in experiments and used as a proxy of net-baryon number; an example is shown in Fig. 2 [28]. It, however, should be remembered that the net-proton number is not a conserved charge and different from net-baryon number [98, 99]. In fact, it is shown in Refs. [98, 99] that the net-proton and net-baryon number cumulants can take significantly different values and thus the substitution of the former for the latter cannot be justified. In this study it is also shown that the net-baryon number cumulants can be determined experimentally without measuring of neutrons. We will discuss these issues in Sec. 6.

The experimental measurement of net-strange number has a difficulty at a more fundamental level. The strange charges in heavy ion collisions are dominantly carried by kaons. Among them, charged kaons K^+ and K^- carrying strange numbers $s = \pm 1$, respectively, can be measured by detectors. The strange number is also carried by the neutral kaons, K^0 and \bar{K}^0 having strange numbers $s = \pm 1$, respectively. The decays of these neutral kaons undergo the weak interaction, in which K_L^0 and K_S^0 are eigenstates but not eigenstates of strange number. Because of this mixing, the net-strangeness carried by K_L^0 and K_S^0 can not be observable, even if the detectors measure these particles. Fluctuations of net kaon number, the difference of the numbers of K^- and K^+ , are often considered experimentally as a proxy of net strangeness. One, however, should keep in mind that the substitution of the net-kaon number for net-strangeness contains the same problem as that of net-proton number for net-baryon number.

4.1.2 Coverage to count the particle number

In event-by-event analysis, the particle number arriving at some range of the detector is counted in each event. In order to compare event-by-event fluctuations with thermal ones, it is desirable to choose this range so that it corresponds to a spatial volume of the hot medium. The detectors in heavy ion collisions, however, can only measure the momentum of particles in the final state.

The momentum range in the final state can be related to a spatial volume of the hot primordial medium in coordinate space in some special cases such as the Bjorken scaling flow [71]. In the Bjorken picture, which is well justified for large $\sqrt{s_{NN}}$, the hot medium has boost invariance along the longitudinal direction. To describe such systems, it is convenient to introduce the rapidity y and the

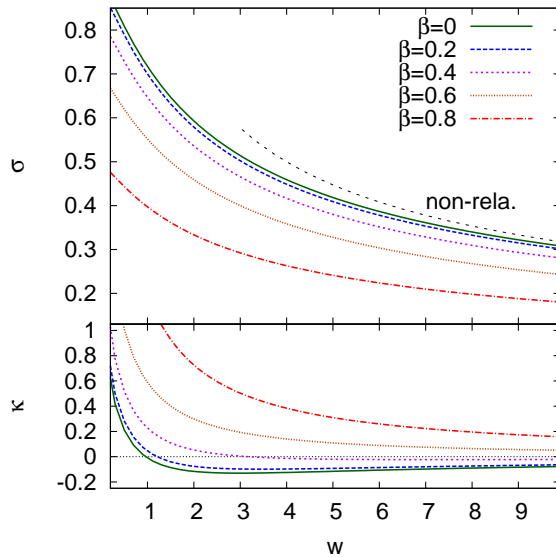


Figure 9: Width σ and kurtosis κ of the thermal distribution in rapidity space calculated in a blast wave model with several values of radial velocity β [127, 128]. The horizontal axis shows $w = m/T_{\text{kin}}$ with the mass of particle m and the freezeout temperature T_{kin} .

coordinate-space rapidity Y ,

$$y = \frac{1}{2} \ln \frac{1 + \beta}{1 - \beta} = \tanh^{-1} \beta, \quad Y = \frac{1}{2} \ln \frac{t + z}{t - z}, \quad (127)$$

respectively. Here, β is the velocity along the longitudinal direction; for particles it is given by $\beta = p_z/E$ with the longitudinal momentum p_z and energy E . t and z represent the time and longitudinal coordinate, respectively. Rapidities y and Y obey an additional law under the Lorentz boost; with the boost of a system with velocity β_0 , rapidities are transformed as

$$y' = y + \beta_0, \quad Y' = Y + \beta_0. \quad (128)$$

Because of the boost invariance, in the Bjorken picture the rapidity y of a *fluid element* is equal to its coordinate-space rapidity Y . Therefore, up to the thermal motion of individual particles the rapidity of particles at y is identical to the coordinate-space one, Y . Using this correspondence, one can count the particle number in an (approximate) coordinate space interval from the momentum distribution in the final state. In typical event-by-event analyses, the range to count the particle number is chosen to a (pseudo-)rapidity interval Δy , while the transverse momentum p_T and the azimuthal angle are integrated out. This range then can approximately be identified with the spatial volume in the corresponding coordinate-space rapidity $\Delta Y = \Delta y$

It, however, should be remembered that the correspondence between y and Y is valid only for the fluid element, and it does not hold for the rapidities of individual particles in the volume element, because individual particles have nonzero velocity against the fluid element due to the thermal motion. Because of the thermal motion, the correspondence between the particle distribution in Y space and in y space is blurred. The use of y as a proxy of Y is valid only up to the resolution brought by this thermal motion. The rapidity window Δy to measure event-by-event particle distribution has to be taken sufficiently large compared with the resolution width brought by the thermal motion in rapidity space $\Delta y_{\text{thermal}}$ in order to suppress the effect of the blurring; otherwise, the information of fluctuations in a volume in ΔY is lost. In the upper panel of Fig. 9, we plot the width of the thermal motion

$\sigma = \Delta y_{\text{thermal}}$ calculated in a simple blast wave model [127, 128]. The parameter $w = m/T_{\text{kin}}$ is the ratio between the particle mass m and the kinetic-freezeout temperature T_{kin} , while β is the radial velocity. For central collisions at the top-RHIC and LHC energies, the blast wave fit to the transverse momentum spectra gives $\beta \simeq 0.6$ and $T_{\text{kin}} \simeq 100$ MeV [129]. Assuming that particles are emitted from the medium at the kinetic-freezeout surface with the thermal distribution and using these values of β and T_{kin} , one obtains that the thermal width is $\Delta y_{\text{thermal}} \simeq 0.5$ for pions ($w = m/T_{\text{kin}} \simeq 1.5$) and $\Delta y_{\text{thermal}} \simeq 0.25$ for nucleons ($w \simeq 9$); see Fig. 9. On the other hand, the maximum rapidity window of the STAR detector is $\Delta y = 1.0$. For the analysis of net-electric charge fluctuation, this width is comparable with $\Delta y_{\text{thermal}}$, and thus may not be large enough to suppress the effect of thermal motion [127, 128]. More quantitative estimate of this effect on cumulants [127, 128, 70] will be discussed in Sec. 5. In the lower panel of Fig. 9, the kurtosis of the thermal distribution in rapidity space is also plotted. The panel suggests that the non-Gaussianity of the distribution is not large for the kinetic freezeout parameters except for the case of pions. In fact, it is shown from an explicit calculation of the cumulants that the effects of the non-Gaussianity are well suppressed in the cumulants [127, 128].

We emphasize that the above argument on the approximate correspondence between y and Y is based on the Bjorken picture for medium expansion. When the Bjorken picture breaks down for low energy collisions, further subtle discussion is needed for the relation between y and Y , and the interpretation of event-by-event fluctuations in a rapidity interval Δy . This would particularly be the case for the BES energy, $\sqrt{s_{\text{NN}}} \simeq 7.7 - 20$ GeV, at RHIC. In the interpretation of fluctuation observables in this energy range (for example, Fig. 2), therefore, careful arguments on these issues, which should be carried out with the aid of dynamical models and information of various observables, is required.

The other remark concerning the choice of Δy is that the observed event-by-event fluctuations are those in the final state in heavy ion collisions, and not those in some early stage, such as at chemical freezeout time, in the time evolution. Even if clear signals in fluctuation observables are well developed reflecting thermodynamics in some early time, they are modified during the time evolution in later stages before the detection. Here, it is worth emphasizing that event-by-event fluctuations continue to change until *kinetic* freezeout. This is contrasted with *average* particle abundances, which are almost frozen at *chemical* freezeout time. The modification of event-by-event fluctuations after chemical freezeout is easily understood from the fact that the particle number in a coordinate-space rapidity interval ΔY in a collision event is modified due to the motion of individual particles. When one compares event-by-event fluctuations with thermal fluctuations in early stage, this effect has to be also taken into account. In Sec. 5, we argue that the effects of the time evolution after chemical freezeout and the thermal width $\Delta y_{\text{thermal}}$ are simultaneously described as a diffusion process. It will also be discussed that the magnitude of these effects can be examined experimentally from the Δy dependences of the cumulants.

Finally, we note that in general the coverages in the p_T and azimuthal direction of detectors are not perfect, although the coverages are desirable to be taken as large as possible to measure the event-by-event fluctuations in a volume in coordinate-space. The imperfect coverages also modify fluctuation observables. In fact, in a recent analysis of net-proton number cumulants by STAR Collaboration the dependence on the p_T coverage is reported [32]; see the right panel in Fig. 2. It should also be remembered that the azimuthal coverage of the PHENIX detector is significantly limited compared with the STAR detector. The effect of finite acceptance is in part treated as an efficiency effect as discussed in Sec. 6. The effects of the p_T cut on event-by-event analysis are recently investigated, for example, in Refs. [130, 131, 132].

4.1.3 Canceling spatial volume dependences

The cumulants of thermal fluctuations are proportional to the spatial volume of the system as discussed in Sec. 3.1. In order to give a physical meaning to the magnitude of cumulants observed by the event-by-event analyses, therefore, one has to know the spatial volume of the hot medium besides the value

of the cumulants. Moreover, because the hot medium created in relativistic heavy ion collisions is an expanding system, the spatial volume is changing with time evolution.

In order to eliminate the spatial volume dependence, in relativistic heavy ion collisions cumulants are usually discussed in terms of the ratios between extensive observables. Here, the extensive observables have to be taken as conserved quantities or their cumulants. By taking the ratio of these quantities observed in a rapidity window Δy , the effect of the spatial volume and its time evolution can be canceled out under the Bjorken picture as follows. As discussed previously, the rapidity window Δy approximately corresponds to the one of coordinate-space rapidity $\Delta Y = \Delta y$. Although the spatial volume of the medium in ΔY changes during the time evolution in a nontrivial way, the amount of a conserved quantity in ΔY is conserved if we neglect the effect of diffusion, i.e. exchange of the quantity with adjacent volume elements [21, 22]. The ratio of conserved quantities in ΔY , therefore, does not depend on the time evolution of spatial volume when the effect of diffusion is negligible.

Before the measurement of higher order cumulants has started, the magnitude of the second-order cumulant was discussed in terms of the ratio with entropy density [21, 22], which is a conserved quantity in non-dissipative hydrodynamic expansion. The use of a quantity called the D -measure,

$$D = 4 \frac{\langle N_Q^2 \rangle_c}{\langle N_{\text{tot}} \rangle}, \quad (129)$$

as an experimental observable with the net-electric charge N_Q and the number of total charge N_{tot} , i.e. the sum of the positively and negatively charged particle numbers, was suggested in Ref. [22]. Here, N_{tot} is used as a proxy of the entropy density. It is estimated that the D -measure takes $D = 3 \sim 4$ in the HRG model while the value of D is about twice or more smaller if the deconfined medium is created [22]. Figure 1 shows the D -measure measured by ALICE collaboration [27]. The experimental result shows the suppression of this quantity compared with the hadronic value especially for large $\Delta\eta$. This result suggests the survival of the thermal fluctuation created in the deconfined medium. The origin of the $\Delta\eta$ dependence in the figure will be discussed in Sec. 5. Later, the use of the ratio between cumulants of conserved charges was proposed in Ref. [23]. This choice removes the ambiguity in the relation between the entropy and N_{tot} in the definition of the D -measure. The top and bottom panels in the right figure of Fig. 2, for example, show the ratio of net-proton number cumulants,

$$\kappa\sigma^2 = \frac{\langle N_p^4 \rangle_c}{\langle N_p^2 \rangle_c}, \quad \frac{S\sigma}{\text{Skellam}} = \frac{\langle N_p^3 \rangle_c}{\langle N_p \rangle_c}, \quad (130)$$

respectively, where the skewness S and kurtosis κ are defined in Sec. 2.5. As discussed in Sec. 3, these ratios become exactly unity in the HRG model. These ratios thus are suitable in exploring the existence of physics which cannot be described by the HRG model. The experimental results in Fig. 2 show that these ratios show statistically-significant deviation from unity. This result thus cannot be described solely by the thermal fluctuation in the hadronic medium. Non-hadronic or non-thermal physics come into play in these observables, which should be understood in future studies.

4.2 Global charge conservation

Above, we discussed that larger rapidity window Δy has to be taken to suppress the burring effects due to the thermal motion of individual particles. When Δy becomes larger, however, another problem due to the finiteness of the system, or global charge conservation, shows up.

The hot medium created by relativistic heavy ion collisions is a finite-size system. If one measures a conserved charge in the total system, it is always fixed to the sum of those in the colliding nuclei and does not fluctuate. This fact is called the global charge conservation. Conserved charges can have event-by-event fluctuations when measurement is performed for subsystems. Even if measurement is

performed for a subsystem, when the subsystem is not small enough compared with the total system the global charge conservation affects event-by-event fluctuations.

The effect of the global charge conservation on fluctuation observables in an equilibrated medium is investigated in Refs. [22, 133, 134, 135, 136]. These analyses suggest that the effect of global charge conservation tends to reduce the magnitude of fluctuation observables. In Ref. [137], the effect of global charge conservation is studied by incorporating non-equilibrium effects in the time evolution of the hadronic medium. In this study it is argued that the effect of the global charge conservation tends to be suppressed owing to non-equilibrium effects, which stem from the finiteness of the diffusion speed, compared with those in Refs. [22, 133]. In particular, it is pointed out that the experimental result on net-electric charge fluctuation at ALICE [27] is not affected by this effect [137].

As the collision energy $\sqrt{s_{\text{NN}}}$ is lowered, the length of the hot medium along the rapidity direction becomes smaller, and the effect of the global charge conservation becomes more prominent with fixed rapidity window Δy . It is not a priori clear whether there exists a range of Δy in which both the effects of thermal blurring and global charge conservation are well suppressed in low energy collisions as realized in the BES program, or not. The breakdown of the Bjorken picture would also modify the justification of the use of Δy in place of ΔY . An answer to this question would be obtained by experimental study of the Δy dependences of various cumulants [68, 137, 70] and by theoretical study of the transportation of conserved charges without assuming the Bjorken picture.

4.3 Non-thermal event-by-event fluctuations

Collision events in heavy ion collisions have various event-by-event fluctuations besides the thermal ones discussed so far. For example, the energy per unit rapidity and shape of the initial state just after the collision are fluctuating [138, 139], even with fixed collision energy and after a centrality selection. These fluctuations give rise to additional event-by-event fluctuations besides the thermal ones. Production of jets in high energy collisions will be another source of event-by-event fluctuations. When experimentally observed event-by-event fluctuations are directly compared with thermal ones, it is implicitly assumed that these non-thermal fluctuations are well suppressed compared with thermal fluctuations. This assumption, however, has to be examined carefully. When the contribution of non-thermal fluctuations is not small, they have to be eliminated in order to isolate the thermal fluctuations.

An example of non-thermal event-by-event fluctuations is that of the energy density in the initial state. Even with fixed impact parameter, the energy density of the produced medium after the collision is fluctuating event by event. Under the Bjorken picture, the event-by-event fluctuation of energy density per unit rapidity is translated to that of spatial volume with a fixed temperature. Because cumulants of thermal fluctuations are proportional to the spatial volume, the energy fluctuation in the initial state directly affects the magnitude of event-by-event fluctuations [140, 141]. Similarly, the finite size of the centrality bins also gives rise to event-by-event fluctuations of the volume. In experimental analyses, in order to remove this fluctuation as much as possible analyses of cumulants are performed with narrow centrality bins, and then summed up [61]. On the theoretical side, the effect of the volume fluctuation on cumulants can be estimated by superposing the events with different spatial volumes. The event-by-event cumulants are then represented by the cumulants of thermal and volume fluctuations; see Appendix A. Another possibility to take account of the volume fluctuation is to employ so-called strongly-intensive quantities [142, 143, 144], which are combinations of cumulants in which the spatial volume fluctuations are canceled out. Although strongly-intensive quantities are usually defined for non-conserved quantities [142, 143], if they were defined solely with conserved quantities their physical meaning would become more apparent.

In high energy collisions, production of jets would also disturb fluctuation observables in a rapidity window Δy . The total conserved charges carried by jets are typically small, because the charges carried by primary partons (gluon or quark) except energy, momentum, and angular momentum, are negligibly

small. As a first approximation, therefore, the effects of jets on the conserved-charge fluctuations would be well suppressed. They, however, give rise to fluctuation of energy density along the rapidity direction, and would modify the cumulants in a rapidity window. To the best of the authors' knowledge, these effects have not been discussed in the literature.

A qualitative observation on these non-thermal event-by-event fluctuations is that they tend to enhance the magnitude of fluctuations. In particular, for the second-order cumulant both thermal and non-thermal fluctuations take positive values. Assuming that they are uncorrelated, the total cumulant is simply given by their sum. In this sense, the suppression of the second-order cumulant of net-electric charge observed by ALICE collaboration [27] in Fig. 1 is quite interesting; because all non-thermal fluctuations tend to enhance event-by-event fluctuations, the suppression is most probably attributed to the thermal fluctuation [19].

4.4 Other problems

Besides the above problems, there are various issues which should be considered in the interpretation of the event-by-event fluctuations.

1. **Fluctuations in the pre-equilibrium stage:** For $\sqrt{s_{\text{NN}}}$ larger than the top RHIC energy, the pre-equilibrium state is dominated by gluons. Because gluons do not carry conserved charges except energy, momentum and angular momentum, with the absence of quarks the fluctuations of conserved charges in the pre-equilibrium system should be small. Only after the pair creation of quarks, which carry conserved charges, fluctuations of conserved charges start to increase. If the equilibration of fluctuations is not established during the time evolution, the cumulants in the final state would be suppressed as a remnant of the small fluctuation in the pre-equilibrium stage. In low energy collisions, on the other hand, the magnitude of fluctuations in the pre-equilibrium system would be determined by the fluctuation of baryon stopping.
2. **Limitation of detector's ability:** The finite efficiency and acceptance of detectors modify the result of event-by-event analysis [98, 99, 67]. These effects will be addressed in Sec. 6. The effect of the particle misidentifications by detectors on event-by-event analysis has to be investigated separately from efficiency problems [29, 145].
3. **Final state hadronic interactions:** The decays of resonance states modify event-by-event fluctuation in a rapidity window [99, 146]. To the first approximation, the effect of the resonance decays can be treated as a part of diffusion. In Ref. [145], the effect of secondary (knockout) protons is investigated. The effect of deuteron formation is studied in Ref. [147].

5 Time evolution of fluctuations in diffusive processes

In Sec. 3 we have seen that the cumulants in equilibrated QCD medium show characteristic behaviors when the medium undergoes phase transitions. The goal of the measurement of fluctuations in relativistic heavy ion collisions is to find these behaviors in the cumulants measured by event-by-event analysis. As we have already discussed in Sec. 4, however, fluctuations measured by event-by-event analysis are not the same as the thermal fluctuations. In particular, it is to be remembered that the system created by the collisions is a dynamical system, although all analyses discussed in Sec. 3 assumes equilibration. Besides the caveats listed in Sec. 4, here we emphasize that in the comparison of thermal fluctuations with event-by-event one, the following two assumptions are implicitly made:

1. The medium establishes a (near-) *equilibration of fluctuations* in the early stage.

2. The signals developed in the early stage survive until the final state; although the fluctuations tend to be shifted toward the equilibrated values by final state interactions in the hadronic medium and thermal blurring, this effect is assumed to be well suppressed.

The purpose of this section is to consider these issues. To this end, we first introduce a simple stochastic model to illustrate a diffusive process of fluctuations. We elucidate the concept of *equilibration of fluctuations of conserved charges*. It will be shown that this concept can be different from local equilibration; the time scale to establish the former can be significantly longer than that for the latter.

A characteristic feature of the time evolution of conserved-charge fluctuations compared with non-conserved quantities is that the time evolution of the former is typically slow because their evolution is governed by hydrodynamic equations. In particular, it can become arbitrary slow as the spatial volume to define the fluctuation becomes larger. This property is highly contrasted with the one of non-conserved quantities, whose typical time scales are typically short and insensitive to the spatial volume.

In this section, we consider the stochastic diffusion equation (SDE), which is a stochastic version of the diffusion equation with a Langevin-type stochastic term. This equation, which is a part of theory of hydrodynamic fluctuations [95, 148], is suitable to describe the evolution of conserved-charge fluctuations in diffusion processes for second order. By describing the non-equilibrium time evolution of conserved-charge fluctuations in diffusive systems in this model, we illustrate key ingredients associated with the time evolution of fluctuations. We also discuss that this formalism cannot describe the nonzero non-Gaussian fluctuations in equilibrium in a straightforward manner, and thus is not suitable for the description of the non-Gaussianity in relativistic heavy ion collisions. A model to describe the diffusion of non-Gaussianity is introduced in Sec. 5.4.

5.1 Langevin equation for Brownian motion

Before starting the discussion of diffusive processes, however, for pedagogical purposes we first briefly take a look at the Langevin equation for a single Brownian particle, which is a simple stochastic equation. Readers who are familiar with the Langevin equation can skip this subsection.

Let us consider a heavy particle floating in a fluid. We call this particle the Brownian particle in the following. For simplicity we consider the velocity v of this particle only along a one-dimensional direction. When this particle moves with a nonzero velocity it receives a drag force proportional to v from the fluid. The equation of motion of this particle is then given by

$$m \frac{dv}{dt} = -\gamma v, \quad (131)$$

where γ is the drag coefficient. The solution of this equation with an initial condition $v = v_0$ at $t = 0$ is easily obtained as

$$v(t) = v_0 e^{-\gamma' t}, \quad (132)$$

with $\gamma' = \gamma/m$. This solution shows that the velocity of the particle becomes arbitrary slow as t becomes large, and vanishes in equilibrium defined by $t \rightarrow \infty$.

On the other hand, statistical mechanics tells us that particles in an equilibrated medium have thermal motion; from the equi-partition principle in classical statistical mechanics the expectation value of the square of the velocity is given by $\langle v^2 \rangle_{\text{eq}} = T/m$ in equilibrium, where $\langle \cdot \rangle_{\text{eq}}$ denotes the thermal average. When one is concerned with the velocity of order $v \simeq \sqrt{T/m}$, therefore, the solution Eq. (132) is not satisfactory.

The thermal motion of Brownian particles comes from the interaction with atoms composing the fluid [39]. Because the thermal motion of individual atoms is random and not controlled by macroscopic

quantities, even if we start from initial conditions with the same macroscopic observables the motion of the particles would fluctuate to result in different time evolutions of Brownian particles around the solution Eq. (132). To incorporate such stochastic effects in Eq. (131), one may promote Eq. (131) to a Langevin equation by adding a stochastic term $\xi(t)$ as

$$\frac{dv}{dt} = -\gamma'v + \xi(t). \quad (133)$$

Because the average motion of Brownian particles should be well described by Eq. (131) even with $\xi(t)$, the effect of $\xi(t)$ should vanish on average. We thus require

$$\langle \xi(t) \rangle = 0, \quad (134)$$

where the expectation value is taken for different time evolutions.

Next, the correlation of the stochastic terms described by the two-point function $\langle \xi(t_1)\xi(t_2) \rangle$ can take nonzero values. The correlation, however, would vanish when t_1 and t_2 are well separated, because the stochastic terms which come from microscopic interactions should be uncorrelated for macroscopic time separation. When the typical time scale for the variation of v is sufficiently long compared with the one for $\xi(t)$, the correlation function should be well approximated by the delta function,

$$\langle \xi(t_1)\xi(t_2) \rangle = A\delta(t_1 - t_2), \quad (135)$$

with an unknown coefficient A , which will be determined later. The stochastic term obeying Eq. (135) is called the white noise, because the Fourier transform of Eq. (135) is constant as a function of frequency.

The solution of Eq. (133) with an initial condition $v(0) = v_0$ is given by

$$v(t) = v_0e^{-\gamma't} + \int_0^t dt' e^{-\gamma'(t-t')} \xi(t'). \quad (136)$$

The average of $v(t)$ is obtained by taking the expectation values of both sides as

$$\langle v(t) \rangle = \langle v_0 \rangle e^{-\gamma't}, \quad (137)$$

where the second term in Eq. (136) vanishes by Eq. (134). In Eq. (137) we assumed that the statistical average is taken over both the stochastic effect and the fluctuation of the initial condition, and replaced v_0 by its average. The result Eq. (137) is equivalent with Eq. (132); the introduction of the stochastic term does not modify the average of the velocity.

The characteristic of Eq. (133) is that its solution can fluctuate around the average Eq. (137). To see the magnitude of the fluctuation, we take the average of the square of $v(t)$,

$$\langle (v(t))^2 \rangle = \langle v_0^2 \rangle e^{-2\gamma't} + 2e^{-\gamma't} \int_0^t dt' e^{-\gamma'(t-t')} \langle v_0 \xi(t') \rangle + \int_0^t dt_1 dt_2 e^{-\gamma'(t-t_1)} e^{-\gamma'(t-t_2)} \langle \xi(t_1)\xi(t_2) \rangle. \quad (138)$$

Since the stochastic term originates from microscopic effects, $\xi(t)$ would be uncorrelated with the fluctuation of the initial condition v_0 . Under this assumption, $\langle v_0 \xi(t') \rangle$ in the second term on the right-hand side vanishes. Substituting Eq. (135) into the last term, and subtracting the average Eq. (137), one obtains

$$\langle (\delta v(t))^2 \rangle = \langle (v(t) - \langle v(t) \rangle)^2 \rangle = \langle \delta v_0^2 \rangle e^{-2\gamma't} + \frac{A}{2\gamma'} (1 - e^{-2\gamma't}), \quad (139)$$

where $\langle \delta v_0^2 \rangle = \langle v_0^2 \rangle - \langle v_0 \rangle^2$ is the fluctuation in the initial condition. This result shows that the fluctuation of $v(t)$ relaxes from the initial value to the equilibrated one, $A/2\gamma'$, with the relaxation time $1/2\gamma'$.

The fluctuation in equilibrium is given by the equi-partition principle as $\langle v^2 \rangle_{\text{eq}} = T/m$. Because this condition should be satisfied in the $t \rightarrow \infty$ limit in Eq. (139), one obtains $A/2\gamma' = \langle v^2 \rangle_{\text{eq}} = T/m$, or

$$\langle \xi(t_1)\xi(t_2) \rangle = 2\gamma' \langle v^2 \rangle_{\text{eq}} \delta(t_1 - t_2) = \frac{2\gamma'T}{m} \delta(t_1 - t_2). \quad (140)$$

This relation is known as the fluctuation dissipation relation (of first-kind), which relates the magnitude of the microscopic random force with macroscopic observables [39].

Several comments are in order. First, the stochastic process described by the Langevin equation Eq. (133) with a white noise is a Markov process. In fact, Eq. (133) can be converted to an equivalent Fokker-Planck equation, which is a partial differential equation for a distribution function, which is of the first-order in time derivative [73]. This means that the stochastic process is a Markov process. Second, having obtained the fluctuation dissipation relation for Gaussian fluctuation, Eq. (140), it may look possible to extend this relation to higher order cumulants, in such a way that the non-Gaussian cumulants $\langle v^n \rangle_{c,\text{eq}}$ would be related to higher order correlation $\langle \xi(t_1)\xi(t_2) \cdots \xi(t_n) \rangle_c$. This idea, however, results in failure. It is shown that the stochastic term should be of Gaussian and all correlations higher than the second-order vanish

$$\langle \xi(t_1)\xi(t_2) \cdots \xi(t_n) \rangle_c = 0 \quad (n \geq 3), \quad (141)$$

for Markov processes if the stochastic variable $v(t)$ varies continuously [73]. With Eq. (141), it is easy to check that all higher order cumulants of v vanish in the $t \rightarrow \infty$ limit. For the third-order case, for example, $\langle v(t)^3 \rangle_c$ is calculated to be

$$\begin{aligned} \langle (v(t))^3 \rangle &= \langle v_0^3 \rangle e^{-3\gamma't} + 3 \int_0^t dt' \langle v_0^2 \xi(t') \rangle e^{-2\gamma't} e^{-\gamma'(t-t')} \\ &\quad + 3 \int_0^t dt_1 dt_2 \langle v_0 \xi(t_1) \xi(t_2) \rangle e^{-\gamma't} e^{-\gamma'(t-t_1)} e^{-\gamma'(t-t_2)} \\ &\quad + \int_0^t dt_1 dt_2 dt_3 \langle \xi(t_1) \xi(t_2) \xi(t_3) \rangle e^{-\gamma'(t-t_1)} e^{-\gamma'(t-t_2)} e^{-\gamma'(t-t_3)}. \end{aligned} \quad (142)$$

In the large t limit the first three terms depending on the initial condition vanish owing to the $e^{-\gamma't}$ factor, while the last term also vanishes because of Eq. (141). This result shows that the Langevin equation Eq. (133) is not suitable for the description of the relaxation of non-Gaussian fluctuations toward nonzero equilibrated values.

5.2 Stochastic diffusion equation

5.2.1 Formalism

Now, we have come to the main subject of this section, the stochastic process in diffusive systems. To treat this problem, we introduce the stochastic diffusion equation (SDE). This formalism, which can be regarded as a counterpart of the theory of hydrodynamic fluctuations [95, 148], serves as a useful tool to describe the time evolution of fluctuations around the solution of the diffusion equation. Although we limit our attention to one dimensional cases, the generalization to multi-dimensional ones is straightforward.

The time evolution of a conserved charge $n(x, t)$ is given by the equation of continuity,

$$\frac{\partial}{\partial t} n(x, t) = -\frac{\partial}{\partial x} j(x, t), \quad (143)$$

with the current $j(x, t)$. It is phenomenologically known that $j(x, t)$ in various systems well obeys the constitutive equation called the Fick's law,

$$j = -D \frac{\partial}{\partial x} n(x, t), \quad (144)$$

where D is the diffusion constant. By combining Eqs. (143) and (144), one obtains the diffusion equation

$$\frac{\partial}{\partial t} n(x, t) = D \frac{\partial^2}{\partial x^2} n(x, t). \quad (145)$$

The solution of Eq. (145) is easily obtained in Fourier space. In the $t \rightarrow \infty$ limit, $n(x, t)$ approaches a uniform form $n(x, t) = n_0$ without fluctuations.

In thermal systems, on the other hand, $n(x, t)$ should be fluctuating. In fact, the integral of $n(x, t)$ in some spatial extent with length L ,

$$Q_L(t) = \int_0^L dx n(x, t), \quad (146)$$

is the number of the conserved charge in L , and as we have seen in Sec. 3 this quantity is fluctuating in equilibrium. This means that $n(x, t)$ is also fluctuating in equilibrium. When one considers the time evolution of $n(x, t)$ with a resolution that this thermal fluctuation is not negligible, the property of Eq. (145) that $n(x, t)$ becomes static in the $t \rightarrow \infty$ is not satisfactory.

To describe the approach of fluctuations toward the thermal one in diffusive systems, one may modify Eq. (145) by introducing a stochastic term similarly to the procedure in Sec. 5.1. The stochastic term should be introduced in the constitutive equation Eq. (144), because this is a phenomenological relation: Although the current $j(x, t)$ in a macroscopic scale should obey Eq. (144), microscopically $j(x, t)$ should be fluctuating around Eq. (144), because of the random thermal motions of the microscopic constituents of the fluid. We thus modify Eq. (144) as

$$j(x, t) = -D \frac{\partial}{\partial x} n(x, t) + \xi(x, t), \quad (147)$$

where $\xi(x, t)$ represents the stochastic effect depending on x and t . The conservation law Eq. (143), on the other hand, is an exact relation and should not be altered. Substituting Eq. (147) into Eq. (143), one obtains

$$\frac{\partial}{\partial t} n(x, t) = D \frac{\partial^2}{\partial x^2} n(x, t) - \frac{\partial}{\partial x} \xi(x, t). \quad (148)$$

Because the stochastic term should not modify the average motion of $n(x, t)$, the average of the stochastic term should vanish,

$$\langle \xi(x, t) \rangle = 0, \quad (149)$$

where the meaning of the statistical average is understood similarly to the one in the previous subsection. The two-point correlation $\langle \xi(x_1, t_1) \xi(x_2, t_2) \rangle$, on the other hand, can take nonzero values. We require that the correlation of the stochastic term is temporarily and spatially local, i.e.

$$\langle \xi(x_1, t_1) \xi(x_2, t_2) \rangle = A \delta(x_1 - x_2) \delta(t_1 - t_2). \quad (150)$$

This requirement will be justified if the length and temporal scales of the motion of $n(x, t)$ described by Eq. (148) is sufficiently large compared with the microscopic scales responsible for $\xi(x, t)$. The overall

coefficients A will be determined later. Equation (148) together with Eqs. (149) and (150) is referred to as the SDE.

Equation (148) is solved in Fourier space similarly to Eq. (133) in the previous subsection. By defining the Fourier transform of $n(x, t)$ as

$$n(k, t) = \int dx e^{-ikx} n(x, t), \quad (151)$$

we obtain

$$\frac{\partial}{\partial t} n(k, t) = -Dk^2 n(k, t) + ik\xi(k, t). \quad (152)$$

The solution of Eq. (152) with the initial condition $n(k, 0) = n_0(k)$ is given by

$$n(k, t) = n_0(k) e^{-Dk^2 t} + \int_0^t dt' e^{-Dk^2(t-t')} ik\xi(k). \quad (153)$$

The Fourier transform of the stochastic term satisfies

$$\begin{aligned} \langle \xi(k, t) \rangle &= \int dx e^{-ikx} \langle \xi(x, t) \rangle = 0, \\ \langle \xi(k_1, t_1) \xi(k_2, t_2) \rangle &= \int dx_1 dx_2 e^{-ik_1 x_1 - ik_2 x_2} \langle \xi(x_1, t_1) \xi(x_2, t_2) \rangle \\ &= \int dx_1 dx_2 e^{-ik_1 x_1 - ik_2 x_2} A \delta(x_1 - x_2) \delta(t_1 - t_2) \\ &= 2\pi A \delta(k_1 + k_2) \delta(t_1 - t_2). \end{aligned} \quad (154)$$

$$(155)$$

By taking the expectation value of Eq. (153) and using Eq. (154), one obtains

$$\langle n(k, t) \rangle = \langle n_0(k) \rangle e^{-Dk^2 t}, \quad (156)$$

which is equivalent with the solution of the diffusion equation. Next, by taking the average of the product of Eq. (153) with Eq. (155), one obtains

$$\langle n(k_1, t) n(k_2, t) \rangle = \langle n_0(k_1) n_0(k_2) \rangle e^{-D(k_1^2 + k_2^2)t} + \frac{\pi A}{D} \delta(k_1 + k_2) (1 - e^{-2Dk_1^2 t}), \quad (157)$$

where it has been assumed that the stochastic term is uncorrelated with the initial condition $n_0(k)$, i.e. $\langle n_0(k_1) \xi(k_2, t) \rangle = 0$. This result with Eq. (156) gives

$$\langle \delta n(k_1, t) \delta n(k_2, t) \rangle = \langle \delta n_0(k_1) \delta n_0(k_2) \rangle e^{-D(k_1^2 + k_2^2)t} + \frac{\pi A}{D} \delta(k_1 + k_2) (1 - e^{-2Dk_1^2 t}). \quad (158)$$

Next, let us consider the large t limit of Eq. (158). In this limit, the fluctuation of $n(x, t)$ should approach the equilibrium one. The first term in Eq. (158) is suppressed in this limit owing to the exponential factor; although the zero mode fluctuation $\langle \delta n_0(0) \delta n_0(0) \rangle$ in the initial condition is not damped in this limit, this term has a negligible contribution unless the initial condition has a long range correlation. One then obtains

$$\lim_{t \rightarrow \infty} \langle \delta n(k_1, t) \delta n(k_2, t) \rangle = \frac{\pi A}{D} \delta(k_1 + k_2). \quad (159)$$

The correlation function in spatial coordinate in this limit is given by

$$\begin{aligned} \lim_{t \rightarrow \infty} \langle \delta n(x_1, t) \delta n(x_2, t) \rangle &= \lim_{t \rightarrow \infty} \int \frac{dk_1}{2\pi} \frac{dk_2}{2\pi} e^{ik_1 x_1} e^{ik_2 x_2} \langle \delta n(k_1, t) \delta n(k_2, t) \rangle \\ &= \frac{A}{2D} \delta(x_1 - x_2). \end{aligned} \quad (160)$$

This form of the correlation function is consistent with Eq. (84), which is the correlation function in an equilibrated medium. The coefficient of this term is thus identified as the susceptibility,

$$\frac{A}{2D} = \chi_2. \quad (161)$$

With Eqs. (160) and (161), the fluctuation of Q_L in Eq. (146) is calculated to be

$$\lim_{t \rightarrow \infty} \langle (\delta Q_L(t))^2 \rangle = \lim_{t \rightarrow \infty} \int_0^L dx_1 dx_2 \langle \delta n(x_1, t) \delta n(x_2, t) \rangle = \chi_2 L. \quad (162)$$

This result shows that the fluctuation of Q_L in equilibrium is proportional to L , which is the result obtained in Sec. 3.1.1. Substituting Eq. (161) into Eq. (150), one obtains

$$\langle \xi(x_1, t_1) \xi(x_2, t_2) \rangle = 2D \chi_2 \delta(x_1 - x_2) \delta(t_1 - t_2). \quad (163)$$

In Eq. (163), the property of the stochastic term is given through the macroscopic observables D and χ_2 . This is the fluctuation dissipation relation in the SDE.

5.2.2 Time evolution in SDE

Next, we investigate the time evolution of fluctuation in the SDE. To simplify the problem, in this article we limit our attention to the solution of the SDE for an initial condition satisfying

$$\langle \delta n(x_1, 0) \delta n(x_2, 0) \rangle = \sigma_0 \delta(x_1 - x_2). \quad (164)$$

In this initial condition we assume that the fluctuation is local similarly to the equilibrium case Eq. (84), but the proportionality coefficient σ_0 takes a different value from the susceptibility χ_2 . With Eq. (164), the fluctuation of Q_L is an extensive variable, $\langle (\delta Q_L)^2 \rangle = \sigma_0 L$ in the initial condition. By substituting Eq. (164) into Eq. (158), the solution in Fourier space for this initial condition is given by

$$\langle \delta n(k_1, t) \delta n(k_2, t) \rangle = \pi \left(\sigma_0 e^{-2Dk_1^2 t} + \chi_2 (1 - e^{-2Dk_1^2 t}) \right) \delta(k_1 + k_2). \quad (165)$$

The fluctuation of Q_L is obtained by performing the inverse Fourier transformation as

$$\langle (\delta Q_L)^2 \rangle = L(\sigma_0 F_2(X) + \chi_2(1 - F_2(X))), \quad (166)$$

where we have introduced a dimensionless variable $X = \sqrt{2Dt}/L$ and

$$F_2(X) = \int dz [I_X(z/L)]^2, \quad (167)$$

$$I_X(\zeta) = \int_{-1/2}^{1/2} d\xi \int \frac{dp}{2\pi} e^{-X^2 p^2/2} e^{ip(\xi+\zeta)} = \frac{1}{2} \left(\operatorname{erf} \left(\frac{\zeta + 1/2}{\sqrt{2X}} \right) - \operatorname{erf} \left(\frac{\zeta - 1/2}{\sqrt{2X}} \right) \right), \quad (168)$$

with the error function $\operatorname{erf}(x) = (2/\sqrt{\pi}) \int_0^x dt e^{-t^2}$; see Ref. [70] for manipulations. The same result is obtained in Ref. [149] using the Fokker-Planck equation. We remark that the solution depends on t

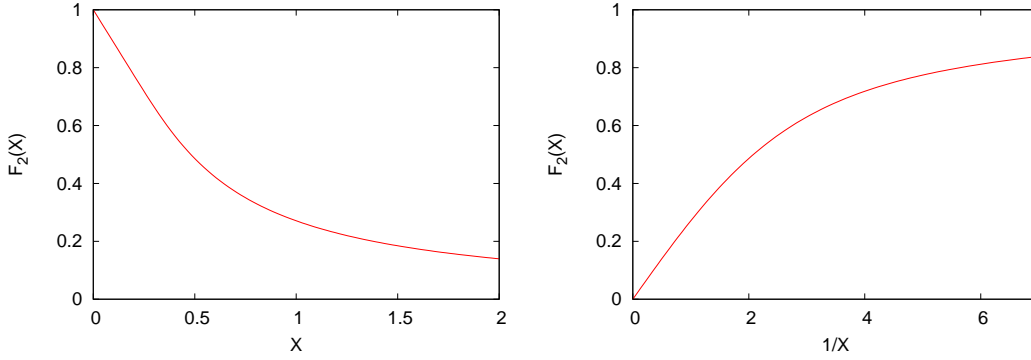


Figure 10: Function $F_2(X)$ in Eq. (167).

and L only through X . Here, $\sqrt{2Dt}$ is the diffusion distance of particles in the system described by Eq. (145).

In Fig. 10, we plot $F_2(X)$ as functions of X and $1/X$. The left panel can be interpreted as the \sqrt{t} dependence of $\langle(\delta Q_L)^2\rangle$ with a fixed L . Substituting this behavior of $F_2(X)$ into Eq. (166), one sees that $\langle(\delta Q_L)^2\rangle$ approaches the equilibrated value χ_2 from the initial value σ_0 as t becomes larger. Because Eq. (166) depends on t only through X , the variation is slower for larger L . From the right panel of Fig. 10, one can read off the L dependence of $\langle(\delta Q_L)^2\rangle$ for a given t . The panel shows that the value of $\langle(\delta Q_L)^2\rangle$ with fixed t approaches the equilibrated (initial) value as L becomes smaller (larger).

The right panel of Fig. 10 with Eq. (166) also shows that $\langle(\delta Q_L)^2\rangle$ is not proportional to L for finite $t > 0$. This behavior is contrasted to the extensive nature of fluctuations in equilibrium. The L dependence of $\langle(\delta Q_L)^2\rangle/L$ comes from the nonzero correlation $\langle n(x_1, t)n(x_2, t)\rangle$ at $x_1 \neq x_2$, which vanishes in the large t limit. Intuitively, the “memory” of the initial condition gives rise to this correlation. Only when the particles composing the system completely forget the initial condition in the $t \rightarrow \infty$ limit, the equilibrium property Eq. (160) is realized.

An important comment here is that the local equilibration and the equilibration of conserved-charge fluctuations are different concepts. In particular, the latter is not a necessary condition of the former. To see this, we note that the SDE is reasonably obtained if one assumes the local equilibration of the medium. In fact, the local equilibration well justifies the use of the modified Fick’s law Eq. (147) with a diffusion constant. Moreover, the value of susceptibility in equilibrium is used in SDE through the fluctuation dissipation relation, although the SDE is an equation to describe non-equilibrium density profile $n(x, t)$. A reasonable justification for the use of the equilibrium values would be to assume that the microscopic time scales establishing the local equilibration is sufficiently shorter than the typical one of $n(x, t)$. The difference between the time scales comes from the conserving nature of the charge. Because the charge is conserved, the variation of the local density $n(x, t)$ is achieved only through diffusion, i.e. transfer of charges. It, however, can become arbitrary slow as the length scale becomes longer, as shown in the L dependence of Eq. (166). For non-conserving quantities, on the other hand, the variation of the local density is typically insensitive to the length scale.

5.2.3 Discussions

Next, we comment on the description of non-Gaussian cumulants of Q_L or $n(x, t)$ in the SDE. As in the previous section, it is easy to show that the fluctuation of Q_L becomes of Gaussian in the $t \rightarrow \infty$ limit; $\langle Q_L^n \rangle_c = 0$ for $n \geq 3$ in this limit. When one wants to describe the time evolution of non-Gaussian cumulants toward the *nonzero* equilibrated value, the SDE Eq. (148) with Eq. (163) is not suitable. One may try to introduce higher order correlation of $\xi(x, t)$ so that Q_L in the $t \rightarrow \infty$ limit becomes

non-Gaussian. However, similarly to the argument in Sec. 5.1 it is rigorously shown that the stochastic term in the SDE must be of Gaussian and higher order correlations vanish [73]

$$\langle \xi(x_1, t_1) \cdots \xi(x_n, t_n) \rangle_c = 0 \quad \text{for } n \geq 3. \quad (169)$$

It is possible to introduce nonzero higher order correlation of $\xi(x, t)$ by brute force ignoring the theorem. This trial, however, results in failure with unphysical long-range correlations in higher order correlations of $\xi(x, t)$ [150]. Another way to make the distribution of Q_L in equilibrium non-Gaussian in the SDE is to make the susceptibility $n(x, t)$ dependent. With $n(x, t)$ dependent χ_2 , Q_L in equilibrium becomes non-Gaussian even with the Gaussian stochastic term. In this case, however, the SDE becomes nonlinear and analytic treatment of the equation becomes difficult. In Sec. 5.4, we consider another model for diffusion processes which can describe nonzero non-Gaussian fluctuations in equilibrium.

The fluctuation dissipation relation for the SDE discussed in this subsection can be generalized to hydrodynamic equations in a similar manner [95]. Besides Eq. (143), the hydrodynamic equations are constructed from the conservation law of energy-momentum tensor

$$\partial_\mu T_{\mu\nu} = 0, \quad (170)$$

and the constitutive equations for the elements of $T_{\mu\nu}$. In a usual dissipative hydrodynamic equations, the constitutive equations are deterministic. With a motivation similar to that with which we have introduced the SDE, it is possible to promote these equations to those with stochastic terms. Assuming the locality of the stochastic terms, their magnitudes are determined by macroscopic observables including viscosity via the fluctuation dissipation relation [95]. This procedure is extended to relativistic systems in Ref. [148], in which an application of the stochastic equations to relativistic heavy ion collisions is addressed. The stochastic equations constructed in this way are called theory of hydrodynamic fluctuations or stochastic hydrodynamics. The SDE is regarded as a counterpart of this formalism.

5.3 Diffusion of fluctuations in heavy ion collisions

The purpose of event-by-event analysis in relativistic heavy ion collisions is to measure anomalous behaviors in thermal fluctuations which occur in the early stage of the time evolution. As discussed in Sec. 4 already, however, the experimental detectors can only measure the fluctuations in the final state. Even if anomalous thermal fluctuations are well developed in the early stage, the fluctuations are modified in the hadronic medium owing to diffusion. For conserved charges, this time evolution is caused by diffusion process [21, 22, 149], and would be well described by the SDE.

Under the Bjorken expansion, the diffusion of conserved charges takes place in coordinate-space rapidity space, and rapidity window ΔY to count the particle number serves as the length L in Eq. (146). It is thus expected that the magnitude of conserved-charge fluctuations is more QGP like as ΔY becomes wider, while the magnitude becomes more hadronic for narrower ΔY . Assuming the correspondence between ΔY and the (momentum-space) rapidity interval $\Delta\eta$, such a behavior is in fact observed by ALICE collaboration in net-electric charge fluctuation as shown in Fig. 1 [27]. In the figure, the right vertical axis represents the D -measure Eq. (129), a quantity proportional to net-electric charge fluctuation $\langle N_Q^2 \rangle_c / \Delta\eta$. The figure shows that as $\Delta\eta$ becomes larger the magnitude of $\langle N_Q^2 \rangle_c / \Delta\eta$ is more suppressed. If the magnitude of $\langle N_Q^2 \rangle_c$ is small in the early stage in the time evolution, this $\Delta\eta$ dependence is reasonably understood as a result of the diffusion process discussed in the previous subsection.

In Sec. 4.1.2, we discussed that the experimental measurements are performed in a (pseudo-)rapidity window, $\Delta\eta$. On the other hand, thermal fluctuations are defined in a coordinate-space rapidity window ΔY , and the diffusion process also takes place in coordinate space. As discussed in Sec. 4.1.2, there is only an approximate correspondence between the rapidities Y and η even if the Bjorken picture holds

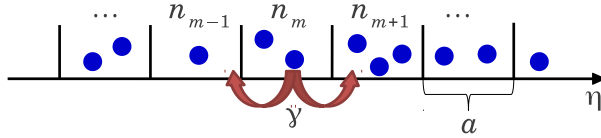


Figure 11: System described by the diffusion master equation Eq. (171).

for the flow of the medium; the measurement in rapidity η is accompanied with a blurring arising from the thermal motion of individual particles at kinetic freezeout. However, the effect of the blurring due to the rapidity conversion can be regarded as if it were a part of the diffusion effects, because the distribution of the thermal motion in y space is almost Gaussian as already discussed in Sec. 4.1.2. Therefore, the above interpretation on the $\Delta\eta$ dependence of Fig. 1 hardly changes even after including the effect of blurring, although in this case the value of diffusion length $\sqrt{2Dt}$ has to be understood as the one including the effects of blurring [127, 128].

The time evolution of fluctuations of conserved charges has also been investigated in molecular dynamical models in Refs. [133, 151]. Extension of the SDE to include the memory effect by introducing higher order time derivative(s) to the diffusion equation is discussed in Refs. [152, 153].

The D -measure has also been measured at RHIC [154, 155, 156]. Contrary to the ALICE result, these results are consistent with the value in the hadronic medium ($\sqrt{s_{\text{NN}}}$ dependence of the D -measure is nicely summarized in Fig. 4 in Ref. [27]). The maximum $\Delta\eta$ in these experiments, $\Delta\eta = 1.0$, determined by the structure of the detectors, however, is smaller than the one of the ALICE, $\Delta\eta = 1.6$. As is evident in Fig. 1, the narrower $\Delta\eta$ makes $\langle N_Q^2 \rangle_c$ more hadronic. This difference in $\Delta\eta$ in these experiments would be one of the origins of the contradiction.

When the hot medium passes through near the QCD critical point, besides the diffusion of conserved charges, the dynamical time evolution of sigma field $\sigma = \langle \bar{\psi}\psi \rangle$, which is the order parameter of the chiral phase transition, has to be considered simultaneously. Although the fluctuation of σ diverges at the critical point in equilibrium, in dynamical system the approach to the equilibrium value is limited due to the critical slowing down. The growth of the fluctuation of σ is investigated in terms of the correlation length of σ field in Refs. [157, 158]. These studies suggest that the growth of the correlation length is limited to $\xi \simeq 2$ fm even if the system passes exactly on the critical point. The time evolution of the third- and fourth-order cumulants of σ near the critical point is discussed in Ref. [159]. To describe the time evolution of conserved-charge fluctuations near the critical point, the coupling of σ with the conserved charge [107, 108] should play a crucial role. Attempts to model the time evolution of fluctuations incorporating both σ and conserved-charge fields in a stochastic formalism are made in Refs. [160, 161, 162, 163]. When the hot medium undergoes a first-order phase transition, the fluctuation would be enhanced owing to domain formation [163] and spinodal instabilities [164, 165, 166]. Understanding these highly dynamical processes, especially the growth of fluctuations and their effects on experimental signals, is an interesting future subject.

5.4 $\Delta\eta$ dependence of higher order cumulants

In Sec. 5.2, we have seen that the SDE is suitable to describe the diffusion process of Gaussian fluctuations. As discussed there, however, in this model it is difficult to describe nonzero non-Gaussian fluctuations in equilibrium. Accordingly, this formalism is not suitable to describe the approach of non-Gaussian cumulants toward nonzero equilibrated value, which would happen in heavy ion collisions.

For a description of the time evolution of non-Gaussian cumulants in diffusive systems, a model called the diffusion master equation (DME) [73] is employed in Refs. [145, 137, 70]. A feature of

these studies is that the discrete nature of particle number is explicitly treated. In the DME for one dimensional problems, the coordinate is divided into discrete cells with an equal length a (see, Fig. 11). We denote the number of particles in each cell, labeled by an integer m , as n_m . We then introduce the probability distribution function $P(\mathbf{n}, t)$ that each cell contains n_m particles at time t with $\mathbf{n} = (\dots, n_{m-1}, n_m, n_{m+1}, \dots)$. It is also assumed that each particle moves to adjacent cells with a probability γ per unit time, as a result of microscopic interactions and random motion. The probability $P(\mathbf{n}, t)$ then obeys the differential equation

$$\begin{aligned} \partial_\tau P(\mathbf{n}, \tau) = & \gamma(t) \sum_m [(n_m + 1)\{P(\mathbf{n} + \mathbf{e}_m - \mathbf{e}_{m+1}, \tau) + P(\mathbf{n} + \mathbf{e}_m - \mathbf{e}_{m-1}, \tau)\} \\ & - 2n_m P(\mathbf{n}, \tau)], \end{aligned} \quad (171)$$

where \mathbf{e}_m is the vector that all components are zero except for the m th-one, which takes unity. Equation (171) is referred to as the DME [73].

The time evolution of the cumulants and correlation functions of particle number described by the DME, Eq. (171), can be solved analytically [68]. To obtain the solution for arbitrary initial conditions, it is convenient to use the formula of superposition of probability distribution functions given in Appendix A [68, 70]. One then takes the continuum limit, $a \rightarrow 0$, of this solution. It is shown that the time evolution of average density $\langle n(x, t) \rangle$ after taking the continuum limit is consistent with the one obtained with the diffusion equation Eq. (145) with the diffusion constant $D(t) = \gamma(t)a^2$. Moreover, the time evolution of the second-order cumulant with the DME is also consistent with that with the SDE.

In the DME, motion of the individual particles composing the system is given by random walk without correlations with one another. The time evolution of the particle distribution thus is given by the superposition of these uncorrelated particles. In this sense, it is reasonable that the solution of the DME is consistent with those in the diffusion equation and the SDE. In the $t \rightarrow \infty$ limit, each particle exists any position with an equal probability irrespective of the initial condition, and they are uncorrelated with each other. The particle number Q_L in an interval L , therefore, is simply given by the Poisson distribution in this limit when L is sufficiently smaller than the length of the system (see, Sec. 2.4.2). The cumulants of Q_L in this limit thus are given by

$$\langle Q_L^n \rangle_c = \langle Q_L \rangle = \rho L \quad (172)$$

with the average density ρ .

The time evolution of the second-order cumulant in the DME agrees with that in the SDE with $\chi_2 = \rho$. On the other hand, higher order cumulants in the DME take nonzero values in equilibrium as shown in Eq. (172) contrary to the case of the SDE. Therefore, the DME is regarded as an extension of the SDE to describe the approach of the higher order cumulants toward nonzero equilibrium values.

The DME can be extended to the system with multi-particle species. This allows us to define the difference of two particle numbers. Because the distributions of two particle numbers in an interval L become Poissonian in equilibrium, the difference of the particle numbers in the interval is given by the the Skellam distribution in equilibrium. This property is suitable for the description of diffusion process of net-baryon number in the hadronic medium in heavy ion collisions, because its fluctuations in the HRG model are given by the Skellam distribution as discussed in Sec. 3.3.1.

Now we consider the time evolution in the DME. To compare the result with fluctuations in heavy ion collisions, we call the spatial coordinate as rapidity η , and the difference of the particle numbers as net-particle number. We also denote the net-particle number in a rapidity interval $\Delta\eta$ as $Q_{(\text{net})}$. Similarly to the case of the solution of SDE in Sec. 5.2, the time evolution of the cumulants $\langle Q_{(\text{net})}^n \rangle_c$ depends on $\Delta\eta$ and the proper time τ only through a combination $X = d(\tau)/\Delta\eta$, where $d(\tau)$ is the

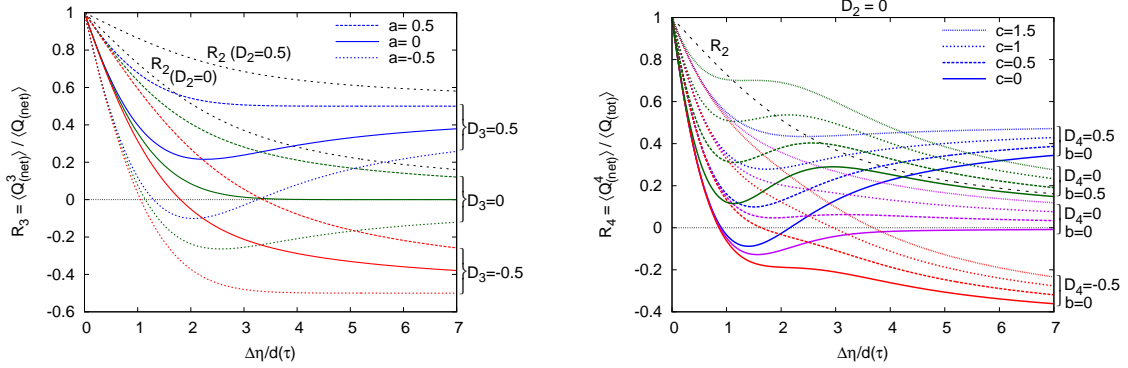


Figure 12: Example of the solution of Eq. (171) [70]. Behaviors of the third- and fourth-order cumulants as functions of rapidity window ($\Delta\eta$) for various initial conditions.

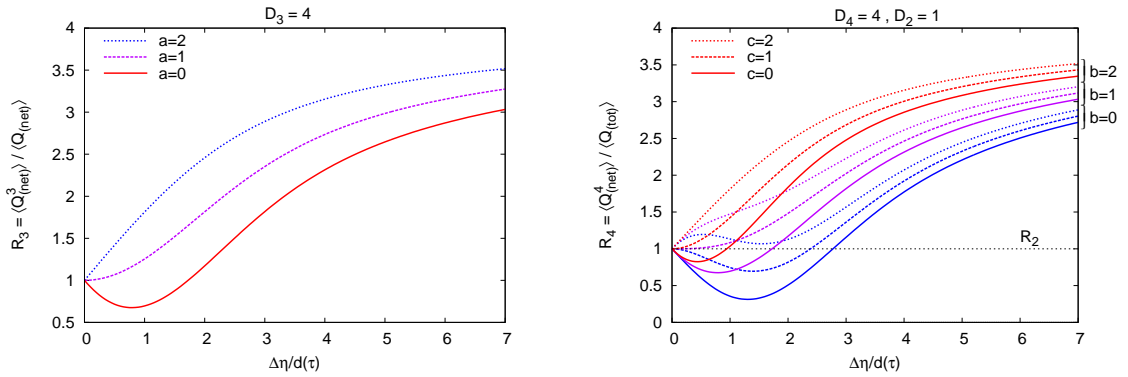


Figure 13: Same as Fig. 12, but with initial condition with larger higher order cumulants.

diffusion distance in rapidity space,

$$d(\tau) = \sqrt{2 \int_{\tau_{\text{initial}}}^{\tau} d\tau D(\tau)}. \quad (173)$$

As discussed in Sec. 5.3, one has to distinguish the coordinate- and momentum-space rapidities. Because the effect of thermal blurring accompanied with the conversion of these rapidities can be regarded as a part of diffusive process as discussed in Sec. 5.3, in this subsection we do not distinguish the rapidities. We, however, have to reinterpret the meaning of $d(\tau)$ to include the effect of the blurring.

In Figs. 12 and 13, we show some examples of the $\Delta\eta$ dependences of third- (left) and fourth- (right) order cumulants obtained in the DME [70]. In these figures, the cumulants are normalized by their equilibrated values. These quantities thus become unity at $\Delta\eta = 0$. The initial conditions are chosen so as to satisfy the locality condition Eq. (84), with the coefficients in front of the delta-function, D_2 , D_3 , D_4 , a , b and c , are treated as free parameters. Here, D_n is the n th-order susceptibility of the net charge in the initial condition. Figure 12 shows the results for initial conditions with small susceptibilities D_3 and D_4 , while in Fig. 13 D_3 and D_4 are taken large. The figures show that the $\Delta\eta$ dependences of higher order cumulants are sensitive to the initial condition. In particular, it is interesting that the third- and fourth-order cumulants can have non-monotonic dependences on $\Delta\eta$. These $\Delta\eta$ dependences can directly be compared with the experimental results [32, 167]. The comparison of the $\Delta\eta$ dependences in these experiments with those in the DME in Figs. 12 and 13 will lead us to deeper understanding on the fluctuation observables, such as the effects of diffusion in the hadronic stage and thermal blurring accompanied with the rapidity conversion. It would also enable us to extract the initial values of cumulants. Experimental measurement of the non-monotonic $\Delta\eta$ dependences in Figs. 12 and 13 is also an interesting subject.

6 Binomial model

In this section, we address two problems associated with the experimental measurement of conserved-charge fluctuations which are not covered in Secs. 4 and 5. One of them is concerned with the measurement of net-baryon number cumulants. As discussed in Sec. 3, among the thermal fluctuations of conserved charges that of net-baryon number shows the most clear signal of the phase transitions. The present experimental detectors, however, are not capable of their measurement because the detectors cannot count neutral baryons, in particular neutrons. As proxies of net-baryon number cumulants, those of net-proton number are measured [26, 28, 32] and compared with theoretical studies on the net-baryon number cumulants in the literature. The systematic error arising from this substitution has to be estimated carefully [98, 99]. The second issue is the effect of the finite efficiency and acceptance of detectors. The real detectors cannot observe all particles entering them, but lose some of them with some nonzero probability. The probability to observe a particle is called efficiency⁵ The detectors also have limitation in acceptance. For example, some azimuthal angles are not covered by the detectors, or hidden by materials in front of the detectors, and the particles arriving at such azimuthal angles are not detected. The finite efficiency and acceptance modify the event-by-event fluctuation [99, 67]. These two problems are in fact understood simultaneously. In fact, the measurement of net-proton number in place of the net-baryon number is regarded as 50% efficiency loss. In this section, in order to describe these effects, we employ a model for probability distribution that we call the “binomial model”. The binomial model is first introduced in Ref. [98] to discuss the similarity and difference between the

⁵This definition of efficiency is an ideal one and different from ones used in most of experiments, in which acceptance and efficiency cannot be separated uniquely for various reasons such as the existence of magnetic field, non-zero probability of simultaneous hits, and so forth.

net-baryon and net-proton number cumulants, and then extended to investigate the effect of efficiency correction [99, 67]. The purpose of this section is to review the binomial model and deal with these problems.

6.1 A model for efficiency

For an illustration of the binomial model, let us first consider the following simple problem. We consider a probability distribution function $P(N)$ for an integer stochastic variable N . To be specific, we suppose that N is the number of some particles in each “event” in some experiment. In order to determine $P(N)$ experimentally, one would repeat the measurements of the particle number for individual events. If measurements of the particles are carried out exactly for each event without any loss, one can determine the histogram corresponding to $P(N)$ and the corresponding cumulants. By increasing the number of measurements, the error of the cumulants can be suppressed arbitrarily.

Now, suppose that we are in a situation where our detector is not perfect, and can count particles only with a probability less than unity. The particle number observed in each event, n , then would be smaller than the actual number N . In this case, the histogram $\tilde{P}(n)$ for the detected particle number n is of course different from $P(N)$. Accordingly, the cumulants of $\tilde{P}(n)$, i.e. those constructed from the experimental result, are not the same as the real cumulants of $P(N)$, either. The question is how to obtain the cumulants of $P(N)$ in this incomplete experiment.

This problem can be solved completely when the probability to detect a particle is a constant for all events and *uncorrelated with one another for individual particles* in an event. Let us denote the probability p . Then, if the actual particle number in an event is N , the probability to find n particles in this event is given by the binomial distribution function $B_{p,N}(n)$ in Eq. (26). The distribution function $\tilde{P}(n)$ is then given by

$$\tilde{P}(n) = \sum_N B_{p,N}(n)P(N). \quad (174)$$

We refer to Eq. (174) as the binomial model.

When Eq. (174) is justified, the cumulants of $P(N)$ can be written by using those of $\tilde{P}(n)$. To understand the origin of such relations, we note that Eq. (174) is a linear relation connecting two distribution functions. In fact, this equation can be rewritten using an infinite-dimensional matrix $M(n, N)$ as $\tilde{P}(n) = \sum_N M(n, N)P(N)$ with $M(n, N) = B_{p,N}(n)$ [99]. Moreover, the matrix $M(n, N)$ is upper triangular in the sense that $M(n, N) = 0$ for $n > N$. The inverse of $M(n, N)$ thus can be constructed iteratively. Using the inverse matrix $M(N, n)^{-1}$, $P(N)$ can be represented as

$$P(N) = \sum_n M(N, n)^{-1}\tilde{P}(n). \quad (175)$$

Unfortunately, however, it is easily shown that $M(N, n)^{-1}$ has a singular behavior, and the determination of the distribution function $P(N)$ itself from Eq. (175) with the information on $\tilde{P}(n)$ is not possible. Nevertheless, in the binomial model Eq. (174) the cumulants of $P(N)$ can be represented by those of $\tilde{P}(n)$, and vice versa. The results up to the fourth-order are given by [99, 65]

$$\langle n \rangle = \xi_1 \langle N \rangle, \quad (176)$$

$$\langle n^2 \rangle_c = \xi_1^2 \langle N^2 \rangle_c + \xi_2 \langle N \rangle, \quad (177)$$

$$\langle n^3 \rangle_c = \xi_1^3 \langle N^3 \rangle_c + 3\xi_1 \xi_2 \langle N^2 \rangle_c + \xi_3 \langle N \rangle, \quad (178)$$

$$\langle n^4 \rangle_c = \xi_1^4 \langle N^4 \rangle_c + 6\xi_1^2 \xi_2 \langle N^3 \rangle_c + (3\xi_2^2 + 4\xi_1 \xi_3) \langle N^2 \rangle_c + \xi_4 \langle N \rangle, \quad (179)$$

and

$$\langle N \rangle = \xi_1^{-1} \langle n \rangle, \quad (180)$$

$$\langle N^2 \rangle_c = \xi_1^{-2} \langle n^2 \rangle_c - \xi_2 \xi_1^{-3} \langle n \rangle, \quad (181)$$

$$\langle N^3 \rangle_c = \xi_1^{-3} \langle n^3 \rangle_c - 3\xi_2 \xi_1^{-4} \langle n^2 \rangle_c + (3\xi_2^2 \xi_1^{-5} - \xi_3 \xi_1^{-4}) \langle n \rangle, \quad (182)$$

$$\langle N^4 \rangle_c = \xi_1^{-4} \langle n^4 \rangle_c - 6\xi_2 \xi_1^{-5} \langle n^3 \rangle_c + (15\xi_2^2 \xi_1^{-6} - 4\xi_3 \xi_1^{-5}) \langle n^2 \rangle_c - (15\xi_2^3 \xi_1^{-7} - 10\xi_2 \xi_3 \xi_1^{-6} + \xi_4 \xi_1^{-5}) \langle n \rangle, \quad (183)$$

where ξ_n are the coefficient of the cumulants of the binomial distribution function defined in Eqs. (30) and (31). The derivation of these results is found in Ref. [65], which makes use of the relations of cumulants summarized in Appendix. A. The equivalent result can be obtained on the basis of the factorial moments [67]. Equations (180) – (183) show that the cumulants of $P(N)$ can be reconstructed from the incomplete information obtained in experiments.

To apply the binomial model to the analysis of net-particle number in relativistic heavy ion collisions, the model has to be extended to probability distribution functions for at least two stochastic variables representing particle and anti-particle numbers. Suppose that the probability that N particles and \bar{N} anti-particles arrive at the detector for each event is given by $P(N, \bar{N})$. We then assume that the detector finds these particles and anti-particles with probabilities p and \bar{p} , respectively, which are independent for individual particles. The distribution function $\tilde{P}(n, \bar{n})$ that n particles and \bar{n} anti-particles are found by the detector in each event is then given by

$$\tilde{P}(n, \bar{n}) = \sum_{N, \bar{N}} B_{p, N}(n) B_{\bar{p}, \bar{N}} P(N, \bar{N}). \quad (184)$$

Assuming this factorization, the cumulants of N and \bar{N} can again be given by those of n and \bar{n} [99, 67]. The model can also be extended to multi variable cases [69, 168, 65]. In the analysis of fluctuations by STAR collaboration, the efficiency correction is taken into account using the binomial model [28, 30, 32]. We note that a similar statistical model is also applied in [169, 170].

When one applies the binomial model, however, it has to be remembered that this model is justified only when the efficiency to measure particles is independent for individual particles. It has been recently pointed out that the violation of this assumption in real detectors can significantly modify the reconstructed values of the cumulants especially for higher order ones [171].

6.2 Net-baryon vs net-proton number cumulants

Now, let us consider the relation between the net-baryon and net-proton number cumulants [98, 99]. In this discussion, we use the fact that an (anti-)baryon arriving at the detector is an (anti-)proton with some probability about 50%. If the probability that an (anti-)baryon is an (anti-)proton is uncorrelated for individual (anti-)baryons, one thus can apply the binomial model to relate the (anti-)baryon and (anti-)proton numbers. Similarly to the previous case, the probability $\mathcal{G}(N_p, N_{\bar{p}})$ to observe N_p protons and $N_{\bar{p}}$ anti-protons in an event is related to the probability $\mathcal{F}(N_B, N_{\bar{B}})$ that N_B baryons and $N_{\bar{B}}$ antibaryons enters the detector in the event as

$$\begin{aligned} \mathcal{G}(N_p, N_{\bar{p}}) &= \sum_{N_B, N_{\bar{B}}} \mathcal{P}(N_p, N_{\bar{p}}; N_B, N_{\bar{B}}) \\ &= \sum_{N_B, N_{\bar{B}}} B_{r, N_B}(N_p) B_{\bar{r}, N_{\bar{B}}}(N_{\bar{p}}) \mathcal{F}(N_B, N_{\bar{B}}), \end{aligned} \quad (185)$$

where r (\bar{r}) is the probability that a baryon (an anti-baryon) arriving at the detector is a proton (anti-proton). Using Eq. (185), one can relate the net-proton number cumulants with those of net-baryons,

and vice versa; explicit formulas are given in Ref. [99]. Using these formulas, it is possible to obtain the net-baryon number cumulants experimentally by measuring only protons and anti-protons.

An important point of this argument is that in this case the assumption on the independence of the probabilities required for the validity of the binomial model Eq. (185) can be justified from a microscopic argument for sufficiently large $\sqrt{s_{\text{NN}}}$ [98, 99]. Therefore, the use of the binomial model is well justified in this problem. The key ingredient for this discussion is $N\pi$ reactions in the hadronic stage mediated by $\Delta(1232)$ resonances having the isospin $I = 3/2$. These reactions frequently take place even after chemical freezeout in the hadronic medium during the time evolution of the fireballs, and in fact are the most dominant reactions of nucleons in the hadronic medium. These reactions contain charge exchange reactions, which alter the third component of the isospin of the nucleon, or the nucleon isospin for short, in the reaction. The reactions of a proton to form Δ are:

$$p + \pi^+ \rightarrow \Delta^{++} \rightarrow p + \pi^+, \quad (186)$$

$$p + \pi^0 \rightarrow \Delta^+ \rightarrow p(n) + \pi^0(\pi^+), \quad (187)$$

$$p + \pi^- \rightarrow \Delta^0 \rightarrow p(n) + \pi^-(\pi^0). \quad (188)$$

Among these reactions, Eqs. (187) and (188) are responsible for the change of the nucleon isospin. The ratio of the cross sections of a proton to form Δ^{++} , Δ^+ , and Δ^0 is $3 : 1 : 2$, which is determined by the isospin $SU(2)$ symmetry of the strong interaction. The isospin symmetry also tells us that the branching ratios of Δ^+ (Δ^0) decaying into the final state having a proton and a neutron are $1 : 2$ ($2 : 1$). Using these ratios, one obtains the ratio of the probabilities that a proton in the hadron gas forms Δ^+ or Δ^0 with a reaction with a thermal pion, and then decays into a proton and a neutron, respectively, $P_{p \rightarrow p}$ and $P_{p \rightarrow n}$, as

$$P_{p \rightarrow p} : P_{p \rightarrow n} = 5 : 4, \quad (189)$$

provided that the hadronic medium is isospin symmetric and that the three isospin states of pions are equally distributed in the medium. Because of the isospin symmetry of the strong interaction one also obtains the same conclusion for neutron reactions:

$$P_{n \rightarrow n} : P_{n \rightarrow p} = 5 : 4. \quad (190)$$

Similar results are also obtained for anti-nucleons. Equations (189) and (190) show that these reactions act to randomize the isospin of nucleons during the hadronic stage. Moreover, the mean time of protons to undergo the charge exchange reaction is $3 \sim 4$ fm for $T = 150 \simeq 170$ MeV in the hadronic gas [99]. Because this mean time is shorter than the typical lifetime of the hadronic stage in heavy ion collisions, all nucleons have chances to undergo the above reaction several times. Because of the charge exchange reaction, the isospins of (anti-)baryons in the final state is randomized almost completely. Although various effects on this conclusion is investigated in Ref. [99], this conclusion is not altered. This is sufficient to justify the binomial model Eq. (185) for the relation between (anti-)baryon and (anti-)proton number distributions.

7 Summary

In this article, we have reviewed physics of bulk fluctuations in relativistic heavy ion collisions. Now, let us recall the experimental results in Figs. 1 and 2. After reading this review, the readers should be able to understand how to interpret these experimental results. In the experimental result of the second-order cumulant of net-electric charge fluctuation in Fig. 1, the second-order cumulant shows a suppression compared with the hadronic value, and the suppression is more prominent for larger rapidity window

$\Delta\eta$. As discussed in Sec. 3, the thermal fluctuations are suppressed when the medium undergoes a deconfinement phase transition. The experimental result in Fig. 1 thus can be interpreted as the remnant of the small fluctuations in the primordial stage. In Sec. 5, we have seen that the $\Delta\eta$ dependence in this experimental result can also be understood reasonably in this picture. The readers should also be able to understand the reason why the quantities plotted in Fig. 2, especially their deviations from unity, contain important information. In Sec. 3, we have learned that these ratios should take unity if the cumulants are well described by hadronic degrees of freedom in equilibrium. Interestingly, the ratios of the cumulants in Fig. 2 show deviations compared to this “baseline” behavior. This deviation clearly shows that the fluctuation carries information of non-hadronic and/or non-thermal physics in relativistic heavy ion collisions. The origin of the deviations, however, is still in debate and is not settled when this manuscript is written. As discussed in Secs. 4, 5 and 6, there are many subtle problems in the comparison between event-by-event fluctuations with theoretical studies on thermal fluctuations. These problems have to be revealed in the cooperation between experimental and theoretical researches as well as numerical analysis in lattice QCD. The experimental analysis of rapidity window dependence discussed in Sec. 5 and its theoretical description are one of the important subjects.

As these examples show, bulk fluctuations are important observables in heavy ion collisions, which encode nontrivial physics on the early thermodynamics of the hot medium and diffusion processes in later stages. The fluctuation observables are expected to become one of the most important quantities in the study of the QCD phase structure in future experimental programs with intermediate collision energies, $3 \lesssim \sqrt{s_{\text{NN}}} \lesssim 20$ GeV, such as the beam-energy scan II (BES-II) program [15] at RHIC, and those planned in FAIR, NICA and J-PARC. Careful analyses of fluctuation observables in these experiments will provide us plenty of information on the QCD phase structure.

Acknowledgment

A large part of this review is written on the basis of a lecture by M. K. at Tsukuba University on Oct. 29–31, 2014. He thanks members of the high energy nuclear experiment group at Tsukuba University, especially Shin-ichi Esumi and Hiroshi Masui for the invitation and discussions during his stay, which are reflected in this article. The authors also thank for many invitations to international workshops on fluctuations and active discussions there, especially Adam Bzdak, Bengt Friman, Frithjof Karsch, Volker Koch, Xiaofeng Luo, Tapan Nayak, Krzysztof Redlich and Nu Xu. The authors thank Hiroshi Horii and Miki Sakaida for reading the manuscript. This work is supported in part by JSPS KAKENHI Grant Numbers 23540307, 25800148 and 26400272.

A Superposition of probability distribution functions

In this appendix, we consider cumulants of a probability distribution function which is given by a superposition of probability distribution functions [99, 70].

Let us consider a probability distribution function $P(x)$ for an integer stochastic variable x , and assume that $P(x)$ consists of the superposition of sub-probabilities as

$$P(x) = \sum_N F(N) P_N(x), \quad (191)$$

where $P_N(x)$ are sub-probabilities labeled by integer N . Each sub-probability is summed with a weight $F(N)$ satisfying $\sum_N F(N) = 1$, which is also regarded as a probability. The purpose of this appendix is to represent the cumulants of $P(x)$ using those of $P_N(x)$ and $F(N)$. Although we write down the results explicitly up to the fourth-order in this article, the result can be extended to higher orders straightforwardly.

We start from the cumulant generating function of Eq. (191),

$$K(\theta) = \log \sum_x e^{\theta x} P(x) = \log \sum_N F(N) \sum_x e^{\theta x} P_N(x) \quad (192)$$

$$= \log \sum_N F(N) \sum_x e^{K_N(\theta)} \quad (193)$$

where $K_N(\theta) = \log \sum_x e^{\theta x} P_N(x)$ is the cumulant generating function for $P_N(x)$. Using the cumulant expansion Eq. (67), Eq. (193) is written as

$$\begin{aligned} K(\theta) &= \sum_m \frac{1}{m!} \sum_F [K_N(\theta)]_c^m \quad (194) \\ &= \sum_F K_N(\theta) + \frac{1}{2} \sum_F (\delta K_N(\theta))^2 + \frac{1}{3!} \sum_F (\delta K_N(\theta))^3 \\ &\quad + \frac{1}{4!} \sum_F [K_N(\theta)]_c^4 + \dots, \quad (195) \end{aligned}$$

where \sum_F is a shorthand notation for $\sum_N F(N)$, and $\sum_F [K_N(\theta)]_c^m$ is the m th-order cumulant of K_N for the sum over F , whose explicit forms up to the fourth-order are given on the far right hand side with

$$\sum_F (\delta K_N(\theta))^n = \sum_F \left(K_N(\theta) - \sum_F K_N(\theta) \right)^n, \quad (196)$$

$$\sum_F [K_N(\theta)]_c^4 = \sum_F (\delta K_N(\theta))^4 - 3 \left(\sum_F (\delta K_N(\theta))^2 \right)^2. \quad (197)$$

Cumulants of $P(x)$ are given by derivatives of $K(\theta)$ as

$$\langle x^n \rangle_c = \left. \frac{\partial^n}{\partial \theta^n} K(\theta) \right|_{\theta} \equiv K^{(n)}. \quad (198)$$

All cumulants can be obtained with Eqs. (198) and (195). In order to calculate the cumulants explicitly, we first note that the normalization condition $\sum_x P_N(x) = 1$ yields $K_N(0) = 0$. From this property, it is immediately concluded that all $K_N(\theta)$ in each term on the far right hand side of Eq. (195) must receive at least one differentiation so that the term gives nonzero contribution to Eq. (198). This means that the m th-order term in Eq. (195) can affect Eq. (198) only if $m \leq n$. Keeping this rule in mind, derivatives of Eq. (195) with $\theta = 0$ is given by

$$K^{(1)} = \sum_F K_N^{(1)}, \quad (199)$$

$$K^{(2)} = \sum_F K_N^{(2)} + \sum_F (\delta K_N^{(1)})^2, \quad (200)$$

$$K^{(3)} = \sum_F K_N^{(3)} + 3 \sum_F \delta K_N^{(1)} \delta K_N^{(2)} + \sum_F (\delta K_N^{(1)})^3, \quad (201)$$

$$\begin{aligned} K^{(4)} &= \sum_F K_N^{(4)} + 4 \sum_F \delta K_N^{(1)} \delta K_N^{(3)} + 3 \sum_F (\delta K_N^{(2)})^2 + 6 \sum_F (\delta K_N^{(1)})^2 \delta K_N^{(2)} \\ &\quad + \sum_F (\delta K_N^{(1)})_c^4, \quad (202) \end{aligned}$$

with $K_N^{(n)} = \left. \frac{\partial^n K_N(\theta)}{\partial \theta^n} \right|_{\theta=0}$ being the cumulants of the sub-probabilities $P_N(x)$. Equations (199) - (202) relate the cumulants $K^{(n)}$ with $K_N^{(n)}$.

The above relations are further simplified when the cumulants of $P_N(x)$ are at most linear with respect to N , i.e.

$$K_N^{(n)} = N\xi_{(n)} + \zeta_{(n)}, \quad (203)$$

where $\xi_{(n)}$ and $\zeta_{(n)}$ are constants which do not depend on N . Substituting Eq. (203) into Eqs. (199) - (202) one obtains

$$K^{(1)} = \zeta_{(1)} + \xi_{(1)} \langle N \rangle_F, \quad (204)$$

$$K^{(2)} = \zeta_{(2)} + \xi_{(2)} \langle N \rangle_F + \xi_{(1)}^2 \langle \delta N^2 \rangle_F, \quad (205)$$

$$K^{(3)} = \zeta_{(3)} + \xi_{(3)} \langle N \rangle_F + 3\xi_{(1)}\xi_{(2)} \langle \delta N^2 \rangle_F + \xi_{(1)}^3 \langle \delta N^3 \rangle_F, \quad (206)$$

$$K^{(4)} = \zeta_{(4)} + \xi_{(4)} \langle N \rangle_F + (4\xi_{(1)}\xi_{(3)} + 3\xi_{(2)}^2) \langle \delta N^2 \rangle_F + 6\xi_{(1)}^2 \xi_{(2)} \langle \delta N^3 \rangle_F + \xi_{(1)}^4 \langle \delta N^4 \rangle_{c,F}, \quad (207)$$

where $\langle O(N) \rangle_F = \sum_N O(N)F(N)$ denotes the average over $F(N)$; these averages in the above formulas represent cumulants of the probability $F(N)$.

Extension of these results to the case of multi variable distribution functions is addressed in Ref. [70].

References

- [1] M. Cheng, N. H. Christ, S. Datta, J. van der Heide, C. Jung, F. Karsch, O. Kaczmarek and E. Laermann *et al.*, Phys. Rev. D **74**, 054507 (2006).
- [2] Y. Aoki, G. Endrodi, Z. Fodor, S. D. Katz and K. K. Szabo, Nature **443**, 675 (2006).
- [3] M. Asakawa and K. Yazaki, Nucl. Phys. A **504** (1989) 668.
- [4] M. Kitazawa, T. Koide, T. Kunihiro and Y. Nemoto, Prog. Theor. Phys. **108** (2002) 929 [hep-ph/0207255].
- [5] M. A. Stephanov, Proc. Sci. LAT2006 (2006) 024. [arXiv:hep-lat/0701002].
- [6] K. Fukushima and T. Hatsuda, Rept. Prog. Phys. **74** (2011) 014001 [arXiv:1005.4814 [hep-ph]].
- [7] O. Philipsen, Acta Phys. Polon. Supp. **5** (2012) 825
- [8] I. Arsene *et al.* [BRAHMS Collaboration], Nucl. Phys. A **757**, 1 (2005); B. B. Back *et al.* [PHOBOS Collaboration], Nucl. Phys. A **757**, 28 (2005); J. Adams *et al.* [STAR Collaboration], Nucl. Phys. A **757**, 102 (2005); K. Adcox *et al.* [PHENIX Collaboration], Nucl. Phys. A **757**, 184 (2005).
- [9] B. Muller, J. Schukraft and B. Wyslouch, Ann. Rev. Nucl. Part. Sci. **62**, 361 (2012) [arXiv:1202.3233 [hep-ex]].
- [10] A. Andronic, P. Braun-Munzinger and J. Stachel, Phys. Lett. B **673** (2009) 142 [Phys. Lett. B **678** (2009) 516] [arXiv:0812.1186 [nucl-th]].
- [11] L. Kumar [STAR Collaboration], Nucl. Phys. A **904-905** (2013) 256c [arXiv:1211.1350 [nucl-ex]].
- [12] P. Braun-Munzinger, K. Redlich and J. Stachel, arXiv:nucl-th/0304013.
- [13] J. Randrup and J. Cleymans, Phys. Rev. C **74** (2006) 047901 [hep-ph/0607065].
- [14] STAR Collaboration, "Experimental Study of the QCD Phase Diagram & Search for the Critical Point: Selected Arguments for the Run-10 Beam Energy Scan," STAR Notes SN0493, <https://drupal.star.bnl.gov/STAR/starnotes/public/sn0493> (2009).

- [15] STAR Collaboration, “Studying the Phase Diagram of QCD Matter at RHIC,” STAR Notes SN0598, <https://drupal.star.bnl.gov/STAR/starnotes/public/sn0598> (2014).
- [16] R. Rapp *et al.*, Lect. Notes Phys. **814** (2011) 335.
- [17] “Design and construction of nuclotron-based ion collider facility (NICA) conceptual design report”, http://nica.jinr.ru/files/NICA_CDR.pdf (2008).
- [18] M. A. Stephanov, K. Rajagopal, and E. V. Shuryak, Phys. Rev. Lett. **81** (1998) 4816.
- [19] M. Kitazawa, Nucl. Phys. A **931** (2014) 92.
- [20] V. Koch, arXiv:0810.2520 [nucl-th].
- [21] M. Asakawa, U. W. Heinz, and B. Müller, Phys. Rev. Lett. **85** (2000) 2072.
- [22] S. Jeon and V. Koch, Phys. Rev. Lett. **85** (2000) 2076.
- [23] S. Ejiri, F. Karsch, and K. Redlich, Phys. Lett. **B633** (2006) 275.
- [24] M. A. Stephanov, K. Rajagopal and E. V. Shuryak, Phys. Rev. D **60** (1999) 114028 [hep-ph/9903292].
- [25] Y. Hatta and M. A. Stephanov, Phys. Rev. Lett. **91** (2003) 102003 [Phys. Rev. Lett. **91** (2003) 129901] [hep-ph/0302002].
- [26] M. M. Aggarwal *et al.* [STAR Collaboration], Phys. Rev. Lett. **105** (2010) 022302.
- [27] B. Abelev *et al.* [ALICE Collaboration], Phys. Rev. Lett. **110** (2013) 152301.
- [28] L. Adamczyk *et al.* [STAR Collaboration], Phys. Rev. Lett. **112** (2014) 032302.
- [29] T. Anticic *et al.*, Phys. Rev. C **89** (2014) 5, 054902 [arXiv:1310.3428 [nucl-ex]].
- [30] L. Adamczyk *et al.* [STAR Collaboration], Phys. Rev. Lett. **113** (2014) 092301. [arXiv:1402.1558 [nucl-ex]].
- [31] J. T. Mitchell [PHENIX Collaboration], Nucl. Phys. A904-905 (2013) 903c; [arXiv:1211.6139 [nucl-ex]].
- [32] X. Luo [STAR Collaboration], PoS CPOD **2014** (2015) 019 [arXiv:1503.02558 [nucl-ex]].
- [33] A. Adare *et al.* [PHENIX Collaboration], arXiv:1506.07834 [nucl-ex].
- [34] H. T. Ding, F. Karsch and S. Mukherjee, Int. J. Mod. Phys. E **24** (2015) 10, 1530007 [arXiv:1504.05274 [hep-lat]].
- [35] S. Borsanyi, Proc. Sci. **LATTICE2015** (2015) 015 [arXiv:1511.06541 [hep-lat]].
- [36] M. A. Stephanov, Phys. Rev. Lett. **102** (2009) 032301.
- [37] M. Asakawa, S. Ejiri, and M. Kitazawa, Phys. Rev. Lett. **103** (2009) 262301 [arXiv:0904.2089 [nucl-th]].
- [38] R. Landauer, Nature **392** (1998) 658.
- [39] A. Einstein, Annalen der Physik **17** (1905) 549.
- [40] J. Perrin, Annales de chimie et de physique VIII **18** (1909) 5.
- [41] P. A. R. Ade *et al.* [Planck Collaboration], Astron. Astrophys. **571** (2014) A1 [arXiv:1303.5062 [astro-ph.CO]].
- [42] D. Baumann, arXiv:0907.5424 [hep-th].
- [43] J. M. Maldacena, JHEP **0305** (2003) 013 [astro-ph/0210603].
- [44] N. Bartolo, E. Komatsu, S. Matarrese and A. Riotto, Phys. Rept. **402** (2004) 103 [astro-ph/0406398].
- [45] P. A. R. Ade *et al.* [Planck Collaboration], Astron. Astrophys. **571** (2014) A24 [arXiv:1303.5084 [astro-ph.CO]].
- [46] J. B. Johnson, Phys. Rev. **32** (1928) 97.

- [47] H. Nyquist, Phys. Rev. **32** (1928) 110.
- [48] W. Schottky, Ann. der Phys. **57** (1918) 541.
- [49] X. Jehl, *et al.*, Nature **405** (2000) 50.
- [50] L. Saminadayar, D. C. Glattli, Y. Jin, and B. Etienne, Phys. Rev. Lett. **79**, 2526 (1997).
- [51] See, for example, L. S. Levitov and G. B. Lesovik, JETP Lett., **58** (1993) 230; B. Reulet, J. Senzier and D. E. Prober, Phys. Rev. Lett. **91** (2003) 196601; S. Gustavssona, *et al.*, Surf. Sci. Rep. **64** (2009) 191.
- [52] S. Pratt, Phys. Rev. Lett. **108** (2012) 212301.
- [53] S. A. Bass, P. Danielewicz, and S. Pratt, Phys. Rev. Lett. **85** (2000) 2689.
- [54] S. Jeon and S. Pratt, Phys. Rev. C **65** (2002) 044902.
- [55] B. Ling, T. Springer and M. Stephanov, Phys. Rev. C **89** (2014) 6, 064901.
- [56] K. Pearson, “On the General Theory of Skew Correlation and Non-linear Regression,” (Dulau and Co., London, 1905).
- [57] D. J. Gross, R. D. Pisarski, and L. G. Yaffe, Rev. Mod. Phys. **53** (1981) 43.
- [58] C. Bonati, M. D’Elia, H. Panagopoulos and E. Vicari, Phys. Rev. Lett. **110**, no. 25, 252003 (2013) [arXiv:1301.7640 [hep-lat]].
- [59] R. Kitano and N. Yamada, arXiv:1506.00370 [hep-ph].
- [60] S. Borsanyi *et al.*, arXiv:1508.06917 [hep-lat].
- [61] X. Luo, J. Phys. G **39** (2012) 025008 [arXiv:1109.0593 [physics.data-an]].
- [62] K. Morita, B. Friman, K. Redlich, and V. Skokov, Phys. Rev. C **88** (2013) 034903 [arXiv:1301.2873 [hep-ph]].
- [63] K. Morita, V. Skokov, B. Friman and K. Redlich, Eur. Phys. J. C **74** (2014) 2706 [arXiv:1211.4703 [hep-ph]].
- [64] K. Morita, B. Friman and K. Redlich, Phys. Lett. B **741** (2015) 178 [arXiv:1402.5982 [hep-ph]].
- [65] M. Kitazawa, arXiv:1602.01234 [nucl-th].
- [66] J. W. Negele and H. Orland, “Quantum Many-particle Systems” (Perseus, 1998).
- [67] A. Bzdak and V. Koch, Phys. Rev. C **86** (2012) 044904.
- [68] M. Kitazawa, M. Asakawa, and H. Ono, Phys. Lett. B **728** (2014) 386 [arXiv:1307.2978].
- [69] X. Luo, Phys. Rev. C **91** (2015) 3, 034907 [arXiv:1410.3914 [physics.data-an]].
- [70] M. Kitazawa, Nucl. Phys. A **942** (2015) 65 [arXiv:1505.04349 [nucl-th]].
- [71] K. Yagi, T. Hatsuda, and Y. Miake, “Quark-Gluon Plasma” (Cambridge University Press, 2005).
- [72] J. I. Kapusta and C. Gale, “Finite-Temperature Field Theory” (Cambridge University Press, 2006).
- [73] Crispin Gardiner, “Stochastic Methods: A Handbook for the Natural and Social Sciences” (Springer Series in Synergetics, 2009).
- [74] R. V. Gavai and S. Gupta, Phys. Lett. B **696**, 459 (2011) [arXiv:1001.3796 [hep-lat]].
- [75] C. Schmidt, Prog. Theor. Phys. Suppl. **186**, 563 (2010) [arXiv:1007.5164 [hep-lat]].
- [76] S. Mukherjee, J. Phys. G **38**, 124022 (2011) [arXiv:1107.0765 [nucl-th]].
- [77] S. Borsanyi, *et al.*, JHEP **1201**, 138 (2012) [arXiv:1112.4416 [hep-lat]].
- [78] K. Nagata and A. Nakamura, JHEP **1204** (2012) 092 [arXiv:1201.2765 [hep-lat]].
- [79] A. Bazavov *et al.* [HotQCD Collaboration], Phys. Rev. D **86** (2012) 034509.
- [80] A. Bazavov, *et al.*, Phys. Rev. Lett. **109** (2012) 192302.
- [81] A. Bazavov, *et al.*, Phys. Rev. Lett. **111** (2013) 082301.

- [82] A. Nakamura and K. Nagata, arXiv:1305.0760 [hep-ph].
- [83] S. Borsanyi, Z. Fodor, S. D. Katz, S. Krieg, C. Ratti and K. K. Szabo, Phys. Rev. Lett. **111** (2013) 062005 [arXiv:1305.5161 [hep-lat]].
- [84] R. Bellwied, *et al.*, Phys. Rev. Lett. **111** (2013) 202302.
- [85] A. Bazavov *et al.*, Phys. Rev. D **88** (2013) 9, 094021 [arXiv:1309.2317 [hep-lat]].
- [86] S. Borsanyi, *et al.*, Phys. Rev. Lett. **113** (2014) 052301.
- [87] A. Bazavov, *et al.*, Phys. Lett. B **737** (2014) 210.
- [88] A. Bazavov *et al.*, Phys. Rev. Lett. **113** (2014) 7, 072001 [arXiv:1404.6511 [hep-lat]].
- [89] S. Gupta, N. Karthik and P. Majumdar, Phys. Rev. D **90** (2014) 3, 0340010.
- [90] A. Nakamura, S. Oka and Y. Taniguchi, arXiv:1504.04471 [hep-lat].
- [91] A. Bazavov *et al.*, arXiv:1509.05786 [hep-lat].
- [92] The Review of Particle Physics, K. Nakamura, *et al.* (Particle Data Group), J. Phys. G **37**, 075021 (2010).
- [93] J. Cleymans and K. Redlich, Phys. Rev. Lett. **81**, 5284 (1998) [arXiv:nucl-th/9808030].
- [94] L.D. Landau and E.M. Lifshitz, “Statistical Physics: Part 1”, (Pergamon, Oxford, 1980).
- [95] L.D. Landau and E.M. Lifshitz, “Statistical Physics: Part 2”, (Pergamon, Oxford, 1980).
- [96] V. Koch, A. Majumder and J. Randrup, Phys. Rev. Lett. **95** (2005) 182301 [nucl-th/0505052].
- [97] F. Karsch and K. Redlich, Phys. Lett. B **695** (2011) 136 [arXiv:1007.2581 [hep-ph]].
- [98] M. Kitazawa and M. Asakawa, Phys. Rev. C **85** (2012) 021901 [arXiv:1107.2755 [nucl-th]];
- [99] M. Kitazawa and M. Asakawa, Phys. Rev. C **86** (2012) 024904 [Erratum-ibid. C **86** (2012) 069902] [arXiv:1205.3292 [nucl-th]].
- [100] S. Mogliacci, J. O. Andersen, M. Strickland, N. Su and A. Vuorinen, JHEP **1312** (2013) 055 [arXiv:1307.8098 [hep-ph]].
- [101] N. Haque, M. G. Mustafa and M. Strickland, JHEP **1307** (2013) 184 [arXiv:1302.3228 [hep-ph]].
- [102] N. Haque, J. O. Andersen, M. G. Mustafa, M. Strickland and N. Su, Phys. Rev. D **89** (2014) 6, 061701 [arXiv:1309.3968 [hep-ph]].
- [103] D. T. Son and M. A. Stephanov, Phys. Rev. D **70** (2004) 056001 [hep-ph/0401052].
- [104] Y. Minami, Phys. Rev. D **83** (2011) 094019 [arXiv:1102.5485 [hep-ph]].
- [105] P. C. Hohenberg and B. I. Halperin, Rev. Mod. Phys. **49** (1977) 435.
- [106] Y. Hatta and T. Ikeda, Phys. Rev. D **67** (2003) 014028 [hep-ph/0210284].
- [107] H. Fujii, Phys. Rev. D **67** (2003) 094018 [hep-ph/0302167].
- [108] H. Fujii and M. Ohtani, Phys. Rev. D **70** (2004) 014016 [hep-ph/0402263].
- [109] T. Kunihiro, Phys. Lett. B **271** (1991) 395.
- [110] C. Sasaki, B. Friman and K. Redlich, Phys. Rev. D **75** (2007) 054026 [hep-ph/0611143].
- [111] C. Sasaki, B. Friman and K. Redlich, Phys. Rev. D **75** (2007) 074013 [hep-ph/0611147].
- [112] K. Fukushima, Phys. Rev. D **77** (2008) 114028 [Phys. Rev. D **78** (2008) 039902] [arXiv:0803.3318 [hep-ph]].
- [113] B. J. Schaefer, M. Wagner and J. Wambach, Phys. Rev. D **81** (2010) 074013 doi:10.1103/PhysRevD.81.074013 [arXiv:0910.5628 [hep-ph]].
- [114] W. j. Fu, Y. x. Liu and Y. L. Wu, Phys. Rev. D **81** (2010) 014028 doi:10.1103/PhysRevD.81.014028 [arXiv:0910.5783 [hep-ph]].
- [115] V. Skokov, B. Friman and K. Redlich, Phys. Rev. C **83** (2011) 054904 doi:10.1103/PhysRevC.83.054904 [arXiv:1008.4570 [hep-ph]].

- [116] T. Ichihara, K. Morita and A. Ohnishi, arXiv:1507.04527 [hep-lat].
- [117] B. Friman, F. Karsch, K. Redlich, and V. Skokov, Eur. Phys. J. C **71** (2011) 1694.
- [118] M. A. Stephanov, Phys. Rev. Lett. **107** (2011) 052301.
- [119] S. Gupta, *et al.*, Science **332** (2011) 1525.
- [120] C. Athanasiou, K. Rajagopal and M. Stephanov, Phys. Rev. D **82** (2010) 074008 [arXiv:1006.4636 [hep-ph]].
- [121] P. Braun-Munzinger, B. Friman, F. Karsch, K. Redlich and V. Skokov, Phys. Rev. C **84**, 064911 (2011) [arXiv:1107.4267 [hep-ph]].
- [122] P. Braun-Munzinger, B. Friman, F. Karsch, K. Redlich and V. Skokov, Nucl. Phys. A **880**, 48 (2012) [arXiv:1111.5063 [hep-ph]].
- [123] K. Fukushima, Phys. Rev. C **91** (2015) 4, 044910 [arXiv:1409.0698 [hep-ph]].
- [124] M. Bluhm, P. Alba, W. Alberico, R. Bellwied, V. Mantovani Sarti, M. Nahrgang and C. Ratti, Nucl. Phys. A **931** (2014) 814 [arXiv:1408.4734 [hep-ph]].
- [125] M. Albright, J. Kapusta and C. Young, Phys. Rev. C **92** (2015) 4, 044904 [arXiv:1506.03408 [nucl-th]].
- [126] F. Karsch, Central Eur. J. Phys. **10** (2012) 1234 [arXiv:1202.4173 [hep-lat]].
- [127] M. Asakawa, M. Kitazawa, Y. Ohnishi and M. Sakaida, talk given in Quark Matter 2015.
- [128] Y. Ohnishi, M. Asakawa, M. Kitazawa, in preparation.
- [129] B. Abelev *et al.* [ALICE Collaboration], Phys. Rev. C **88** (2013) 044910 [arXiv:1303.0737 [hep-ex]].
- [130] P. Alba, W. Alberico, R. Bellwied, M. Bluhm, V. Mantovani Sarti, M. Nahrgang and C. Ratti, Phys. Lett. B **738** (2014) 305 [arXiv:1403.4903 [hep-ph]].
- [131] K. Morita and K. Redlich, PTEP **2015** (2015) 4, 043D03 [arXiv:1409.8001 [hep-ph]].
- [132] F. Karsch, K. Morita and K. Redlich, arXiv:1508.02614 [hep-ph].
- [133] M. Bleicher, S. Jeon, and V. Koch, Phys. Rev. C **62**, 061902 (2000).
- [134] V. V. Begun, M. Gazdzicki, M. I. Gorenstein and O. S. Zozulya, Phys. Rev. C **70** (2004) 034901 [nucl-th/0404056].
- [135] V. V. Begun, M. Gazdzicki, M. I. Gorenstein, M. Hauer, V. P. Konchakovski and B. Lungwitz, Phys. Rev. C **76** (2007) 024902 [nucl-th/0611075].
- [136] A. Bzdak, V. Koch and V. Skokov, Phys. Rev. C **87** (2013) 1, 014901 [arXiv:1203.4529 [hep-ph]].
- [137] M. Sakaida, M. Asakawa and M. Kitazawa, Phys. Rev. C **90** (2014) 6, 064911.
- [138] S. Cao, G. Y. Qin and S. A. Bass, Phys. Rev. C **92** (2015) 5, 054909 doi:10.1103/PhysRevC.92.054909 [arXiv:1505.01869 [nucl-th]].
- [139] H. Niemi, K. J. Eskola and R. Paatelainen, arXiv:1505.02677 [hep-ph].
- [140] V. Skokov, B. Friman and K. Redlich, Phys. Rev. C **88** (2013) 034911 [arXiv:1205.4756 [hep-ph]].
- [141] P. Alba, R. Bellwied, M. Bluhm, V. M. Sarti, M. Nahrgang and C. Ratti, arXiv:1504.03262 [hep-ph].
- [142] M. I. Gorenstein and M. Gazdzicki, Phys. Rev. C **84** (2011) 014904 [arXiv:1101.4865 [nucl-th]].
- [143] V. V. Begun, M. Gazdzicki and M. I. Gorenstein, Phys. Rev. C **88** (2013) 2, 024902 [arXiv:1208.4107 [nucl-th]].
- [144] E. Sangaline, arXiv:1505.00261 [nucl-th].
- [145] H. Ono, M. Asakawa and M. Kitazawa, Phys. Rev. C **87** (2013) 041901 R.
- [146] M. Nahrgang, M. Bluhm, P. Alba, R. Bellwied and C. Ratti, arXiv:1402.1238 [hep-ph].
- [147] Z. Feckova, J. Steinheimer, B. Tomasik and M. Bleicher, arXiv:1510.05519 [nucl-th].

- [148] J. I. Kapusta, B. Muller and M. Stephanov, Phys. Rev. C **85** (2012) 054906 [arXiv:1112.6405 [nucl-th]].
- [149] E. V. Shuryak and M. A. Stephanov, Phys. Rev. C **63** (2001) 064903.
- [150] H. Ono, Master thesis, Osaka University (2013).
- [151] S. Haussler, S. Scherer and M. Bleicher, Phys. Lett. B **660** (2008) 197 [hep-ph/0702188 [HEP-PH]].
- [152] M. A. Aziz and S. Gavin, Phys. Rev. C **70** (2004) 034905.
- [153] C. Young, J. I. Kapusta, C. Gale, S. Jeon and B. Schenke, Phys. Rev. C **91** (2015) 4, 044901 [arXiv:1407.1077 [nucl-th]].
- [154] K. Adcox *et al.* [PHENIX Collaboration], Phys. Rev. Lett. **89** (2002) 082301 [nucl-ex/0203014].
- [155] J. Adams *et al.* [STAR Collaboration], Phys. Rev. C **68** (2003) 044905 [nucl-ex/0307007].
- [156] B. I. Abelev *et al.* [STAR Collaboration], Phys. Rev. C **79** (2009) 024906 [arXiv:0807.3269 [nucl-ex]].
- [157] B. Berdnikov and K. Rajagopal, Phys. Rev. D **61** (2000) 105017 [hep-ph/9912274].
- [158] C. Nonaka and M. Asakawa, Phys. Rev. C **71** (2005) 044904 [nucl-th/0410078].
- [159] S. Mukherjee, R. Venugopalan and Y. Yin, Phys. Rev. C **92** (2015) 3, 034912 [arXiv:1506.00645 [hep-ph]].
- [160] M. A. Stephanov, Phys. Rev. D **81** (2010) 054012 [arXiv:0911.1772 [hep-ph]].
- [161] M. Nahrgang, S. Leupold, C. Herold and M. Bleicher, Phys. Rev. C **84** (2011) 024912 [arXiv:1105.0622 [nucl-th]].
- [162] M. Nahrgang, C. Herold, S. Leupold, I. Mishustin and M. Bleicher, J. Phys. G **40** (2013) 055108 [arXiv:1105.1962 [nucl-th]].
- [163] C. Herold, M. Nahrgang, Y. Yan and C. Kobdaj, J. Phys. G **41** (2014) 11, 115106.
- [164] C. Sasaki, B. Friman and K. Redlich, Phys. Rev. Lett. **99** (2007) 232301 [hep-ph/0702254 [HEP-PH]].
- [165] J. Steinheimer and J. Randrup, Phys. Rev. Lett. **109** (2012) 212301 [arXiv:1209.2462 [nucl-th]].
- [166] J. Steinheimer, J. Randrup and V. Koch, Phys. Rev. C **89** (2014) 3, 034901 [arXiv:1311.0999 [nucl-th]].
- [167] J. THAEDER, for STAR Collaboration, presentation at Quark Matter 2015, Kobe, Japan, 27 Sep. – 3 Oct., 2015.
- [168] A. Bzdak and V. Koch, Phys. Rev. C **91** (2015) 2, 027901 [arXiv:1312.4574 [nucl-th]].
- [169] M. I. Gorenstein, Phys. Rev. C **84** (2011) 024902 [arXiv:1106.4473 [nucl-th]].
- [170] A. Rustamov and M. I. Gorenstein, Phys. Rev. C **86** (2012) 044906 [arXiv:1204.6632 [nucl-th]].
- [171] R. Holzmann, talk given in “HIC for FAIR Workshop on Fluctuation and Correlation Measured in Nuclear Collisions 2015,” Jul. 29-31, FIAS, Frankfurt, Germany, and “EMMI Workshop on Fluctuations in Strongly Interacting Hot and Dense Matter: Theory and Experiment,” Nov. 2-6, 2015, GSI, Darmstadt, Germany; private communication with R. Holzmann, A. Bzdak and V. Koch.